FIELD THEORY FOR ANDERSON TRANSITIONS IN HIGH DIMENSIONS

Inaugural-Dissertation

zur

Erlangung des Doktorgrades

der Mathematisch-Naturwissenschaftlichen Fakultät

der Universität zu Köln

vorgelegt von

Julian Arenz

aus Brühl

UNIVERSITÄT
ZU KÖLN

Köln, 2026

Berichterstatter: Prof. Dr. Martin R. Zirnbauer
Prof. Dr. Sebastian Diehl
Prof. Dr. Margherita Disertori

Vorsitzender der Prüfungskommission: Prof. Dr. Alexander Drewitz

Tag der mündlichen Prüfung: 02.06.2026

Abstract

Disordered electron systems can undergo a quantum phase transition, known as the Anderson transition, from a metallic phase for weak disorder to an insulating phase at strong disorder. In low dimensions ($d = 2 + \varepsilon$), an efficient tool for studying the transition is an effective field theory called the nonlinear σ-model. The renormalization group treatment of this effective model supports a one-parameter scaling hypothesis for the Anderson transition, where the conductance is the only relevant scaling variable.

In the present work, we investigate the Anderson transition in the opposite case of high lattice dimensions. Here the critical point moves into the strong coupling regime, and a field-theoretical description, similar to the nonlinear $\sigma-$model in low dimensions, is lacking at present. The plan here is to identify a field-theoretical mechanism that describes the critical regime in high dimensions. The main finding is a distinct mechanism of spontaneous symmetry breaking. In the metallic phase, the hyperbolic symmetry of the field theory breaks down to a maximal compact subgroup, whereas at criticality it breaks down to a nilpotent subgroup. This distinct symmetry-breaking mechanism naturally leads to a singular continuous spectrum of the underlying random Hamiltonian–a spectral type that has not yet been widely appreciated in the physics literature.

The explicit microscopic model we analyze is a variant of the standard Anderson model, namely the Wegner $N = 1$-orbital model, which belongs to symmetry class A in the Tenfold Way. The model is analyzed using an approximation that goes back to Abou-Chacra, Anderson, Thouless (AAT). In this approximation, one obtains self-consistent equations for advanced and retarded Green's functions. It is exact on tree-like lattices and is expected to capture the essential physics of Anderson transitions in high lattice dimensions.

Kurzzusammenfassung

In ungeordneten Elektronensystemen kann es einen Quantenphasenübergang, den Anderson-Übergang, zwischen einer metallischen Phase bei schwacher Unordnung und einer Isolatorphase bei starker Unordnung geben. In niedriger Raumdimension ($d = 2 + \varepsilon$), kann man den Übergang durch eine effektive Feldtheorie, das nichtlineare σ-Modell, studieren. Die Renormierungsgruppe dieses Modells unterstützt eine Ein-Parameter-Skalenhypothese, in der die einzig relevante Skalenvariable die Leitfähigkeit ist.

In dieser Dissertation betrachten wir den Anderson-Übergang im Falle hoher Raumdimension. Nun ist der kritische Punkt im Regime starker Kopplung, und eine feldtheoretische Beschreibung in diesem Regime ist deutlich subtiler. Das Ziel dieser Arbeit ist es, einen neuen feldtheoretischen Mechanismus, der das kritische Verhalten in hoher Dimension beschreibt, zu identifizieren. Das Hauptresultat ist eine neue Art der spontanen Symmetriebrechung. Während in der metallischen Phase die hyperbolische Symmetrie der Feldtheorie zu einer maximal kompakten Untergruppe bricht, bricht sie am kritischen Punkt zu einer nilpotenten Untergruppe. Dieser neue Symmetriebrechungsmechanismus führt physikalisch zu singulär kontinuierlichem Spektrum des zugrunde liegenden Zufallshamiltonians.

Als explizites mikroskopisches Modell analysieren wir eine Variante des Standard-Anderson-Modells, nämlich das Wegner $N = 1$-Orbital-Modell. Dieses gehört zu der Symmetrieklasse A des "Tenfold Way". Wir werden das Modell in der sogenannten Abou-Chacra, Anderson, Thouless (AAT)-Näherung lösen. Im Rahmen dieser Näherung erhält man selbstkonsistente Gleichungen für avancierte und retardierte Greensche Funktionen. Während die Näherung auf unendlichen Baumgraphen exakt ist, erwartet man, dass sie zumindest für lokale Observablen eine gute Näherung in hoher Dimension liefert.

Contents

1 Introduction

> Wenn man gut durch geöffnete Türen kommen will, muß man die Tatsache achten, daß sie einen festen Rahmen haben: dieser Grundsatz [...] ist einfach eine Forderung des Wirklichkeitssinns. Wenn es aber Wirklichkeitssinn gibt, und niemand wird bezweifeln, daß er seine Daseinsberechtigung hat, dann muß es auch etwas geben, das man Möglichkeitssinn nennen kann.
>
> Robert Musil, *Der Mann ohne Eigenschaften*

The progress in the study of mesoscopic properties of condensed matter over the last century is one of the great achievements of both modern experimental and theoretical physics. The constituents of a condensed matter system are interacting particles, such as electrons, in an environment, for example, given by static heavy nuclei surrounded by bound electrons. In a mathematical model, the environment can be simulated by a lattice $\mathbb{G}$ and the dynamics of the interacting particles by a many-body Hamiltonian on that lattice. A typical condensed matter system consists of a macroscopic number of particles, say 10^{23}, interacting with their neighbors. It is hopeless to simulate their collective microscopic dynamics. A key insight that enables the study of the low-energy (or long wavelength) behavior of a variety of different models is the fact that the exact microscopic details are irrelevant for the low-energy behavior. Rather, it can be deduced by analyzing a few (instead of 10^{23}) collective degrees of freedom of the system. An efficient tool to analyze these collective degrees of freedom is quantum field theory. It categorizes the microscopic theories into a comparably small number of universality classes, classified by the fundamental symmetries of the theory [7] and (!) their symmetry-breaking mechanism.

There are two major challenges when analyzing condensed matter systems. The first one is that the interactions between the constituents can be quite strong, i.e., the problem at hand may be non-perturbative around the non-interacting limit. An example is the Hubbard model for Mott insulators [11]. The second one is that the

impurities of the underlying lattice can be quite large, making the problem non-perturbative around the limit where impurities are absent. The impurities can be simulated by a random potential V which consists of independent random variables $V(j),\ j \in \mathbb{G}$. The strength of the fluctuations of the random potential (its variance) is called disorder. An example of this is the Anderson transition in high lattice dimensions.

1.1 Anderson localization and Anderson transition

A strategy to gain analytical understanding of these strongly coupled problems is to either investigate the strongly interacting case with disorder absent or the strongly disordered case with interactions absent. The present dissertation addresses the second case. We treat the electrons in the non-interacting (or mean-field) approximation on a high-dimensional lattice with disorder present. Since the pioneer work of A.W. Anderson [10], it has been understood that disorder can localize the electron wave function due to quantum interferences. A heuristic argument goes as follows: To analyze the transition probability for the electron from an initial site n to a different site n', one can write the propagation amplitude $\langle n', \mathrm{e}^{-\mathrm{i}tH}\, n\rangle$ as a sum over contributions from different lattice paths starting at site n and ending at site n'. Each path accumulates a complex amplitude determined by the values of the disorder potential on this path. After summing, one takes the squared absolute value [28]. For large separations between n and n', typically, the contributing paths explore largely disjoint spatial regions. For large disorder strength, the fluctuations of the disorder potential are strong, so the spatially separated paths probe essentially independent regions of the configurations of the disorder potential. As a consequence, the corresponding amplitudes have effectively uncorrelated complex phases and tend to interfere destructively when summed.

By contrast, for paths that remain in the vicinity of the initial site n, there is a significant spatial overlap. Now the complex phases of the path amplitudes are correlated, and the degree of destructive interference is smaller.

As a result, for sufficiently strong disorder, the electron tends to stay in the vicinity of the initial site n and the electron wave function remains localized.

In high enough lattice dimension ($d > 2$ for cubic lattices) and for weak disorder, the above argument no longer applies. The electron wave function delocalizes, and the system turns into a metallic state. This implies that electrons undergo a quantum phase transition, known as the Anderson transition, from a metallic state at weak disorder to an insulating state at strong disorder. When tuning the energy

instead of the disorder strength, the corresponding critical energy is called *mobility edge*. The concept of a mobility edge separating metallic and insulating states on the energy axis was first introduced by Mott [62].

1.2 One-parameter scaling hypothesis and nonlinear σ-model

It took almost 20 years after the seminal work of Anderson to make progress in understanding the nature of the Anderson transition, theoretically and experimentally. Detailed reviews of these developments are given in [53, 57, 23]. Based on earlier works [85, 95], in [2] a one-parameter scaling hypothesis for the Anderson transition was proposed: the conductance g is the only relevant scaling variable near the transition. Its flow when varying the system size L is given by

$$\beta(g) = \frac{\mathrm{d}\ln(g)}{\mathrm{d}\ln(L)}. \tag{1.1}$$

The qualitative behavior of the vector field β was obtained by investigating the asymptotic behavior for large and small conductances. A remarkable consequence of the one-parameter scaling hypothesis is that, in symmetry class A, in dimensions $d = 1, 2$ (for $\mathbb{G} = \mathbb{Z}^d$), the conductance flows to zero in the thermodynamic limit. This implies that in dimensions one and two, the electron wave function is always localized. The Anderson transition can therefore only occur for $d \geq 3$. Furthermore, an analytical milestone was the investigation of the Anderson transition by Abou-Chacra, Anderson, and Thouless (AAT) [1]. They derived a self-consistent equation (AAT equation) for the self-energy, which is exact on an infinite tree-like lattice, the Bethe lattice [13]. A stability analysis of the AAT equation enabled them to infer the location of the critical points. The present work is based on the self-consistent theory derived by AAT.

Support for the one-parameter scaling hypothesis came from the renormalization group (RG) treatment of an effective field theory, the nonlinear σ-model [92], analyzed in the weak-coupling regime in two or near two space dimensions [39, 91]. In this effective field theory, the metal-insulator transition is encoded in a spontaneous symmetry-breaking mechanism: in the metallic phase, the symmetry is spontaneously broken, whereas in the insulating phase, the symmetry is restored. Indeed, in [102], the symmetry-breaking mechanism of the nonlinear σ-model on the Bethe lattice has been connected to the correct analytical behavior of the two-point Green's function in the metallic and insulating phases. A first microscopic deriva-

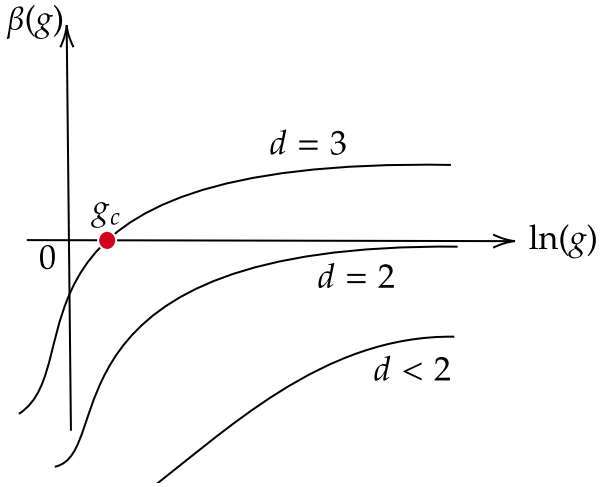

Figure 1.1: One-parameter scaling hypothesis for Anderson transitions: For $d \leq 2$ the vector field β is always negative, even for large conductances g. When increasing the system size L, the system always flows to the insulating limit. For $d = 3$, the vector field β changes sign at the critical value $g = g_c$. For $g > g_c$, the system flows to the metallic fixed point.

tion of the nonlinear σ-model has been achieved in several works [24, 47, 78] using the replica trick. A derivation using the supersymmetry method was first performed by Efetov [22].

We note that, also numerically [76, 33, 74, 58], the Anderson transition in low dimensions has been understood quite early.

1.3 The debate in high lattice dimension

While the validity of the one-parameter scaling hypothesis and the nonlinear σ-model is undisputed near two dimensions, the situation becomes more complicated in high dimensions. The established thought is that the one-parameter scaling hypothesis and the nonlinear σ-model are still applicable [61], but there are also skeptics [38]. The reason for this subtlety is that the Anderson transition point moves into the strong coupling regime in increasing dimension, and there exists no proof of renormalizability of the nonlinear σ-model at strong coupling. The discussion about the validity of the one-parameter scaling hypothesis, the applicability of the nonlinear σ-model, and, more generally, the nature of the Anderson transition in high dimensions is still an ongoing debate. We now give a short overview of this debate:

According to the traditional theory, there exist two phases: (i) the metallic state at weak disorder, and (ii) the insulating state at strong disorder. At the critical point, analytical and numerical investigations reveal that the wave functions turn

out to be multifractal [93, 16], meaning that the scaling of the moments of the inverse participation ratio with the system size is characterized by an infinite set of critical exponents. An informative overview about the multifractality of wave functions is given in Ref. [27]. Multifractality of wave functions here relies on the restriction to finite systems and finite-size scalings. However, it remains elusive how multifractality arises from a field-theoretical mechanism directly in the thermodynamic limit, in the same structural sense as metallic and insulating phases, which are characterized by well-defined symmetry-breaking patterns.

Some time ago, it was proposed [8, 54] that there may exist a third phase, called NEE for non-ergodic extended, in the Anderson model on infinite-dimensional lattices, such as the Bethe lattice, where the electron eigenstates are fractal. While this third phase is realized in simple models of random-matrix type [55], strong evidence [86, 34, 14, 36, 79] excludes its realization in the Anderson model on tree-like graphs. Nevertheless, there does exist recent evidence that the Anderson model on high-dimensional random graphs does not conform to the usual one-parameter scaling hypothesis. Indeed, using large-scale numerical simulations of small-world networks, the authors of Refs. [35, 36] found that two relevant parameters are needed to describe the critical behavior: In the insulating phase, the wave functions have a large localization length along some rare branches. This length diverges at the critical point. The transverse localization length is much smaller and converges to a finite value at criticality. On the metallic side of the transition, the wave function remembers the critical properties on small scales, i.e., here it is non-ergodic, but ergodicity is recovered on larger scales.

A more recent scaling analysis of the Anderson model on random regular graphs is that of Ref. [89], where two scaling parameters are again involved, although for large system sizes one-parameter scaling is recovered.

The above reveals that the critical properties of the Anderson transition in high dimensions are an active subject of modern research. This brings us to the first motivation for the present dissertation: Our goal is to shed new light on the critical behavior of the Anderson transition in high dimensions by using field theory. That is, our plan here is to detect a field-theoretical mechanism at criticality that is distinct from the symmetry-breaking mechanism in the insulating and metallic phases.

1.4 Anderson transition via spectral types

A different viewpoint on the subject emerges from mathematical physics, where the Anderson transition is often formulated in terms of the spectral decomposition of the

underlying random Hamiltonian [6, 67]. From this angle, the distinction between the phases is encoded in the nature of the spectral measure. Pure point (pp) spectrum (i.e., isolated eigenvalues) corresponds to the insulating phase, absolutely continuous (ac) spectrum (i.e., a dense collection of "eigenvalues") corresponds to the metallic phase. Indeed, the corresponding eigenfunctions in the pp case are elements of $\ell^2(\mathbb{G})$, thus localized, while in the ac case they are not square-summable because they are extended over the whole lattice. In particular, it is by now well understood why, for strong disorder and/or low dimension, random Hamiltonians possess pp spectrum [31, 3, 15, 81]. In contrast, the proof of the existence of parameter regions where the spectrum is absolutely continuous is significantly harder. On cubic lattices $\mathbb{Z}^d$, especially $d = 3$, it is the subject of ongoing research for the Anderson model. Nevertheless, the existence of a diffusive phase in $d = 3$, as well as a localized phase for any dimension $d \geq 1$ for a simplified version of the nonlinear σ-model, the $H^{2|2}$ model [103], was proved in [20, 19]. Additionally, significant recent progress has been achieved for random band matrices, where delocalization and diffusive behavior have been rigorously established [25, 101].

On tree-like lattices such as the Bethe lattice, the existence of an ac spectrum in the Anderson model is established for energies near band center and sufficiently weak disorder [49, 50, 4, 30]. The emergence of ac spectrum has been proven in wider parameter ranges by identifying a mechanism called *resonant delocalization*: Localized clusters of the wave functions connect due to rare resonances that occur when the energy difference of these clusters is smaller than the tunneling amplitude. Even though the probability of these events is exponentially small for increasing distance, in high enough dimensions, these events still occur due to the exponentially increasing number of sites [5].

Despite the progress in the identification of an ac spectrum for small to moderate disorder, what remains elusive is the spectral type in the critical regime. In that vein, we recall a fact from the spectral theory of random Schrödinger operators (or any self-adjoint operator) in the infinite-volume limit. Apart from pp and ac spectrum, there is also the possibility of *singular continuous* (sc) spectrum [71, 18]. In short, the sc-type "eigenvalues", as opposed to the pp-type eigenvalues, are neither discrete nor do they form proper bands, as opposed to the ac case. Important work on the analysis of operators with singular continuous spectrum was done in [80, 73, 46, 72]. A rather natural idea is to link the characteristic features of fractal eigenstates with those of sc spectrum and, indeed, this link has been pursued in a recent article [9]. This idea suggests that one could expect a singular continuous spectrum in the critical regime. However, a structural field-theoretical

interpretation of such a spectral type is lacking at present. The central claim of this dissertation is the existence of a novel symmetry-breaking mechanism at criticality, which provides a structural interpretation of singular continuous spectrum in high-dimensional Anderson-type models. This mechanism is distinct from the symmetry-breaking mechanism in the ac phase.

1.5 Proposed symmetry-breaking mechanism at criticality and the debate about conformal invariance

Yet there exists a third motivation for our work. A few years ago, Zirnbauer proposed [105] a conformal field theory for the scaling limit of the critical point between plateaus of the integer quantum Hall (IQH) effect. The key ingredient to arrive at the conformal field theory is a mechanism of *partial symmetry breaking*. This mechanism is based on the non-compact nature of the symmetry group and thus is not restricted to the IQH transition or two dimensions. Indeed, the standard Anderson model in high dimensions, or a variant thereof, the Wegner N-orbital model, which we will study in the present work, both belong to the same symmetry class, class A. By invoking the principle of universality, one could expect a similar spontaneous symmetry-breaking mechanism to occur also in the Anderson model and variants thereof in high dimensions. From the present perspective, our goal is to identify a symmetry-breaking mechanism in the field theory for the Wegner N-orbital model at criticality, and investigate whether or not it is similar to the one identified in the field theory for the IQH.

Now is a good time to announce what this symmetry-breaking mechanism in the field theory we develop in the present work looks like: The symmetry group of the field theory turns out to be the non-compact Lie group $G = \mathrm{SU}(1,1)$, or, after making use of a Lie group isomorphism, $G = \mathrm{SL}(2,\mathbb{R})$. In the insulating phase, no spontaneous symmetry breaking occurs; the full symmetry group G is restored. In the metallic phase, the symmetry is spontaneously broken down to a maximal compact subgroup $K \cong \mathrm{U}(1)$. We propose that the symmetry-breaking mechanism at criticality is distinct: Instead of being restored to the full group G, the symmetry is spontaneously broken down to a *nilpotent* subgroup $N \subset G$. The emergence of a nilpotent residual symmetry reflects the non-compact structure of G and has no analogue in compact symmetry-breaking scenarios.

regime	symmetry
insulating	$\mathrm{SL}(2,\mathbb{R}) = G$
metallic	$\mathrm{U}(1) \cong K \subset G$
critical	$\mathbb{R} \cong N \subset G$

Table 1.1: Symmetry-breaking mechanisms in our field theory

Table 1.1 summarizes the central result of this dissertation. To explain one possible consequence, we now state another open discussion about the nature of the critical point for Anderson transitions in high dimensions (presumably meaning $d \geq 3$): The question of whether or not the critical theory is a conformal field theory. A particularly influential argument against conformal invariance was put forward in Ref. [66]. There it was argued that any Abelian conformal field theory in $d > 2$ necessarily implies a parabolic multifractality spectrum at the Anderson transition. Since both analytical results in $d = 2 + \varepsilon$ [26, 63, 70, 48] and numerical results in $d = 3, 4, 5$ [74, 87, 59, 84] demonstrate clear deviations from parabolicity, the authors concluded that conformal invariance is likely absent at Anderson transitions. Importantly, the authors of [66] argue that their conclusion relies on the assumption that the symmetry of the target space, G, is not spontaneously broken at the critical point. The alternative scenario, namely spontaneous symmetry breaking at criticality, was dismissed as unlikely by the authors. The present work addresses precisely this alternative and proposes that partial symmetry breaking at criticality does occur, thereby challenging their key assumption underlying the no-CFT conclusion.

In summary, the three different perspectives portrayed above boil down to the question of the nature of the Anderson transition in high dimensions. In this work, we detect a field-theoretical phenomenon that naturally represents fractal eigenstates and singular continuous spectrum as a distinct non-compact symmetry-breaking mechanism. In the main part of this dissertation, we will mostly focus on the connection between the symmetry-breaking mechanism and singular continuous spectrum. The reason is that the phenomenon of an sc-type spectrum in general has not been addressed very intensively in the physics literature. In the following figures, we summarize the connection between the spectral type, the wave functions, and the symmetry-breaking mechanism in the field theory. $K_{n,\varepsilon}, \quad \varepsilon > 0$ is a correlator introduced below. Its scaling in ε for $\varepsilon \to 0$ distinguishes between the three spectral types and can be calculated in our field-theoretical approach.

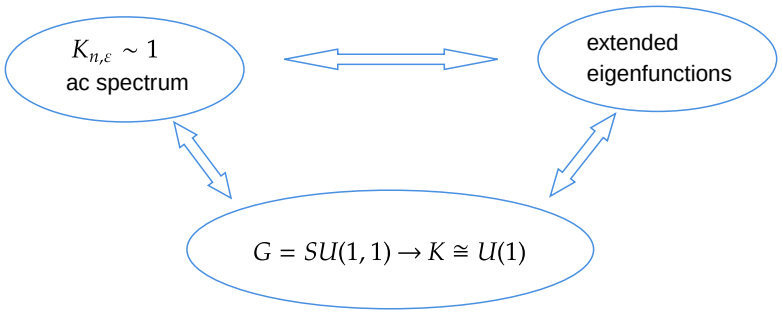

Figure 1.2: Correspondence between spectrum, behavior of eigenfunctions, and symmetry-breaking mechanism in the metallic phase

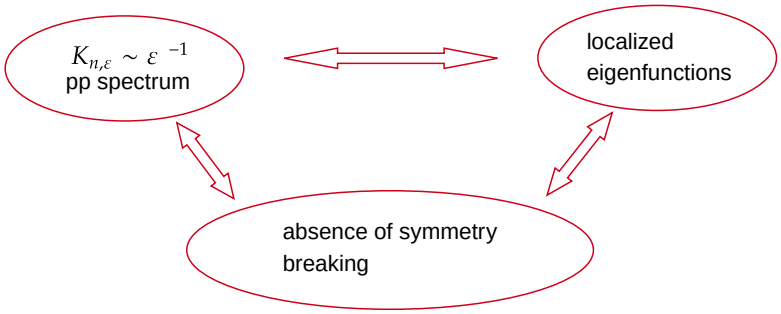

Figure 1.3: Correspondence between spectrum, behavior of eigenfunctions, and symmetry-breaking mechanism in the insulating phase

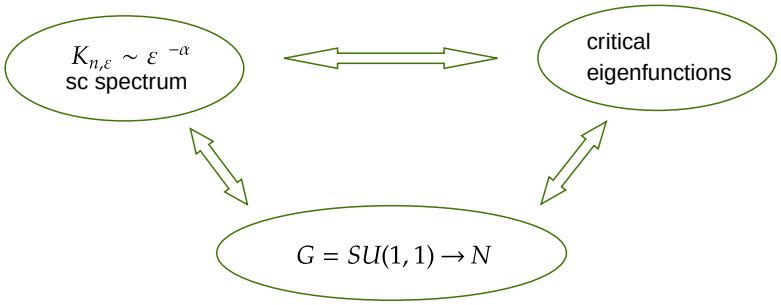

Figure 1.4: Correspondence between spectrum, behavior of eigenfunctions, and symmetry-breaking mechanism at criticality

1.6 Structure of the thesis

For demonstration of the field-theoretical phenomenon, we analyze a variant of the standard Anderson model, namely the Wegner N-orbital model [96] of type A in the Tenfold Way [42]. While previous treatments were mostly concerned with the metallic limit for large N, our focus is on the model for $N = 1$ (i.e., with a single electron orbital per site) in high lattice dimension. The corresponding Hamiltonian is a random Schrödinger operator, H, on an infinite graph, $\mathbb{G}$, for example $\mathbb{G} = \mathbb{Z}^d$:

$$H = \sum h_{n,n'} c_n^\dagger c_{n'}, \tag{1.2}$$

where the sum is over the lattice sites $n, n' \in \mathbb{G}$, and $c_n^\dagger, c_{n'}$ are fermionic creation and annihilation operators. The Hamiltonian matrix elements $h_{n,n'}$ are complex Gaussian random variables. For the definition of the probability law, we refer to the beginning of Chapter 3 where the analysis of the model begins.

We shall solve that model in the approximation afforded by Abou-Chacra, Anderson, and Thouless (AAT) [1]. Exact on the Bethe lattice, the AAT approximation is expected to capture the relevant physics in high dimensions [1, 84].

The structure of the rest of this dissertation is as follows: In the preparatory chapter, Chapter 2, we discuss the main mathematical and physical concepts which are needed for the subsequent analysis but go beyond the standard curriculum of a theoretical physicist. One important outcome of Section 2.2 is an argument that the product of retarded and advanced Green's functions

$$K_{n,\varepsilon} = \mathbb{E}(|G_n|^2), \quad G_n \equiv G_{n,n}(E + \mathrm{i}\varepsilon) \tag{1.3}$$

is an observable suitable for detecting the three spectral types. In Eq. 1.3, the expectation value $\mathbb{E}$ is over the disorder of the Wegner Hamiltonian, and G_n is the retarded Green's function of H at site n and energy E.

Afterwards, in Chapter 3 we first introduce the Wegner 1-orbital model and its probability law in Section 3.1. We show how the problem of calculating the above observable simplifies within the AAT approximation in Section 3.2: Initially, we obtain a self-consistency equation for the retarded Green's function. To calculate the correlator $K_{n,\varepsilon}$, we need both retarded and advanced Green's functions, so next we derive a self-consistency equation for a matrix Green's function:

$${}^g\mathcal{G} = \left(\begin{pmatrix} E-h & 0 \\ 0 & E-h \end{pmatrix} + g \begin{pmatrix} \mathrm{i}\varepsilon & 0 \\ 0 & -\mathrm{i}\varepsilon \end{pmatrix} g^{-1} \right)^{-1}, \quad g \in \mathrm{SU}(1,1). \tag{1.4}$$

For an enhanced perspective, we also include symmetry transformed matrices ${}^g\mathcal{G}, g \neq 1$. [In a later chapter, we will see a connection between the existence of different solutions of the self-consistency equation ${}^g\mathcal{G}$ and the fact that in symmetry-broken phases there is a whole manifold of different extremal Gibbs states]. With the AAT-self consistency equation for ${}^g\mathcal{G}$ in hand, we next introduce the field variables, 4×4 supermatrices $\mathcal{Q}_j$, to map the self-consistency equation to a supersymmetric integral equation 3.50 (called AAT integral equation) for a superanalytic function ${}^g\mathcal{Y}(\mathcal{Q}_j)$ in Section 3.3. The function ${}^g\mathcal{Y}$ contains the information about the Green's functions, and with it one can calculate (among others) the observable $K_{n,\varepsilon}$. In Section 3.4 we connect the solutions ${}^g\mathcal{Y}$ of the integral equation to the notion of extremal Gibbs states of the field theory on arbitrary high-dimensional lattices such as $\mathbb{Z}^d, d \gg 1$. We find that calculating the field operator representing the observable $K_{n,\varepsilon}$ in an extremal Gibbs state, characterized by a symmetry group element g, reduces to performing the integral

$$K_{n,\varepsilon} \stackrel{!}{=} \int \mathrm{d}Q_n \, \mathrm{e}^{-\operatorname{Tr}(\varepsilon\sigma_3)Q_n} \; {}^gY(Q_n), \tag{1.5}$$

where Q_n is the field on site $n \in \mathbb{G}$, and ${}^gY(Q_n)$ is a solution of the supersymmetric AAT integral equation with Grassmann variables set to zero. In the final part of the chapter, 3.5, we naturally proceed by reducing the supersymmetric AAT integral equation to a purely "bosonic" equation, i.e., with Grassmann variables fully absent, Eq. 3.90.

In the following two Chapters, 4, and 5, we analyze the reduced "bosonic" integral equation. In Chapter 4 we first delve deeper into the geometric structure of the field target space, Section 4.1. Afterwards, in Section 4.2 we analyze the "bosonic" AAT integral equation, Eq. 3.90, by imposing $\mathrm{U}(1)_{\mathrm{i}\sigma_3}$ symmetry (i.e. we impose that its solutions do not break the U(1) symmetry generated by the Pauli matrix σ_3). As an outcome, we find explicit expressions for solutions $Y_{\mathrm{pp}}, Y_{\mathrm{ac}}$ deep in the insulating phase (pp spectrum), and deep in the metallic phase (ac spectrum). This happens in Sections 4.3 and 4.4. The final subsection, Subsection 4.4.2, is a preparation for the analysis in Chapter 5. Here we observe that there is a whole continuum of symmetry transformed metallic, or, equivalently, ac-type, solutions ${}^gY_{\mathrm{ac}}$ of the AAT integral equation, and we investigate how these solutions behave for g approaching the boundary of $\mathrm{SU}(1,1)/\mathrm{U}(1)$. This investigation serves as a first inspiration of what might happen at criticality. The analysis of the critical regime happens in Chapter 5. We find an explicit formula for the critical points (the critical manifold)

at strong coupling using harmonic analysis in Section 5.1

$$K(w_c) = \frac{1}{\sqrt{2}} \frac{w_c}{\ln(w_c)} \exp\left(\frac{E^2}{2w_V^2}\right). \tag{1.6}$$

In Eq. (1.6), K is the branching number of the high-dimensional graph. w_V is the on-site disorder strength, w_c is the critical quotient of on-site disorder strength and hopping strength, and E is the energy.

The eigenfunctions of the harmonic analysis also tell about the behavior of the $\mathrm{U}(1)_{\mathrm{i}\sigma_3}$-invariant metallic solutions when approaching criticality from the metallic phase. This aspect is studied in Section 5.2. Most importantly, we calculate the length scale Λ which tells at which radial scale the above close-to-critical metallic solutions decay. In other words, the scale Λ roughly speaking controls the radial field fluctuations; it diverges at criticality. Finally, with the knowledge of the behavior of the metallic solutions Y_{ac} on the way to criticality, we construct the critical, N-invariant solutions, Y_{sc} in Section 5.3. They emerge due to the combination of two effects. First, when approaching the critical point from the metallic phase, the field fluctuations on the symmetry group orbits (the Goldstone manifold) become stronger and stronger. Second, we propose that the $\mathrm{U}(1)_{\mathrm{i}\sigma_3}$ is spontaneously broken and a typical field configuration concentrates around a point on the asymptotic boundary of the Goldstone manifold. To explicitly construct these critical solutions, we subject the $\mathrm{U}(1)_{\mathrm{i}\sigma_3}$-invariant solution Y_{ac} to a coupled limit, where the disorder is tuned to the critical disorder from below, and the action of the symmetry group $Y \to {}^{g}Y$ (a Lorentz boost) is sent to infinity. To wrap up Chapter 5 and to justify the important arrow in Figure 1.4, we next show that the solution Y_{sc} indeed corresponds to sc-type behavior of the observable $K_{n,\varepsilon}$ in Section 5.4.

In the final Chapter 6 before the conclusions, we deliver the symmetry characterization of the three types of solutions $Y_{\mathrm{ac}}, Y_{\mathrm{pp}}, Y_{\mathrm{sc}}$, i.e., we justify the Table 1.1. For that purpose, we delve a bit deeper into the algebraic structure of our symmetry group and discuss the relevant subgroups that determine the symmetries of the solutions Y. As an additional benefit, we will see how the coordinate systems we used throughout this thesis stem from different decompositions of our symmetry group $G = \mathrm{SU}(1,1) \cong \mathrm{SL}(2,\mathbb{R})$.

2 Framework

This chapter introduces the tools that will be used throughout this thesis and that go beyond the standard curriculum of a theoretical physicist.

We begin with an introduction to superanalysis, Section 2.1, where we define superfunctions, the Berezin integral, what is meant by a supersymmetry, and we state the supersymmetric localization theorem. These concepts are required because the field theory we analyze originally contains commuting ("bosonic") variables and anti-commuting ("fermionic", Grassmann) variables and has supersymmetries. Because of these supersymmetries, a localization theorem is at work and ensures the normalization of the field integral. In the course of this work, we will integrate out the Grassmann variables and obtain a purely "bosonic" theory. Nevertheless, some identities of the resulting "bosonic" theory would seem mysterious without an in-depth understanding of the supersymmetric origin, and for this reason, a brief introduction to superanalysis is included. Readers mainly interested in the physical insights may skip this section on first reading.

Next, we summarize the aspects of the spectral theory of self-adjoint operators in infinite volume that are needed in this work (Section 2.2). In particular, we review their three spectral types: pure point (pp), absolutely continuous (ac), and, singular continuous (sc). We give examples of operators that possess purely pp, ac, and sc spectra. Building on that, we introduce self-adjoint operators whose matrix entries are random variables, so-called *random Schrödinger operators* or *random Hamiltonians*. We explain what can be inferred about their spectral types, and, most importantly, we motivate an observable that distinguishes between the three spectral types. This observable will be analyzed in our field-theoretical approach for the Wegner $N = 1$-orbital model. Since one focus of this thesis is the identification of singular continuous spectrum in Anderson transitions in high dimensions, a clear understanding of this section is essential.

Because field theory will be our tool for analysis, next our focus goes to the mechanism of spontaneous symmetry breaking in field theories on an infinite lattice $\mathbb{G}$ (Section 2.3). Of course, this concept is familiar to most theoretical physicists who have a basic education in field theory. Nevertheless, the field theory we analyze

comes with a peculiarity. Its symmetry group is a non-compact group, namely $G = \mathrm{SU}(1,1)$, or, after modding out a trivially-acting subgroup, the Lorentz group

$$G' = \mathrm{SU}(1,1)/\mathbb{Z}_2 \cong \mathrm{SO}(1,2). \tag{2.1}$$

While spontaneous symmetry breaking is well understood for the compact case, the non-compact case is more subtle. In a sense, in this work, we aim to better understand the similarities and differences between the two cases. A main insight will be that the emergence of singular continuous spectrum is closely related to the non-compactness of the symmetry group and, correspondingly, the non-compactness of symmetry group orbits. To pursue the goal of investigating the non-compact symmetry-breaking mechanism, we find it useful to formulate it in a general and clean way. This is done in the language of so-called *(extremal) Gibbs states* in infinite volume.

Finally, within the field-theoretical approach, a central tool to study the transition from metallic to insulating states will be harmonic analysis on the two-hyperboloid H^2. The reason for this will become clear in the course of the thesis. In short, the transition from metallic to insulating behavior can be located by investigating the maximal eigenvalue of a linear integral equation; the transition occurs when this eigenvalue reaches magnitude one. The linear equation contains one massive degree of freedom and two symmetry (Goldstone) degrees of freedom. The symmetry degrees of freedom parametrize the two-hyperboloid H^2. To find the corresponding eigenfunctions and eigenvalues, we rely on standard results from harmonic analysis. These are introduced in this final section of the present chapter, Section 2.4.

2.1 Superanalysis

Superanalysis is the generalization of analysis to functions that depend on commuting and anti-commuting (Grassmann) variables. In the field-theoretical treatment of Anderson transitions, it is a standard tool: Using the Wegner-Efetov supersymmetry method, one expresses disorder expectation values of Green's functions as an integral over commuting and anti-commuting variables [23]. For more details on the mathematics presented here, we refer to the standard source, Berezin's book [12]. For overviews of the application of the supersymmetry method to mesoscopic systems, we refer to [22, 23, 32, 41, 90, 104]. In this work, we use superanalysis mostly in the early sections, Sections 3.3, 3.4, 3.5, and supersymmetric localization acts in the background in several steps throughout the whole thesis.

2.1.1 $\mathbb{Z}_2$-graded linear algebra

The setting is a $\mathbb{Z}_2$-graded vector space $V = V_0 \oplus V_1$ over a field $\mathbb{K}$ (here $\mathbb{K} = \mathbb{R}$ or $\mathbb{K} = \mathbb{C}$). The elements in V_0 (V_1) are called even- (odd-) homogeneous. To distinguish between the even and odd elements, one introduces the parity function:

$$V \ni v \to |v| = \begin{cases} 0, & v \in V_0 \\ 1, & v \in V_1, \end{cases} \tag{2.2}$$

and extends it to arbitrary $v \in V$ by linearity. When $V_0 = \mathbb{K}^p$ and $V_1 = \mathbb{K}^q$, we simply write $V = \mathbb{K}^{p|q}$. After studying the elements of $\mathbb{Z}_2$-graded vector spaces, we now introduce the linear maps on V, $\mathrm{End}(V)$. Because of the $\mathbb{Z}_2$ grading of V, they decompose in blocks and inherit a $\mathbb{Z}_2$ grading:

$$\mathrm{End}(V) = \mathrm{End}(V_0 \oplus V_1) \cong \mathrm{End}(V)_0 \oplus \mathrm{End}(V)_1 \ni X = \begin{pmatrix} A & 0 \\ 0 & D \end{pmatrix} + \begin{pmatrix} 0 & B \\ C & 0 \end{pmatrix}. \tag{2.3}$$

Here $A \in \mathrm{End}(V_0)$, $D \in \mathrm{End}(V_1)$ constitute the space of even linear maps, $\mathrm{End}(V)_0$, and $B \in \mathrm{Hom}(V_1, V_0)$, $C \in \mathrm{Hom}(V_0, V_1)$ constitute the space of odd linear maps, $\mathrm{End}(V)_1$.

In this thesis, we make use of the generalization of the trace to $\mathbb{Z}_2$-graded vector spaces, the supertrace

$$\mathrm{STr}_V : \mathrm{End}(V) \to \mathbb{K}, \ \mathrm{STr}_V X = \mathrm{Tr} A - \mathrm{Tr} D, \tag{2.4}$$

where Tr denotes the usual trace of a linear map.

2.1.2 Grassmann variables

In physics literature, so-called supervectors and supermatrices contain Grassmann variables. In the next step, these enter the stage. Let Λ denote a Grassmann algebra over $\mathbb{K}$. Since a general element in Λ consists of even and odd monomials in the generators, Λ is a $\mathbb{Z}_2$-graded vector space: $\Lambda = \Lambda_0 \oplus \Lambda_1$, where Λ_0 (Λ_1) contains even (odd) polynomials in the generators. Starting from the vectors in the graded vector space V, the corresponding supervectors, with entries in Λ, are elements of the tensor product $(\Lambda_0 \otimes V_0) \oplus (\Lambda_1 \otimes V_1) = (\Lambda \otimes V)_0$. In math literature, this space is sometimes called the Grassmann envelope, and it is denoted by $V(\Lambda)$. Next, we construct supermatrices. As we have already seen, the space $\mathrm{End}(V)$ is $\mathbb{Z}_2$-graded, so we can repeat the procedure from above. The Grassmann envelope of $\mathrm{End}(V)$ is denoted by $\mathrm{End}(V)(\Lambda)$ and its elements are supermatrices. They can again be represented in terms of block matrices A, B, C, D. Now the entries of these matrices take values in Λ; in A, D (B, C) the matrix elements are even (odd) in the generators of Λ. The algebra $\mathrm{End}(V)(\Lambda)$ naturally acts on $V(\Lambda)$ and can be identified with the linear maps on $V(\Lambda)$: $\mathrm{End}(V)(\Lambda) \cong \mathrm{End}(V(\Lambda))$. Using this and the fact that $V(\Lambda)$, $\mathrm{End}(V)(\Lambda)$ are $\mathbb{Z}_2$-graded, the notion of supertrace for supermatrices is well-defined. For $V = \mathbb{K}^{p|q}$ one writes $V(\Lambda) \equiv \mathbb{K}^{p|q}(\Lambda)$ and $\mathrm{End}(V)(\Lambda) \equiv \mathrm{End}(\mathbb{K}^{p|q})(\Lambda)$.

Another important operation in linear algebra is the determinant. The generalization to supermatrices is called superdeterminant: For $\mathrm{End}(V)(\Lambda) \ni X$, the superdeterminant is defined as:

$$\mathrm{SDet}(X) = \mathrm{SDet}\begin{pmatrix} A & B \\ C & D \end{pmatrix} = \frac{\mathrm{Det}(A - BD^{-1}C)}{\mathrm{Det}(D)} = \frac{\mathrm{Det}(A)}{\mathrm{Det}(D - CA^{-1}B)}, \tag{2.5}$$

where Det denotes the usual determinant.

To put this subsection into perspective, we mention that the original field variables of our field theory are 4×4 supermatrices with complex variables $u, \bar{u}, v, \bar{v}$, and Grassmann variables $\zeta, \bar{\zeta}, \omega, \bar{\omega}$:

$$\mathcal{Q} = \begin{pmatrix} u \\ v \\ \zeta \\ \omega \end{pmatrix} \otimes \begin{pmatrix} \bar{u} & -\bar{v} & \bar{\zeta} & \bar{\omega} \end{pmatrix}. \tag{2.6}$$

The field theory action contains terms such as $\mathrm{STr}(\mathcal{Q}^2)$.

2.1.3 Superfunctions

Superfunctions are functions that depend on commuting and Grassmann variables. They are defined by a power series expansion in the Grassmann variables. The series will eventually terminate because the generators of the Grassmann algebra square to zero. Here we define superfunctions in the linear setting, where the underlying space is a $\mathbb{Z}_2$-graded vector space $V = V_0 \oplus V_1$. This is sufficient for our purposes. Real- or complex-analytic superfunctions are maps $\mathcal{F} : V_0 \to \Lambda(V_1^*)$, i.e., real- or complex analytic functions on V_0 that take values in the Grassmann algebra over the dual space of V_1. They form an associative algebra, and, as announced above, they can be written as a power series:

$$\mathcal{F}(x) = \sum_{n=0}^{\dim(V_1)} \sum_{i_1<i_2<\ldots<i_n} F_{i_1 i_2 \ldots i_n}(x^1, x^2, \ldots, x^{\dim(V_0)})\, \zeta^{i_1}\zeta^{i_2}\ldots\zeta^{i_n}, \tag{2.7}$$

where $F_{i_1,i_2,\ldots,i_n} : V_0 \to \mathbb{K}$ are real- ($\mathbb{K} = \mathbb{R}$) or complex- ($\mathbb{K} = \mathbb{C}$) analytic functions, x^i are coordinates of V_0, and $\zeta^j \in V_1^*$ are generators of $\Lambda(V_1^*)$.

2.1.4 Berezin integral

How can we generalize the integral over the functions $F_{i_1,i_2,\ldots,i_n}$ to the superfunction setting? The answer is that an additional step is needed to map the superfunction (2.7) to a number. This additional step is the elimination of the Grassmann variables. It is often called fermionic integration, even though, actually, one performs derivatives. It maps the superfunction, which contains the odd generators ζ^j, to a function on V_0. This function is then promoted to a top-degree differential form that can be integrated over V_0 (or an open subset thereof). The fermionic integration makes use of the operation of anti-derivation on $\Lambda(V_1^*)$. Fixing a set of generators $\{\zeta^j\}$, it is simply the partial derivative $\partial/\partial\zeta^j$. It anti-commutes with other partial derivatives $\partial/\partial\zeta^k$ and fulfills the anti-Leibniz rule:

$$\frac{\partial}{\partial\zeta^j}\left(\zeta^k\zeta^l\right) = \delta_j^k\zeta^l - \zeta^k\delta_j^l. \tag{2.8}$$

Now in the fermionic integration Ω_f one performs the derivatives with respect to all ζ^j:

$$\Omega_f[\mathcal{F}] = \text{const.}\frac{\partial}{\partial\zeta^n}\frac{\partial}{\partial\zeta^{n-1}}\ldots\frac{\partial}{\partial\zeta^1}\mathcal{F}. \tag{2.9}$$

Hence we have mapped the superfunction to an ordinary function on V_0. Finally, it gets mapped to a top-degree differential form on V_0. The whole procedure is denoted

by $\Omega_{\text{Ber}}[\mathcal{F}]$. Ω_{Ber} is called Berezin integration form (or Berezin measure).

Example

We look at the example of two real vector spaces $V_0 = V_1$ with $\dim(V_0) = n$. Let x^i be coordinate functions on V_0 and ζ^j be basis vectors of V_1^* (and generators of $\Lambda(V_1^*)$). Then, a Berezin integration form is

$$\Omega_{\text{Ber}} = \mathrm{d}x^1 \wedge \mathrm{d}x^2 \wedge ... \wedge \mathrm{d}x^n \otimes \frac{\partial}{\partial \zeta^n} \frac{\partial}{\partial \zeta^{n-1}} ... \frac{\partial}{\partial \zeta^1}, \tag{2.10}$$

and for a superfunction (2.7) the Berezin integration yields:

$$\int_{V_0} \Omega_{\text{Ber}}[\mathcal{F}] = \int_{V_0} \mathrm{d}x^1 \wedge \mathrm{d}x^2 \wedge ... \wedge \mathrm{d}x^n \, F_{12...n}(x^1, ..., x^n). \tag{2.11}$$

2.1.5 Supersymmetry and supersymmetric localization

Throughout this work, we will encounter superfunctions that possess supersymmetries. In the present section, we simplify the notation by again restricting to the case of two real vector spaces $V_0 = V_1$ with $\dim(V_0) = n$. A supersymmetry is a symmetry generated by an odd vector field Q (realized as a first-order differential operator):

$$Q = \sum_{i=1}^{n} \omega^i(x, \zeta) \frac{\partial}{\partial x^i} + a^i(x, \zeta) \frac{\partial}{\partial \zeta^i}, \tag{2.12}$$

where $\omega^i(x, \zeta)$ is odd in the Grassmann generators ζ^j and $a^i(x, \zeta)$ is even. A superfunction F is called supersymmetric with respect to Q if it vanishes upon Q action:

$$Q[\mathcal{F}] = 0. \tag{2.13}$$

We furthermore assume that Q is a Killing vector field of the Berezin integration form Ω_{Ber}:

$$\text{div}_{\Omega_{\text{Ber}}} Q = 0. \tag{2.14}$$

The divergence $\text{div}_{\Omega_{\text{Ber}}}$ is the obvious generalization of the divergence in the ordinary manifold setting:

$$\int_{V_0} \Omega_{\text{Ber}}[(\text{div}_{\Omega_{\text{Ber}}} Q)\mathcal{F}] = -\int_{V_0} \Omega_{\text{Ber}}[Q[\mathcal{F}]], \tag{2.15}$$

for suitable superfunctions $\mathcal{F}$. A beautiful and, for this work, highly relevant result of the integration theory of supersymmetric superfunctions is the so-called supersymmetric localization theorem. A complete proof of a version similar to the one

we use here is given in [77]. We assume that a superfunction $\mathcal{F}$ has a supersymmetry Q, which additionally is a Killing vector field of the Berezin integration form. Furthermore, we assume that the vector field Q has a discrete zero locus. The zero locus of Q is the subset of V_0 on which the number part of Q (i.e., the terms of Q that remain when all Grassmann variables are set to zero) vanishes. Finally, we assume that the odd vector field Q squares to zero $Q^2 = 0$.

Then the Berezin integral over the superfunction $\mathcal{F}$ localizes on the discrete points contained in the zero locus. To be more precise, for even and Q-invariant superfunctions $\mathcal{G}_0$ whose number part equals one in a small neighborhood around the zero locus and equals zero outside a larger neighborhood, we have

$$\int_{V_0} \Omega_{\mathrm{Ber}}[\mathcal{F}] = \int_{V_0} \Omega_{\mathrm{Ber}}[\mathcal{G}_0 \mathcal{F}]. \tag{2.16}$$

We will not give a proof here, but we present a heuristic argument that goes back to Witten [100]. Locally (away from the zero locus of Q), we can find coordinates such that $Q = \partial/\partial\zeta^i$ for some $i = 1, ..., n$. Now, as $\mathcal{F}$ vanishes upon action of Q, it is independent of ζ^i. We have already learned that fermionic integration is nothing but performing partial derivatives with respect to the Grassmann coordinates ζ^j, so the integral over $\mathcal{F}$ vanishes in the region where we can find coordinates such that $Q = \partial/\partial\zeta^i$. Consequently, the integral over $\mathcal{F}$ vanishes everywhere except for the zero locus of Q (here we obviously cannot find coordinates such that $Q = \partial/\partial\zeta^i$).

Example:

We now look at an example on the graded vector space $\mathbb{R}^{2|2}$. We choose the Berezin measure

$$\Omega_{\mathrm{Ber}} = \frac{\mathrm{d}^2 z}{\pi} \otimes \frac{\partial^2}{\partial\bar{\zeta}\partial\zeta}. \tag{2.17}$$

Let $\mathcal{F}$ be an integrable superfunction of the form:

$$\mathcal{F} = \mathcal{F}(\bar{z}z + \bar{\zeta}\zeta). \tag{2.18}$$

$\mathcal{F}$ has several supersymmetries. One is given by the odd vector field

$$Q = \zeta \frac{\partial}{\partial \bar{z}} - z \frac{\partial}{\partial \bar{\zeta}}. \tag{2.19}$$

Its zero locus is the origin $z = 0$. Obviously, $Q^2 = 0$ is fulfilled. Furthermore, it can be checked that Q is divergence-free when acting on superfunctions whose number parts decay quickly enough at infinity. According to the localization theorem (2.16),

the Berezin integral over $\mathcal{F}$ localizes at the origin $z = 0$. Here we use a slightly modified theorem where we replace the function $\mathcal{G}_0$ by a bump function:

$$\mathcal{G}_0^t = \mathcal{G}_0^t(\overline{z}z + \overline{\zeta}\zeta) = \mathrm{e}^{-t(\overline{z}z+\overline{\zeta}\zeta)}, \quad t \in \mathbb{R}^+. \tag{2.20}$$

Clearly, it is also Q-invariant. The Berezin integral over $\mathcal{F}$ then coincides with the limit:

$$\int_{\mathbb{R}^2} \Omega_{\mathrm{Ber}}[\mathcal{F}] = \lim_{t\to\infty} \int_{\mathbb{R}^2} \Omega_{\mathrm{Ber}}[\mathcal{G}_0^t \mathcal{F}]. \tag{2.21}$$

The integral on the r.h.s. can be calculated:

$$\begin{aligned}
&\lim_{t\to\infty} \int_{\mathbb{R}^2} \Omega_{\mathrm{Ber}}[\mathcal{G}_0^t \mathcal{F}] = \lim_{t\to\infty} \int_{\mathbb{R}^2} \frac{\mathrm{d}^2 z}{\pi} \otimes \frac{\partial^2}{\partial\overline{\zeta}\partial\zeta}\ \mathrm{e}^{-t(\overline{z}z+\overline{\zeta}\zeta)}\ \mathcal{F}(\overline{z}z + \overline{\zeta}\zeta) \\
&= \lim_{t\to\infty} \int_{\mathbb{R}^2} \frac{\mathrm{d}^2 z}{\pi} \otimes \frac{\partial^2}{\partial\overline{\zeta}\partial\zeta}\ \mathrm{e}^{-(\overline{z}z+\overline{\zeta}\zeta)}\ \mathcal{F}\left(\frac{\overline{z}z}{t} + \frac{\overline{\zeta}\zeta}{t}\right) = \mathcal{F}(0) \int_{\mathbb{R}^2} \frac{\mathrm{d}^2 z}{\pi} \otimes \frac{\partial^2}{\partial\overline{\zeta}\partial\zeta}\ \mathrm{e}^{-(\overline{z}z+\overline{\zeta}\zeta)} \\
&= \mathcal{F}(0).
\end{aligned} \tag{2.22}$$

Consequently, supersymmetric localization ensures that the Berezin integral over superfunctions $\mathcal{F} = \mathcal{F}(\overline{z}z + \overline{\zeta}\zeta)$ simply yields its value in $z = 0 = \overline{\zeta} = \zeta$, no matter how complicated the function $\mathcal{F}$ might look.

2.2 Spectral types of self-adjoint operators in infinite volume

One main goal of this thesis is to find a field-theoretical mechanism that describes a singular continuous spectrum of the Wegner Hamiltonian. The present section serves as a reminder of the three spectral types a random discrete Schrödinger operator may have on an infinite lattice $\mathbb{G}$: *absolutely continuous* spectrum (ac), *pure point* spectrum (pp), and *singular continuous* spectrum (sc). The following presentation of the characteristics of the spectral types is based on [6].

A suitable observable to distinguish between the spectral types is the integrated local density of states (ILDOS). In short, they can be characterized as follows:

1. **ac spectrum:** The ILDOS is an absolutely continuous function (actually, smooth in most cases). The corresponding eigenstates are (ergodic) extended and thus are not elements of $\ell^2(\mathbb{G})$. For Anderson-type models, an absolutely continuous spectrum corresponds to the metallic phase.

2. **pp spectrum:** The ILDOS is not a continuous function but a step function. A pure point spectrum consists of the proper eigenvalues of the Schrödinger

operator. The ILDOS jumps as soon as the energy argument meets an eigenvalue. The corresponding eigenstates are localized and are elements of $\ell^2(\mathbb{G})$. For Anderson-type models, a pp spectrum corresponds to the insulating phase.

3. **sc spectrum:** The ILDOS is still a continuous function (jumps are absent) but not absolutely continuous; its derivative is singular and does not exist as a function. A function that undergoes such behavior is the Cantor function, an example of a "devil's staircase". Singular continuous spectrum is typically expected to occur at isolated points (critical points) or in fine-tuned models. In this section, we will see an example of a Hamiltonian that possesses singular continuous spectrum in a wide parameter range.

2.2.1 Spectral representation

Let H be a self-adjoint operator on a Hilbert space $\mathcal{H} = \ell^2(\mathbb{G})$, where $\mathbb{G}$ is an infinite lattice. We use the expression Hamiltonian or Schrödinger operator for H interchangeably. The spectral representation for the mean values of a bounded function f of H, in a normalized state $\psi \in \mathcal{H}$, reads:

$$\langle \psi, f(H)\psi \rangle = \int_{\mathbb{R}} \nu_\psi(\mathrm{d}E)\, f(E). \tag{2.23}$$

$\nu_\psi(\mathrm{d}E)$ is a probability measure on $\mathbb{R}$ that describes the spectral distribution of H in the state ψ. While this definition seems rather abstract at first glance, it is the natural generalization of the finite volume analogue:

$$\langle \psi, f(H)\psi \rangle = \sum_k |\langle \psi_k, \psi \rangle|^2 f(E_k), \tag{2.24}$$

where E_k are the eigenenergies and ψ_k are the corresponding eigenvectors. In simpler words, the subtlety about the infinite-volume limit is related to the fact that the spectrum can consist of more than separated eigenvalues. The infinite-volume version (2.24) reduces to the finite volume version (2.24) in the case of pp spectrum, as will become obvious now.

2.2.2 Spectral measure and its Lebesgue decomposition

The measure $\nu_\psi(\mathrm{d}E)$ is called *spectral measure*. It can be Lebesgue-decomposed into three components

$$\nu_\psi(\mathrm{d}E) = \nu_\psi^{\mathrm{ac}}(\mathrm{d}E) + \nu_\psi^{\mathrm{pp}}(\mathrm{d}E) + \nu_\psi^{\mathrm{sc}}(\mathrm{d}E). \tag{2.25}$$

The ac component of the spectral measure is absolutely continuous with respect to the Lebesgue measure on $\mathbb{R}$. In other words, it possesses a density function $\rho_\psi(E) \in L^1(\mathbb{R})$

$$\nu_\psi^{\mathrm{ac}}(\mathrm{d}E) = \rho_\psi(E)\,\mathrm{d}E. \tag{2.26}$$

The pp component is a sum of point measures on the eigenvalues corresponding to proper (square-summable) eigenfunctions $\psi_k \in \ell^2(\mathbb{G})$:

$$\nu_\psi^{\mathrm{pp}}(\mathrm{d}E) = \sum_k |\langle \psi, \psi_k \rangle|^2\, \delta(E - E_k)\,\mathrm{d}E. \tag{2.27}$$

When inserting (2.27) into the general spectral representation (2.23), we obtain the finite volume version (2.24). Finally, the third component $\nu_\psi^{\mathrm{sc}}(\mathrm{d}E)$ is a singular-continuous measure. It is supported on a set of zero Lebesgue measure, yet it has no atoms (it does not charge single points).

2.2.3 Integrated local density of states

After the rather abstract definitions above, we now focus on the state localized at the lattice site $n \in \mathbb{G}$, $|\psi\rangle = |n\rangle$, and the function $f(H) = \Theta(H - E),\ E \in \mathbb{R}$, where Θ is the Heaviside step-function. Using the spectral representation (2.23) we obtain:

$$I_n(E) = \langle n, f(H) n \rangle = \int_{-\infty}^{E} \nu_n(\mathrm{d}E') \tag{2.28}$$

which is the infinite-volume version of the integrated local density of states at energy E and site n. It can also be expressed in terms of the Green's function

$$G_{n,n'}(z) = \langle n, \frac{1}{z - H} n' \rangle, \tag{2.29}$$

where $z \in \mathbb{C}$ can take values in the upper or lower half plane:

$$I_n(E) = \lim_{\varepsilon \to 0} \int_{-\infty}^{E} \frac{\mathrm{d}E'}{2\pi \mathrm{i}} \Big(G_{n,n}(E' - \mathrm{i}\varepsilon) - G_{n,n}(E' + \mathrm{i}\varepsilon) \Big), \quad \varepsilon > 0. \tag{2.30}$$

From this, it follows that the spectral measure can be associated with the local density of states (LDOS):

$$\nu_n(\mathrm{d}E) = \lim_{\varepsilon \to 0} \frac{\mathrm{d}E}{2\pi \mathrm{i}} \left(G_{n,n}(E - \mathrm{i}\varepsilon) - G_{n,n}(E + \mathrm{i}\varepsilon) \right), \tag{2.31}$$

where the limit is meant in the sense of distributions. With this identification in hand, we use the expressions spectral measure and LDOS interchangeably. We now

relate the three different types of measures in the Lebesgue-decomposition of the spectral measure $\nu_n(\mathrm{d}E)$ to the different behaviors of the ILDOS.

1. **ac spectrum**: The ac component of the spectral measure possesses a density function, $\rho_n(E) \in L^1(\mathbb{R})$. In expression (2.30), limit $\varepsilon \to 0$ and integral can be exchanged. The density function equals:

$$\rho_n(E) = \frac{1}{2\pi \mathrm{i}} \lim_{\varepsilon \to 0} \left(G_{n,n}(E - \mathrm{i}\varepsilon) - G_{n,n}(E + \mathrm{i}\varepsilon) \right). \tag{2.32}$$

   Here the limit is a classical limit, which means that the limit is well-defined as a function. Now

$$I_n(E) = \int_{-\infty}^{E} \rho_n(E') \, \mathrm{d}E'. \tag{2.33}$$

   Because $\rho_n(E) \in L^1(\mathbb{R})$, $I_n(E)$ is an absolutely continuous function.

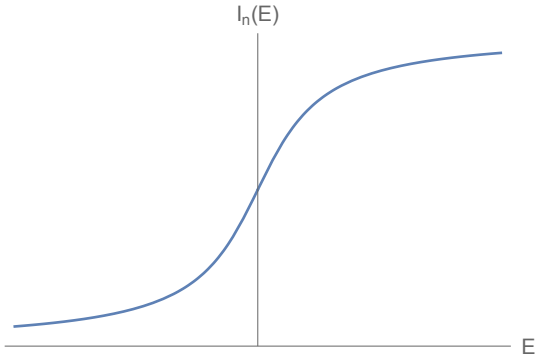

Figure 2.1: A schematic of $I_n(E)$ in the case of ac spectrum. It has an integrable density function and is thus absolutely continuous.

2. **pp spectrum**: The pp component of the spectral measure is a sum of weighted point measures. In other words, the limit

$$\rho_n(E) = \frac{1}{2\pi \mathrm{i}} \lim_{\varepsilon \to 0} \left(G_{n,n}(E - \mathrm{i}\varepsilon) - G_{n,n}(E + \mathrm{i}\varepsilon) \right) \tag{2.34}$$

   only exists in the sense of distributions and yields a sum of weighted delta distributions. When plugging the pp component into (2.28), we obtain a step function:

$$I_n(E) = \sum_{k; E_k \leq E} |\langle n, \psi_k \rangle|^2, \tag{2.35}$$

   where the sum is restricted to eigenstates ψ_k with eigenenergies $E_k \leq E$.

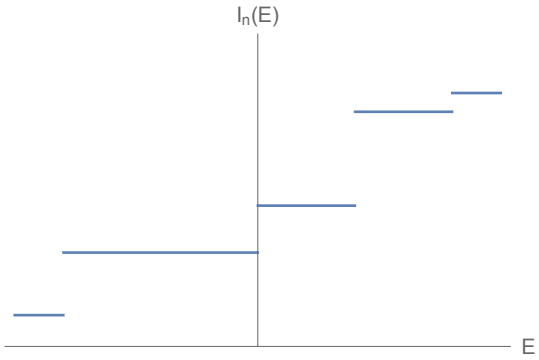

Figure 2.2: A schematic of $I_n(E)$ in the case of pp spectrum. Its density consists of a sum of weighted delta distributions, and thus $I_n(E)$ is a step function.

3. **sc spectrum**: It may happen in principle that $I_n(E)$ is continuous but not absolutely continuous, i.e., one has only the weaker property that there exists a number $\alpha \in (0,1)$ such that

$$\forall \beta \in (0,\alpha] : \lim_{E' \to E} \frac{|I_n(E) - I_n(E')|}{|E - E'|^\beta} = 0. \tag{2.36}$$

As an aside on mathematical terminology, Eq. (2.36) is satisfied by Hölder-continuous functions with Hölder exponent α. Absolute continuity is recovered for $\alpha = 1$. Again, the limit

$$\rho_n(E) = \frac{1}{2\pi \mathrm{i}} \lim_{\varepsilon \to 0} \left(G_{n,n}(E - \mathrm{i}\varepsilon) - G_{n,n}(E + \mathrm{i}\varepsilon) \right) \tag{2.37}$$

only exists in the sense of distributions. However, now the distribution does not charge single points, even though it is supported on a set of Lebesgue measure zero. An example for an sc-type ILDOS is the Cantor function [29], and the corresponding LDOS (the spectral measure) is the distributional derivative of the Cantor function, the Cantor measure. To define the Cantor function, one makes use of the Cantor set C, a subset of the unit interval $[0,1]$. It is the result of the following process: We subdivide the unit interval into three equal intervals $[0,1/3], [1/3,2/3], [2/3,1]$ and remove the middle one. Then we perform the same procedure for the remainder $[0,1/3] \cup [2/3,1]$ and repeat the process ad infinitum. The numbers that have not been removed by this process are the elements of the Cantor set.

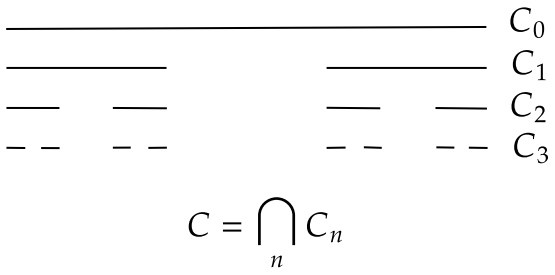

Figure 2.3: The first four iterations of constructing C.

It turns out that every such number has a triadic representation:

$$x = \sum_{k=1}^{\infty} 2x_k \; 3^{-k} \tag{2.38}$$

with $x_i \in \{0, 1\}$ for all i. The Cantor set is uncountable but has Lebesgue measure zero. [It is a fractal with Hausdorff dimension $\ln(2)/\ln(3)$.] The Cantor function is then defined on the Cantor set as

$$f(x) \equiv \sum_{k=1}^{\infty} x_k \; 2^{-k} \tag{2.39}$$

and can be extended to a continuous function $f : [0, 1] \to [0, 1]$:

$$f(y) \equiv \sup \{ f(x); x \in C, x \leq y \} . \tag{2.40}$$

The function so obtained is continuous, but not absolutely continuous. Its derivative exists on $[0, 1] \setminus C$ and it equals zero there, but it is nowhere differentiable on C. The distributional derivative f' defines the Cantor measure, an example of a singular continuous measure:

$$\nu(\mathrm{d}E) = f'(E) \, \mathrm{d}E. \tag{2.41}$$

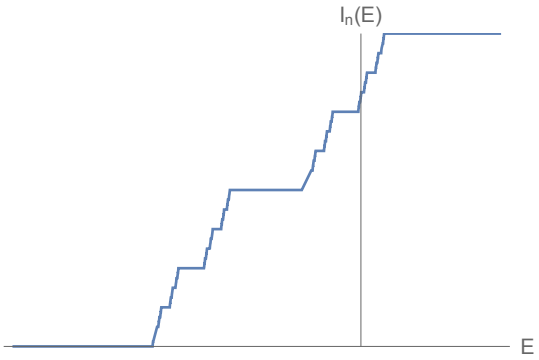

Figure 2.4: A schematic of $I_n(E)$ in the case of sc spectrum, the Cantor function. Its density is a distribution supported on a Lebesgue zero set without charging single points.

2.2.4 Spectral types - Dynamical meaning

Next, we want to relate more concisely the notion of spectral types to the metallic, insulating, and critical structure of the wave function in Anderson transitions. This is quite simple because the spectral measure has an immediate connection to the (time-integrated) probability to find a quantum system that was initiated in a state ψ back in this state at time t. Anticipating that we will analyze a model of Anderson type, we call this probability return probability. Here we again specialize to the state $|n\rangle$. The return probability is given by:

$$\mathrm{Prob}_{n\to n}(t) = \left|\langle n, \mathrm{e}^{-\mathrm{i}tH} n\rangle\right|^2. \tag{2.42}$$

The relation to the spectral measure is an easy consequence of the spectral representation. Indeed, by invoking (2.23) we obtain:

$$\mathrm{Prob}_{n\to n}(t) = \left|\int \nu_n(\mathrm{d}E)\, \mathrm{e}^{-\mathrm{i}tE}\right|^2 = |\hat{\nu}_n(t)|^2, \tag{2.43}$$

where the hat on the right means the Fourier transform of the spectral measure. We again compare the behavior for the three spectral types:

1. **ac spectrum**: We recall that the LDOS is a L^1 function. According to the Riemann-Lebesgue lemma, its Fourier transform vanishes at infinity and thus:

$$\lim_{t\to\infty} \mathrm{Prob}_{n\to n}(t) = 0. \tag{2.44}$$

   In most, if not all, of the physically relevant cases, the LDOS is also an L^2 function: $\rho_n(E) \in L^2(\mathbb{R})$. Using the Plancherel theorem, $|\hat{\nu}_n(t)|^2$ is then integrable and the time-integrated return probability stays finite for infinite times:

$$\lim_{T\to\infty} \int_0^T \mathrm{d}t\ \mathrm{Prob}_{n\to n}(t) < \infty. \tag{2.45}$$

This reflects the fact that the ac-type eigenfunctions are extended: The electron diffuses away from the starting point n fast enough for the time integral (2.45) to converge. More concretely, the states ψ^{ac} corresponding to the ac spectrum leave any finite region around the fixed lattice site n with probability one in the large time limit $t \to \infty$ (they are not recurrent). Absence of recurrence is a property reserved for infinite systems.

2. **pp spectrum**: Now the LDOS is a sum of weighted delta distributions. Consequently, the return probability at time t coincides with the finite volume analogue:

$$\mathrm{Prob}_{n\to n}(t) = \left| \sum_k |\langle n, \psi_k \rangle|^2 \, \mathrm{e}^{-\mathrm{i}tE_k} \right|^2 , \tag{2.46}$$

where E_k are the eigenvalues and ψ_k the corresponding eigenvectors. The return probability is uniformly bounded from below by a positive constant at all times. Hence the time-integrated return probability diverges. For a general spectral measure ν_n, the pp component can be detected by looking at the large time limit of the time-averaged integrated return probability [97]:

$$\lim_{T\to\infty} \frac{1}{T} \int_0^T \mathrm{d}t \; \mathrm{Prob}_{n\to n}(t) = \sum_k \; |\nu_n(\{E_k\})|^2 , \tag{2.47}$$

where again E_k are the discrete eigenvalues, i.e., belong to the pp component of the spectrum. The pp-type eigenfunctions are localized. When the electron is initialized at or near site n, events of nonzero overlap with the state $|n\rangle$ happen again and again *ad infinitum*. In other words, the pp wave functions are confined to a finite region around n for all times t.

3. **sc spectrum**: In the case of sc spectrum, we recall that the integrated local density of states is Hölder continuous with Hölder exponent α. Equivalently, we call the spectral measure ν_n itself uniformly Hölder continuous with exponent $\alpha \in (0,1)$, if for all intervals I with length $|I| < 1$ (in a certain energy regime where sc spectrum is found), one has

$$\nu_n(I) \leq C \, |I|^\alpha , \tag{2.48}$$

where $C < \infty$ is a constant. Again, the pp measure is recovered for $\alpha = 0$ and the ac measure for $\alpha = 1$. Now for sc spectrum the time-integrated return

probability diverges as $T^{1-\alpha}$ in the large time limit [82, 56]:

$$\frac{1}{T}\int_0^T \mathrm{d}t\ \mathrm{Prob}_{n\to n}(t) \leq \frac{c}{T^\alpha}, \tag{2.49}$$

where again $c < \infty$ is a constant. The sc-type eigenfunctions are neither localized nor fully delocalized, but their support is a fractal. The temporal dynamics depopulates the initial site n, but fails to do so quickly enough for the time integral (2.49) to remain convergent for $T \to \infty$. In other words, the eigenfunctions can only show recurrence over vanishing fractions of time in the large time limit $T \to \infty$.

2.2.5 Examples

Here we give examples of Schrödinger operators with absolutely continuous, pure point, and singular continuous spectrum.

1. **ac spectrum**: The standard example of a Schrödinger operator with purely absolutely continuous spectrum is the lattice Laplacian Δ on $\ell^2(\mathbb{Z}^d)$. To show it, one uses Fourier transform $\mathcal{F} : \ell^2(\mathbb{G}) \to L^2([-\pi,\pi]^d)$. For a state ψ and a function f, one obtains:

$$\begin{aligned}&\langle\psi, f(\Delta)\psi\rangle = \langle\mathcal{F}\psi, \mathcal{F}f(\Delta)\mathcal{F}^{-1}\mathcal{F}\psi\rangle = \langle\mathcal{F}\psi, f(\mathcal{F}\Delta\mathcal{F}^{-1})\mathcal{F}\psi\rangle\\ &= \int_{[-\pi,\pi]^d} \frac{\mathrm{d}^d k}{(2\pi)^d}\, |(\mathcal{F}\psi)(k)|^2\ \ f(2\sum_{j=1}^d \cos(k_j)).\end{aligned} \tag{2.50}$$

   By changing coordinates, we obtain:

$$\langle\psi, f(\Delta)\psi\rangle = \int_{\mathbb{R}} \nu_\psi(\mathrm{d}\lambda)\, f(\lambda) \tag{2.51}$$

   where the spectral measure ν_ψ is supported on $[-2d, 2d]$ and obviously is absolutely continuous. The "eigenvectors" of the lattice Laplacian are plane waves:

$$\psi_k(n) = \mathrm{e}^{ik\cdot n},\ k \in [-\pi,\pi]^d,\ n \in \mathbb{G}. \tag{2.52}$$

   They are not elements in $\ell^2(\mathbb{G})$ and are extended over the whole lattice.

2. **pp spectrum**: A simple example of an operator with pp spectrum is a multiplication operator on $\ell^2(\mathbb{G})$, i.e., a real-valued sequence $V \in \ell^\infty(\mathbb{G})$. In this

case:

$$\langle\psi, f(V)\psi\rangle = \sum_{n\in\mathbb{G}} |\psi(n)|^2 f(V(n)) = \int_{\mathbb{R}} \sum_{n\in\mathbb{G}} |\psi(n)|^2 \delta(\lambda - V(n))\,\mathrm{d}\lambda\, f(\lambda). \quad (2.53)$$

From this, we see that the spectral measure is a sum of weighted point measures, and the spectrum is pure point. The eigenvectors are supported on single lattice points:

$$\psi_n(n') = \delta_{nn'}. \quad (2.54)$$

They belong to the space $\ell^2(\mathbb{G})$.

3. **sc spectrum**: As one can anticipate, it is considerably more demanding to come up with an example of an operator with a purely singular continuous spectrum. In many interesting cases, a singular continuous spectrum is associated with critical points. Indeed, in this thesis, we provide strong evidence that the Wegner Hamiltonian exhibits singular continuous spectral behavior at criticality. Nevertheless, there are examples of Hamiltonians that possess a purely singular continuous spectrum. One example is the Fibonacci Hamiltonian, which is relevant to the study of the electronic properties of quasicrystals. It is a Schrödinger operator on $\ell^2(\mathbb{Z})$:

$$H_{\lambda,\omega} = \Delta + V_{\lambda,\omega}, \quad (2.55)$$

where Δ is the lattice Laplacian and V is a multiplication operator, the Fibonacci potential:

$$V_{\lambda,\omega}(n) = \lambda\,\chi_{[1-\alpha,1)}((n\alpha+\omega)\,\mathrm{mod}1). \quad (2.56)$$

Here χ_I is the indicator function on the interval I, $\lambda > 0$ is the coupling constant, $\alpha = (\sqrt{5}-1)/2$ is the frequency, and $\omega \in \mathbb{R}/\mathbb{Z}$ is the phase. It can be shown that the spectrum of the Hamiltonian $H_{\lambda,\omega}$ is independent of the phase ω and for every $\lambda > 0$ is a set of zero Lebesgue measure. At the same time, the Hamiltonian has no proper eigenvalues for all $\lambda > 0$. Hence the Hamiltonian indeed has singular continuous spectrum, a Cantor-type set, and its spectral measures are purely singular continuous, Cantor-type measures [83, 17]. Proving these statements is a hard task that clearly goes beyond the purpose of this introduction. Nevertheless, we try to give some intuition as to why a singular continuous spectrum appears in this model. The deterministic potential $V_{\lambda,\omega}$ exhibits long-range order: it has self-similar patterns that repeat on all scales.

Nevertheless, it is not periodic. In short, the Fibonacci Hamiltonian exactly lies at the sweet spot where two effects balance. The lack of periodicity prevents the wave function from becoming a Bloch-type wave, which would be extended over the whole lattice and would correspond to an ac spectrum. At the same time, the self-similarity at all scales leads to resonances that prevent the wave function from localizing. Consequently, the spectrum is neither ac nor pp, but sc.

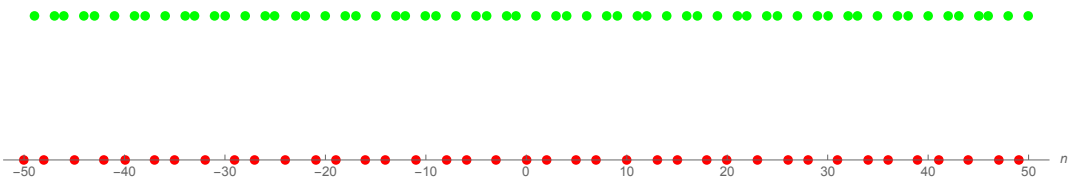

Figure 2.5: The values of the Fibonacci potential $V_{1,0}$ on the sublattice $\mathbb{Z} \cap [-50, 50]$.

We remark that the Anderson or Wegner Hamiltonian consists of both a lattice Laplacian (a hopping term) with purely absolutely continuous spectrum and a multiplication operator, the random potential, with purely pure point spectrum. For vanishing disorder potential, the two models reduce to the lattice Laplacian and thus trivially have an ac spectrum. In the opposite case of vanishing hopping strength, they reduce to the multiplication operator given by the random potential and trivially have a pp spectrum. The combination of both allows for a competition of both operators, enabling a transition between absolutely continuous, pure point, and singular continuous spectrum in different parameter regimes.

2.2.6 Random operators and observable for detection of spectral types

In the final subsection of this section about spectral types of Schrödinger operators, we comment on *random* Schrödinger operators. Until now, we have discussed Schrödinger operators without randomness. Of course, when speaking about Anderson-type transitions, randomness in the Hamiltonian is the central property that simulates the disorder on the lattice. Eventually, we introduce the observable that will be the main object of analysis in this work and motivate why it is suitable to distinguish between the three spectral types.

A random Schrödinger operator H (also called a random Hamiltonian) is a function on a probability space and maps every element from the underlying set, ω, to

a self-adjoint operator, $H(\omega)$, in a common Hilbert space. We restrict ourselves to so-called ergodic operators. For them, the probability distribution of the random Hamiltonians $H(\omega)$ is invariant under a group of measure-preserving graph automorphisms. On $\mathbb{Z}^d$, these are simply the translations. A prominent example is the Anderson Hamiltonian on $\mathbb{Z}^d$:

$$H(\omega) = -\Delta + V(\omega) \tag{2.57}$$

acting in $\ell^2(\mathbb{Z}^d)$. V is a random potential, i.e., a multiplication operator whose values on different lattice sites are independent and identically distributed (iid) and follow a certain probability law. For numerical investigations, one chooses a box distribution, whereas for analytical purposes, a Gaussian distribution is often more suitable. $H(\omega)$ is translation-invariant (for iid random variables $(\omega(i))_{i\in\mathbb{Z}^d}$) and $H(\omega)$ forms a standard ergodic operator.

A theorem that dates back to L. Pastur [67] guarantees that for ergodic operators (such as the Anderson or Wegner Hamiltonian on cubic lattices or also the Bethe lattice) the spectrum of the random Hamiltonian is almost-surely non-random: With probability one it coincides with a fixed set $\Sigma \subset \mathbb{R}$. Furthermore, the same applies to the three spectral components ac, pp, and sc.

The central question now is: What is a good observable that, on the one hand, can be analyzed in our field-theoretic approach and, on the other hand, contains information about the almost-sure spectrum? The answer is given by the expectation values of products of Green's functions. In the light of the discussion in the preceding subsections, a good starting point is the ε-regularized LDOS (its density function):

$$\rho_{n,\varepsilon}(E) = \frac{1}{2\pi\mathrm{i}} \left(G_{n,n}(E - \mathrm{i}\varepsilon) - G_{n,n}(E + \mathrm{i}\varepsilon) \right). \tag{2.58}$$

Now we anticipate that, as in the standard field-theoretical approach to Anderson transitions, our approach also gives access to disorder averages of Green's functions (averages with respect to the distribution of H). Naively, one could hope that the ε-regularized, averaged LDOS $\mathbb{E}(\rho_{n,\varepsilon}(E))$ does the job of distinguishing between the spectral types at energy E (or rather in an arbitrary small interval around E). In some sense, the whole subtlety of the study of Anderson transitions (e.g., the emergence of hyperbolic symmetry in the field theory) is a consequence of the observation that the average LDOS fails to (!) do the job of detecting the spectral type. Indeed, as was first observed by Wegner [94], for sufficiently regular distributions of H (or

V), the mean spectral measure:

$$\nu_n = \mathbb{E}\left[\langle n, P_{(\cdot)}(H)\, n\rangle\right], \tag{2.59}$$

where $P_{(\cdot)}(H)$ denotes the spectral projection, is always absolutely continuous. Consequently, the limit $\varepsilon \to 0$ of the mean $\varepsilon-$regularized LDOS always exists as a function. Here we give a heuristic argument for this observation. For the pp spectrum, the fluctuations of the distribution of the LDOS are maximal; it has heavy tails. When measuring the LDOS at a certain energy E over many copies of the system, where the dynamics is given by the corresponding copy $H(\omega)$, we will typically measure zero LDOS. However, there are rare events where the LDOS will be extremely high; this happens when the corresponding copy of H has an eigenvalue at the energy E. Hence the typical measurement heavily differs from the mean. In contrast, for the ac spectrum, the typically measured value coincides with the mean. The distribution of the LDOS is narrowly peaked around its mean (e.g., a Gaussian distribution), and most measurements will lead to a similar value for the LDOS at energy E. Outliers are extremely rare. In the sc case, the distribution of the LDOS also has heavy tails, but the fluctuations are less strong than for the pp spectrum. It should now be plausible that all cases (pp, ac, sc) lead to a similar mean LDOS because it cannot distinguish between different typical values. To grasp the spectral types and thus to study the Anderson transition, one needs to look at the fluctuations of the distribution of the LDOS.

The second moment of the distribution, $\mathbb{E}(\rho_{n,\varepsilon}^2)$, provides the desired characterization. We will see now that, dependent on the spectral type, it shows different divergencies in the regulator ε for $\varepsilon \to 0$. By again invoking the spectral representation (2.23) for the ε-regularized LDOS we obtain:

$$\rho_{n,\varepsilon}(E) = \int_{\mathbb{R}} \nu_n(\mathrm{d}\lambda)\, \delta_\varepsilon(E-\lambda),\ \delta_\epsilon(x) = \frac{1}{\pi}\frac{\varepsilon}{x^2+\varepsilon^2}. \tag{2.60}$$

Expression (2.60) reveals that for $\varepsilon \to 0$ the ε-regularized LDOS tells us about the spectrum around the energy E:

$$\rho_{n,\varepsilon}(E) \sim \varepsilon^{-1} \int_{E-\varepsilon}^{E+\varepsilon} \nu_n(\mathrm{d}\lambda) = \varepsilon^{-1}\, \nu_n([E-\varepsilon, E+\varepsilon]). \tag{2.61}$$

Accordingly, the quantity $\mathbb{E}(\rho_{n,\varepsilon}^2)$ entails the information about the fluctuations of the spectral measure around E:

$$\mathbb{E}(\rho_{n,\varepsilon}(E)^2) \sim \varepsilon^{-2}\, \mathbb{E}(\nu_n([E-\varepsilon, E+\varepsilon])^2). \tag{2.62}$$

We now argue how the quantity (2.62) scales with ε for $\varepsilon \to 0$ in the three different cases of ac, pp, and sc spectrum at energy E, i.e., the spectrum in arbitrary small intervals $[E-\varepsilon, E+\varepsilon]$, $\varepsilon \to 0$.

1. **ac spectrum**: In the case of ac spectrum, the distribution of the local spectral measure is narrowly peaked, and thus the expectation of ν_n^2 is not much different from its typical value:

$$\mathbb{E}(\nu_n([E-\varepsilon, E+\varepsilon])^2) \sim \nu_n^{\mathrm{typ}}([E-\varepsilon, E+\varepsilon])^2. \tag{2.63}$$

   Typically, due to the lack of heavy tails, one will measure an ac spectrum in the interval $[E-\varepsilon, E+\varepsilon]$. When the ac LDOS is nonzero in this interval, the spectral measure scales with ε:

$$\nu_n([E-\varepsilon, E+\varepsilon]) \sim \varepsilon, \tag{2.64}$$

   which is because the spectral measure has a density function (non-singular). It then follows that $\mathbb{E}(\rho_{n,\varepsilon}(E)^2)$ stays finite for $\varepsilon \to 0$:

$$\mathbb{E}(\rho_{n,\varepsilon}(E)^2) \sim \varepsilon^{-2}\varepsilon^2 = 1. \tag{2.65}$$

2. **pp spectrum**: Now the distribution of the local spectrum measure has heavy tails. The divergence with ε comes from the rare events with very large local spectral measure (when a $\varepsilon-$regularized delta peak of the LDOS sits in the interval $[E-\varepsilon, E+\varepsilon]$). The fluctuations $\mathbb{E}(\nu_n^2)$ can be estimated by the extremal value of $\nu_n([E-\varepsilon, E+\varepsilon])^2$ and the probability that it occurs. The extremal event is when the $\varepsilon-$regularized pp-type LDOS has a peak in E, and in this case:

$$\nu_n([E-\varepsilon, E+\varepsilon]) \sim 1. \tag{2.66}$$

   To estimate the probability of such an event, we remind ourselves that the $\varepsilon-$regularized pp LDOS consists of regularized delta peaks on the energy axis with width $\sim \varepsilon$. Thus the probability that such a peak overlaps with energy E is $\sim \varepsilon$. We then obtain:

$$\mathbb{E}(\rho_{n,\varepsilon}(E)^2) \sim \varepsilon^{-2} \cdot 1^2 \cdot \varepsilon = \varepsilon^{-1}. \tag{2.67}$$

3. **sc spectrum**: Again, the distribution of the local spectral measure has heavy tails and the ε divergence comes from rare events where the $\varepsilon-$regularized sc-type LDOS has a peak in the interval $[E-\varepsilon, E+\varepsilon]$. In contrast to the pp

case, now the spectral measure of this interval still scales with ε because the sc measure does not charge single points:

$$\nu_n([E-\varepsilon, E+\varepsilon]) \sim \varepsilon^{\alpha}, \alpha \in (0,1). \tag{2.68}$$

The peaks of the ε-regularized sc-type LDOS do not diverge "fast enough" in ε to become proper delta peaks for $\varepsilon \to 0$. How can we estimate the scaling of the width of such a peak? The height of it scales with $\varepsilon^{\alpha-1}$. Indeed, when the peak sits in the interval $[E-\varepsilon, E+\varepsilon]$ then

$$\nu_n([E-\varepsilon, E+\varepsilon]) \sim \varepsilon \times \text{height of peak} \sim \varepsilon\, \varepsilon^{\alpha-1} = \varepsilon^{\alpha}. \tag{2.69}$$

Now, for all three spectral types, the integrated LDOS over macroscopic energy intervals in which the spectrum occurs is finite. For that reason, in all three cases, the product of the width and height of a peak needs to be ~ 1. Consequently, the width of a sc-type peak of the $\varepsilon-$regularized LDOS scales as $\sim \varepsilon^{1-\alpha}$. The probability that a peak of the $\varepsilon-$regularized sc-type LDOS overlaps with energy E then also scales as $\sim \varepsilon^{1-\alpha}$. We finally obtain:

$$\mathbb{E}(\rho_{n,\varepsilon}(E)^2) \sim \varepsilon^{-2}\, \varepsilon^{2\alpha}\, \varepsilon^{1-\alpha} = \varepsilon^{-1+\alpha} = \varepsilon^{-\beta},\ \beta = 1-\alpha \in (0,1). \tag{2.70}$$

The preceding discussion assures that the observable $\mathbb{E}(\rho_{n,\varepsilon}(E)^2)$ is suitable to detect the nature of the local spectrum of a random Schrödinger operator at energy E. By analyticity of the Green's function, the terms $\mathbb{E}(G^+G^+)$ and $\mathbb{E}(G^-G^-)$ in $\mathbb{E}(\rho_{n,\varepsilon})^2)$ cannot develop singular behavior for $\varepsilon \to 0$. So we drop them and focus on the informative quantity

$$K_{n,\varepsilon} = \mathbb{E}\left(G_{n,n}(E+\mathrm{i}\varepsilon)\, G_{n,n}(E-\mathrm{i}\varepsilon)\right). \tag{2.71}$$

The correlator (2.71) will be analyzed in our field-theoretical approach. We summarize its behavior for the three different cases in a table:

spectrum	diagnostic	extremal Gibbs states
ac	$K_{n,\varepsilon} \sim 1$	?
pp	$K_{n,\varepsilon} \sim \varepsilon^{-1}$	?
sc	$K_{n,\varepsilon} \sim \varepsilon^{-\beta},\ \beta \in (0,1)$	?

As a teaser, we have added another column to the table 2.2.6. In this thesis, we address the question of which field-theoretical mechanism leads to an sc type scaling of $K_{n,\varepsilon}$. The answer is the novel mechanism of spontaneous symmetry breaking

already announced in the introduction, Table 1.1. A clean way to describe spontaneous symmetry breaking in general field theories is the notion of (extremal) Gibbs states. This will be the subject of the following section.

2.3 (Extremal) Gibbs states and spontaneous symmetry breaking

After providing a detailed introduction to spectral theory and, most importantly, motivating the observable we want to investigate, we now focus on field theory for the first time. Field theory will be our tool to calculate the spectral type. Furthermore, we recall that the key idea of this work is to relate the emergence of singular continuous spectrum to spontaneous symmetry breaking in the presence of a non-compact symmetry group. On the level of observables which can be expressed as field-theoretical expectation values of field operators $\mathcal{O}$, spontaneous symmetry breaking is reflected in the field-theoretical *state* in which the observable is calculated:

$$\langle \bullet \rangle : \text{space of observables} \to \mathbb{R}. \tag{2.72}$$

On a finite sublattice $\Gamma \subset \mathbb{G}$, the state $\langle \bullet \rangle_\Gamma$ is unique when fixing certain boundary conditions. It is defined via the finite-volume statistical weight e^{-S_Γ} and a single-site measure which is promoted to a product measure on the whole finite lattice. Now, when spontaneous symmetry breaking occurs, this uniqueness breaks down in the thermodynamic limit $\Gamma \to \mathbb{G}$. A whole class of symmetry-broken states arises. Observables that themselves break the symmetry can distinguish between the symmetry-broken states; others, which possess the symmetry, are insensitive to which state is spontaneously chosen by the system. Before we proceed, we announce that the observable we focus on, $K_{n,\varepsilon}$, can be represented as a local field operator in our field theory (localized at site n). In consequence, we will only need the restriction of the states to local field operators, localized at an arbitrary but fixed lattice site n. We now formalize this discussion by introducing the notion of (extremal) Gibbs states. For more details, we refer to a pedagogical presentation of the main physical ideas [88], and three standard references [75, 68, 45].

2.3.1 Finite-volume Gibbs state

Here we stick to general notation: We look at a field theory with Hamiltonian function H on an infinite lattice $\mathbb{G}$ and fix a finite sublattice $\Gamma \subset \mathbb{G}$. We assume that the theory in some parameter regimes undergoes spontaneous symmetry breaking

in the thermodynamic limit, which is denoted by $\Gamma \to \mathbb{G}$. The main objects of a field theory, of course, are the fields, which are maps from the lattice to the target space of the field theory. A field configuration is called ω, and the single-site target space is called Ω. The field configuration lives in the product space: $\omega \in \Omega^{\mathbb{G}}$. [This notation simply means that to every lattice site we attach one copy of the single-site target space.]

On the finite sublattice $\Gamma \subset \mathbb{G}$, the restriction of the Hamiltonian to Γ is called H_Γ. We note that the Hamiltonian H_Γ, evaluated on a field configuration ω, $H_\Gamma(\omega)$, depends on the restriction of ω to Γ and the boundary values connected to Γ via the specific interaction of the model (the hopping terms). Note that in general this interaction could be highly non-local, and H_Γ could depend on the restriction to the whole complement ω_{Γ^c}. Nevertheless, we call this restriction "boundary values". The finite-volume Gibbs state is then generated by the finite-volume partition function:

$$Z_\Gamma(\omega_{\Gamma^c}) = \int \prod_{i\in\Gamma} \mathrm{d}\mu(\omega_i) \exp\left(-H_\Gamma(\omega)\right), \tag{2.73}$$

where $\mathrm{d}\mu$ is some a priori measure on the single-site target space Ω. The single-site measure $\mathrm{d}\mu$ is promoted to a measure on Ω^Γ by simply taking the product measure. Examples for the single-site measures could be the Lebesgue measure on $\mathbb{R}^n$ or $\mathbb{C}^n$, the Haar measure on a Lie group, or, for supersymmetric field theories, a Berezin integration form, like in (2.10). Note that after integrating over the field configurations ω_i, $i \in \Gamma$, the expression (2.73) only depends on the field configuration on the complement ω_{Γ^c}. Now from the partition function (2.73) one constructs the finite-volume Gibbs state $\pi_\Gamma(\omega_{\Gamma^c}, \bullet)$ on Γ with boundary condition ω_{Γ^c}. It is a functional on physical observables, i.e., measurable functions $\mathcal{O} : \Omega^{\mathbb{G}} \to \mathbb{R}$:

$$\pi_\Gamma(\omega_{\Gamma^c}, \mathcal{O}) = \frac{1}{Z_\Gamma(\omega_{\Gamma^c})} \int \prod_{i\in\Gamma} \mathrm{d}\mu(\omega_i)\, \mathcal{O}(\omega) \exp\left(-H_\Gamma(\omega)\right). \tag{2.74}$$

2.3.2 Infinite-volume Gibbs states

Clearly, the Gibbs state in finite volume 2.74 is unique. A quick way to see that the thermodynamic limit is subtle is the fact that the Hamiltonian function $H_{\mathbb{G}}$ is only defined symbolically for infinite lattices. It diverges for almost all field configurations. Nevertheless, one can describe Gibbs states on the full configuration space $\Omega^{\mathbb{G}}$. The traditional way (and also the way we will use in the present work) is to define the Gibbs states on $\mathbb{G}$ as a weak limit (in a suitable topology) $\Gamma \to \mathbb{G}$ of the finite-volume states (2.74), the *thermodynamic limit*.

As announced above, in general, the infinite-volume Gibbs states are not unique.

This is at the heart of the spontaneous symmetry breaking mechanism. What is then the structure of the set of infinite-volume Gibbs states?

2.3.3 Structure of the set of infinite-volume Gibbs states and their selection

We call the set of infinite volume Gibbs states $\mathcal{G}(\Pi)$. Π denotes the family of the finite volume states $\{\pi_\Gamma\}_{\Gamma\subset\mathbb{G}}$. $\mathcal{G}(\Pi)$ is a convex space. This means that every convex combination of two Gibbs states is again a Gibbs state. The states that cannot be written as a nontrivial convex combination of other ones are called *extremal Gibbs states*. Furthermore, any non-extremal Gibbs state can be written as a convex combination of extremal ones, and this combination is unique, thus $\mathcal{G}(\Pi)$ is a simplex. Physically, the non-extremal Gibbs states represent a preparation of a randomly chosen extremal Gibbs state. The probabilities are the coefficients of the convex combination. Their significance is that they reflect a lack of knowledge of the "experimenter" of the system's macrostate [88]. The system itself is in a well-defined macrostate given by an extremal Gibbs state.

Now, in the phase where spontaneous symmetry breaking is absent, the space $\mathcal{G}$ for fixed parameter values consists of a single element. This element is the fully symmetric Gibbs state. Obviously, it is extremal.

The situation changes when spontaneous symmetry breaking occurs. Now there are several distinct extremal Gibbs states for fixed parameter values that break the symmetry. They can be transformed into each other by a symmetry transformation. Of course, the symmetric Gibbs state still exists, but it is not extremal anymore. It can be written as a convex combination of extremal (symmetry-broken) Gibbs states.

Finally, we state two options of how one can select a specific extremal Gibbs state in the presence of spontaneous symmetry breaking. One option is to impose certain collective boundary conditions in Γ^c which mimic the anticipated macrostates ("alignment" of all fields). The second option is to add an explicit symmetry-breaking term to the field theory, which is sent to zero after (!) performing the thermodynamic limit of finite-volume Gibbs states. This second option is often seen in physics literature. For instance, in the field theory for the Ising model, one adds a small magnetic field h to the field theory action that breaks the $\mathbb{Z}_2$-symmetry and aligns all the spins. It is sent to zero after performing the thermodynamic limit. Also, in the present work, we will sometimes encounter explicit symmetry-breaking terms in the action. The symmetry-breaking "fields" are denoted by $\widetilde{\varepsilon}, \widetilde{\delta}$.

2.3.4 Examples

To finish this interlude on the theory of Gibbs states, we give two short examples. The prototype example is the Ising model on $\mathbb{Z}^d$, $d \geq 2$. At low temperature, $\mathbb{Z}_2$ spontaneous symmetry breaking occurs [65] and there are two distinct extremal Gibbs states $\langle\bullet\rangle^+$ (spin up) and $\langle\bullet\rangle^-$ (spin down) [37]. A general Gibbs state is the convex combination

$$\langle\bullet\rangle = t\,\langle\bullet\rangle^+ + (1-t)\,\langle\bullet\rangle^-, \quad 0 \leq t \leq 1. \tag{2.75}$$

For the $\mathbb{Z}_2$ symmetric state, one chooses $t = 1/2$.

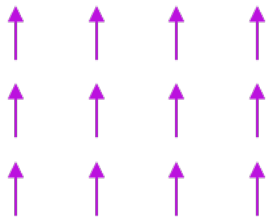

Figure 2.6: Sketch of (an extract of) a typical field configuration in the extremal Gibbs state $\langle\bullet\rangle_+$.

An example with a continuous but compact symmetry group is the SO(3) Heisenberg antiferromagnet on $\mathbb{Z}^d$, $d \geq 3$. At low temperature, the symmetry is spontaneously broken [21] and the Gibbs states are non-unique. The set of extremal Gibbs states can be identified with the order parameter space, the unit sphere S^2. Each extremal Gibbs state $\langle\bullet\rangle_{\mathbf{n}}$ exhibits long-range Néel order with magnetization pointing along the unit vector $\mathbf{n}$. Any other Gibbs state is again a convex mixture of the extremal ones:

$$\langle\bullet\rangle_\mu = \int_{S^2} \mathrm{d}\mu(\mathbf{n})\,\langle\bullet\rangle_{\mathbf{n}}, \tag{2.76}$$

where μ is an arbitrary probability measure on S^2. For the fully symmetric state, one chooses the Haar measure on S^2.

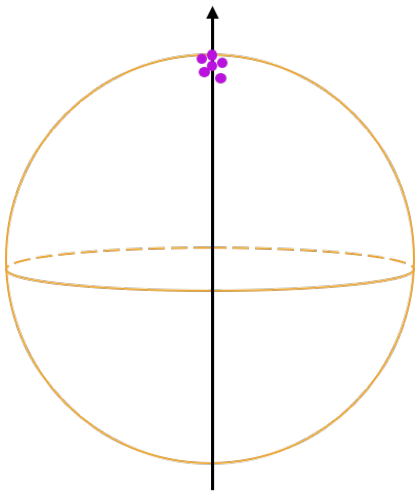

Figure 2.7: Sketch of a typical field configuration in the extremal Gibbs state $\langle\bullet\rangle_{\mathbf{n}=\mathbf{e}_z}$. The field clusters around the north pole of S^2.

One purpose of the present work is to generalize the compact case, such as the example above, to a non-compact situation where the symmetry group is the non-compact group $\mathrm{SU}(1,1)$.

2.4 Harmonic analysis on H^2

In this final section of the introductory chapter, Chapter 2, we review several aspects of harmonic analysis on the two-hyperboloid H^2. As announced above, these will be needed in our approach to studying the transition of the Wegner model. Concretely, the basic results presented in this section are needed in Sections 5.1 and 5.2.

Harmonic analysis is the generalization of Fourier theory on $\mathbb{R}^n$ to symmetric spaces $S \cong G/K$. Here G is a connected Lie group that acts transitively on the manifold S, and K is the isotropy group of a point $x \in S$. H^2 can be identified with the quotient of the symmetry group, $\mathrm{SU}(1,1)$, by its maximal compact subgroup $K = \mathrm{U}(1)$:

$$H^2 \cong \mathrm{SU}(1,1)/\mathrm{U}(1). \tag{2.77}$$

The defining property of a locally symmetric space is that geodesic reflections at any point $x \in S$ are local isometries. Equivalently, the covariant derivative of the curvature tensor vanishes on S. This leads to the intuitive characterization: "The geometry on a symmetric space looks the same everywhere". The locally symmetric space S is called globally symmetric iff the geodesic reflections extend to global isometries. H^2 is an example of a non-compact globally symmetric space.

The goal of harmonic analysis is to expand L^2 functions in terms of a generalized Fourier basis. The basis consists of so-called spherical functions, a certain class of eigenfunctions of the G-invariant Laplace operator. It is quite obvious that harmonic analysis is a strong tool. Analogously to how Fourier theory is used on $\mathbb{R}^n$ to study translation-invariant operators, harmonic analysis on symmetric spaces can be used to study G-invariant operators. Because in this thesis we only need the specific case of the two-hyperboloid, we will not delve deeper into the abstract theory, but derive the Fourier basis in a quite elementary manner here. We refer the interested reader to two standard sources on symmetric spaces [43] and harmonic analysis on them [44].

2.4.1 H^2 as a Riemannian manifold and Laplace-Beltrami operator

We define the two-hyperboloid, H^2, as a manifold embedded into the three-dimensional Minkowski space $\mathbb{R}^{1,2}$ with Cartesian coordinates x_0, x_1, x_2:

$$H^2: \quad -x_0^2 + x_1^2 + x_2^2 = -1 \tag{2.78}$$

and Minkowski metric:

$$g = -\mathrm{d}x_0^2 + \mathrm{d}x_1^2 + \mathrm{d}x_2^2. \tag{2.79}$$

For the present purpose, a suitable coordinate system is given by hyperbolic polar coordinates:

$$\begin{aligned} &i^*x_0 = \cosh(\theta), \quad i^*x_1 = \sinh(\theta)\cos(\phi), \\ &i^*x_2 = \sinh(\theta)\sin(\phi), \quad \theta \in \mathbb{R}^+, \phi \in (0, 2\pi), \end{aligned} \tag{2.80}$$

where θ is the hyperbolic radius and ϕ the hyperbolic angle. We equip H^2 with a metric via pullback: i^*g, where $i : H^2 \to \mathbb{R}^{1,2}$ is the inclusion map. The pullback metric is Riemannian and, in hyperbolic polar coordinates, takes the form:

$$i^*g = \mathrm{d}\theta^2 + \sinh(\theta)^2\,\mathrm{d}\phi^2. \tag{2.81}$$

Next, with the metric, we can construct the Laplace-Beltrami operator:

$$L_{H^2} = \frac{1}{\sqrt{\mathrm{Det}g}}\,\partial_i \sqrt{\mathrm{Det(g)}}\, g^{ij}\,\partial_j = \frac{\partial^2}{\partial\theta^2} + \frac{\cosh(\theta)}{\sinh(\theta)}\frac{\partial}{\partial\theta} + \frac{1}{\sinh(\theta)^2}\frac{\partial^2}{\partial\phi^2}, \tag{2.82}$$

where the sum convention is used.

2.4.2 Spectrum and eigenfunctions of Laplacian

The next step is to look for eigenfunctions φ_λ of the Laplacian (2.82):

$$L_{H^2}\,\varphi_\lambda = -\gamma\,\varphi_\lambda, \quad \gamma \in \mathbb{R}^+. \tag{2.83}$$

It is natural to separate variables and look for the eigenfunctions in different U(1)-sectors:

$$\varphi_\lambda(\theta, \phi) = \sum_{n\in\mathbb{Z}} \varphi_{n,\lambda}(\theta)\,\mathrm{e}^{in\phi}, \tag{2.84}$$

where $\varphi_{n,\lambda}$ fulfills the reduced equation:

$$\left(\frac{\partial^2}{\partial\theta^2}+\frac{\cosh(\theta)}{\sinh(\theta)}\frac{\partial}{\partial\theta}-\frac{n^2}{\sinh(\theta)^2}\right)\varphi_{n,\lambda}(\theta)=-\gamma\,\varphi_{n,\lambda}(\theta). \tag{2.85}$$

To find the spectrum of the Laplacian, we go to the asymptotic limit $\theta \gg 1$, where Eq. (2.85) reduces to a translation-invariant differential equation:

$$\left(\frac{\partial^2}{\partial\theta^2}+\frac{\partial}{\partial\theta}+\gamma\right)\varphi_{n,\lambda}(\theta)=0 \tag{2.86}$$

with eigenfunctions $\exp(\alpha\theta)$ and

$$\alpha=-\frac{1}{2}\pm\sqrt{\frac{1}{4}-\gamma}. \tag{2.87}$$

Eq. (2.87) shows that the spectrum is gapped:

$$\gamma=\frac{1}{4}+\lambda^2,\quad \lambda\in\mathbb{R}. \tag{2.88}$$

The reason is that the "good" eigenfunctions are given by a generalization of plane waves, so-called spherical functions. Analogous to Fourier theory in $\mathbb{R}^n$, their density $|\varphi_{n,\lambda}|^2$ needs to compensate for the growth of the Riemannian measure. Only then can they be utilized to obtain a well-defined pairing with $L^2(H^2)$ functions and consequently serve as a suitable Fourier basis. Because the measure for $\theta \gg 1$ grows as $\sim\exp(\theta)$ the functions $\varphi_{n,\lambda}$ need to decay as $\sim\exp(-\theta/2)$. With this observation, we conclude that

$$\alpha\in-\frac{1}{2}+\mathrm{i}\mathbb{R}. \tag{2.89}$$

Now with the information about the spectrum, we continue with deriving an expression for $\varphi_{0,\lambda}$, $\varphi_{\pm1,\lambda}$ for arbitrary θ (in this thesis, we only need these functions). This is done by mapping (2.85) to the associated Legendre equation. Indeed, by transforming $x=\cosh(\theta)$ we obtain:

$$\begin{gathered}\left(\left(1-x^2\right)\frac{\partial^2}{\partial x^2}-2x\frac{\partial}{\partial x}+\left(l(l+1)-\frac{n^2}{1-x^2}\right)\right)\varphi_{n,\lambda}(x)=0,\\ l(l+1)=-\left(\lambda^2+\frac{1}{4}\right).\end{gathered} \tag{2.90}$$

This equation is solved by the associated Legendre functions (more precisely, conical functions):

$$\varphi_{n,\lambda}(\theta)=P^n_{-\frac{1}{2}-\mathrm{i}\lambda}(\cosh(\theta)). \tag{2.91}$$

2.4.3 Integral identity for certain spherical functions and their asymptotic behavior

In this work, we will make use of two important integral identities [44], which we state here without proof:

$$\begin{aligned}\varphi_{0,\lambda}(\theta) &= \int_0^{2\pi} \frac{\mathrm{d}\phi}{2\pi} \frac{1}{(\cosh(\theta)+\sinh(\theta)\cos(\phi))^{\frac{1}{2}+\mathrm{i}\lambda}} \\ \varphi_{\pm 1,\lambda}(\theta) &= \int_0^{2\pi} \frac{\mathrm{d}\phi}{2\pi} \frac{\cos(\phi)}{(\cosh(\theta)+\sinh(\theta)\cos(\phi))^{\frac{1}{2}+\mathrm{i}\lambda}}.\end{aligned} \tag{2.92}$$

Finally, we derive the asymptotic behavior $\theta \gg 1$ for the functions $\varphi_{\pm 1,\lambda}$. For $\lambda = 0$, this can be rather easily done by making use of the above integral representation, Eq. (2.92). Noting that the dominant contribution comes from the region $\phi \approx \pi$, we expand, and end up with the standardized integral

$$\varphi_{\pm 1,0}(\theta) \sim -\mathrm{e}^{-\frac{\theta}{2}} \int_{-\mathrm{e}^{2\theta}}^{\mathrm{e}^{2\theta}} \mathrm{d}x \, \frac{1}{(1+x^2)^{\frac{1}{2}}} \sim -\mathrm{e}^{-\frac{\theta}{2}} \operatorname{arsinh}(\mathrm{e}^{2\theta}) \sim -\mathrm{e}^{-\frac{\theta}{2}}\, \theta. \tag{2.93}$$

For $\lambda \neq 0$ a similar asymptotic analysis yields two summands, an "incoming" wave $\sim \mathrm{e}^{-\frac{\theta}{2}} \mathrm{e}^{\mathrm{i}\lambda\theta}$, and an "outgoing" wave $\sim \mathrm{e}^{-\frac{\theta}{2}} \mathrm{e}^{-\mathrm{i}\lambda\theta}$. To obtain the correct coefficients (up to global factors), we need to be more careful and go back to the full equation, Eq. (2.91). Using an identity between the conical and hypergeometric functions, and the asymptotic expansion for the hypergeometric functions [64], we end up with:

$$\varphi_{\pm 1,\lambda}(\theta) \sim c_1(\lambda)\, \mathrm{e}^{-\frac{\theta}{2}} \mathrm{e}^{\mathrm{i}\lambda\theta} + c_1(-\lambda)\, \mathrm{e}^{-\frac{\theta}{2}} \mathrm{e}^{-\mathrm{i}\lambda\theta}, \quad c_1(\lambda) = \frac{\Gamma(\mathrm{i}\lambda)}{\Gamma(-\frac{1}{2}+\mathrm{i}\lambda)}. \tag{2.94}$$

We mention in passing that the factor $c_1(\lambda)$ is a Harish-Chandra-c-function for the symmetric space $H^2 \cong \mathrm{SU}(1,1)/\mathrm{U}(1)$.

The asymptotic expression (2.94) will be needed in the analysis in chapter 5, Section 5.2. We will there be interested in the case where $|\lambda| \ll 1$. Using the small argument expansion for the Gamma function

$$\Gamma(\mathrm{i}\lambda) \sim \frac{1}{\mathrm{i}\lambda} - \gamma, \tag{2.95}$$

where γ is the Euler constant, and

$$\frac{1}{\Gamma(-\frac{1}{2}+\mathrm{i}\lambda)} \sim -\frac{1}{2\sqrt{\pi}} \left(1 - \mathrm{i}\lambda(2-\gamma-2\ln(2))\right), \tag{2.96}$$

we obtain

$$\varphi_{\pm 1,\lambda}(\theta) \sim \mathrm{e}^{-\frac{\theta}{2}} \left(-\frac{1}{\lambda} \sin(\lambda\theta) + a\cos(\lambda\theta) \right) \sim -\frac{\mathrm{e}^{-\frac{\theta}{2}}}{\lambda} \sin(\lambda\theta - a\lambda), \tag{2.97}$$

where $a = 2 - 2\ln(2)$.

3 Wegner model, AAT equations, and spontaneous symmetry breaking

After the chapter on the mathematical and physical framework, we are now in a position to initiate the demonstration of the novel symmetry-breaking mechanism for Anderson transitions in high dimensions. The underlying microscopic model is the Wegner $N = 1$-orbital model, defined below. In contrast to the Anderson model, the hopping amplitudes are also random variables in the Wegner model. We begin by deriving the self-consistent equations for the advanced and retarded Green's functions [1], called AAT equations, and we combine both Green's functions in terms of a matrix Green's function, Section 3.2. Finding the Green's functions provides access to our observable of interest, $K_{n,\varepsilon} = \mathbb{E}(|G_{n,n}(E+\mathrm{i}\varepsilon)|^2)$. The self-consistent equations are recursive equations on an infinite lattice, and as such, the solutions may undergo spontaneous symmetry breaking. We will explain in detail how to account for the possibility of spontaneous symmetry breaking by enlarging the solution space of the matrix Green's functions containing the retarded and advanced Green's functions.

Field theory enters the stage by passing from the distribution of the matrix Green's function to its *Fourier-Laplace transform*, Section 3.3. It is a function, $Y(Q)$, of a matrix, which will become the field variable of the field theory. The self-consistent equation for the matrix Green's function naturally extends to a self-consistent integral equation for the Fourier-Laplace transform (3.50). We call it AAT integral equation. Because symmetry breaking may occur at the level of the matrix Green's function, it may also occur at the level of the function $Y(Q)$.

In the following part of this chapter, Section 3.4, we connect the solutions $Y(Q)$ to extremal Gibbs states of the field theory, restricted to local observables. In simple words, the function Y is the result of integrating the statistical weight of the field theory over all sites, except for the distinct site of the operator insertion, say $n \in \mathbb{G}$. This observation connects the rather abstract symmetry-breaking mechanism at the

level of the self-consistent equation for the matrix Green's function or its Fourier-Laplace transform to the well-known fact that in field theories, there may be a large class of different extremal Gibbs states.

After clarifying these connections, we have a clear quest: To analyze the AAT integral equation and to find the symmetry properties of the solutions $Y(Q)$ in different parameter regimes. In consequence, the present chapter lays the groundwork for the Chapters 4,5 that follow.

3.1 The model

We remind the reader that the random Hamiltonian of the Wegner 1-orbital model is given by:

$$H = \sum h_{n,n'} c_n^\dagger c_{n'}, \tag{3.1}$$

where the sum is over the sites n, n' of $\mathbb{G}$. Although H is presented here in basis-independent form using particle creation and annihilation operators, we will analyze it as an operator (h) on the single-particle Hilbert space $\ell^2(\mathbb{G})$. Hence the spectral theory developed in a framework section, Section 2.2.6, holds for this operator.

All Hamiltonian matrix elements are taken to be complex Gaussian independent random variables (subject to the Hermiticity condition $\overline{h_{n,n'}} = h_{n',n}$) with zero mean and variance

$$\mathbb{E}\left(h_{n,n'} h_{l,l'}\right) = \delta_{nl'}\delta_{n'l}\left(\delta_{nn'} w_V^2 + A_{nn'} w_T^2\right), \tag{3.2}$$

where

$$A_{nn'} = A_{nn'}(1-\delta_{nn'}) = A_{n'n} \in \{0,1\} \tag{3.3}$$

is the adjacency matrix of the graph $\mathbb{G}$. The parameter w_V^2 sets the scale of variation of the on-site potentials $h_{n,n} \equiv V_n$, and is called diagonal disorder strength. w_T^2 sets the kinetic-energy scale for hopping between nearest-neighbor pairs and is sometimes called off-diagonal disorder strength or simply hopping strength. Officially known as the Wegner N-orbital model of symmetry class A with $N = 1$ (i.e. a single orbital per site), the model so defined [96] will be referred to simply as the "Wegner model". Our interest is in the almost-sure spectral type of the Wegner Hamiltonian, mostly in the regime of strong diagonal disorder, $w_V^2 \gg w_T^2$, on a regular graph $\mathbb{G}$ with high coordination number $K+1$.

By the probability law (3.2), the ensemble of Hamiltonians (3.1) is invariant under local U(1) phase rotations

$$c_n^\dagger \mapsto c_n^\dagger \mathrm{e}^{\mathrm{i}\alpha_n}, \quad c_{n'} \mapsto \mathrm{e}^{-\mathrm{i}\alpha_{n'}} c_{n'}. \tag{3.4}$$

This property, while not shared by the Anderson model on the lattice scale (where the hopping matrix elements are non-random and constant), is expected to emerge [69] under renormalization on large length scales in the metallic regime (and probably beyond). Its attractive feature is that it facilitates the introduction of matrix variables in the field-theoretical approach.

What can be said at first glance about the local spectrum of the random Hamiltonian (3.1) at energy E in a high lattice dimension? First of all, a high lattice dimension means that there are many paths for the electron to escape to infinity, and that the time-integrated return probability tends to stay finite. Accordingly, the random Hamiltonian (3.1) has an ac spectrum for moderate diagonal disorder, and the system is in the metallic phase. To compensate for this high-dimensional effect, the diagonal disorder strength has to be strong in comparison to the hopping strength (actually $w_V/w_T \gg K$ for energies near the band center $E = 0$). In this limit, the diagonal terms in the sum 3.1 dominate. H approaches a multiplication operator on $\ell^2(\mathbb{G})$, which possesses pp spectrum. The system is then in the insulating phase.

We expect the sc spectrum to emerge in the intermediate (critical) regime $w_V/w_T \sim K$.

3.2 AAT self-consistency equation for Green's functions

In the introductory section, Section 2.2.6, we motivated that a suitable observable for detecting the spectral type is given by the quadratic fluctuations of the distribution of the $\varepsilon-$regularized LDOS at energy E, $\mathbb{E}(\rho_{n,\varepsilon}^2)$. Also, we have argued that the ε-scaling for the different spectral types comes from the correlator:

$$K_{n,\varepsilon} = \mathbb{E}(G_{n,n}(E+\mathrm{i}\varepsilon)\, G_{n,n}(E-\mathrm{i}\varepsilon)). \tag{3.5}$$

We now begin with the analysis of the observable $K_{n,\varepsilon}$. The natural first question is how we can calculate Green's functions of the Wegner Hamiltonian and their disorder expectation values in principle. What helps us here is the fact that we work in a high lattice dimension. We will see that in this regime, we can write down a recursion equation, the AAT self-consistency equation, for the Green's function. In short, the reason is that for increasing lattice dimension, the approximation of the infinite lattice by an infinite tree-like lattice, the Bethe lattice, becomes more and more accurate. The existence of loops in high dimensions is expected to become less

relevant [84], and the Bethe lattice is the limit where loops are completely absent.

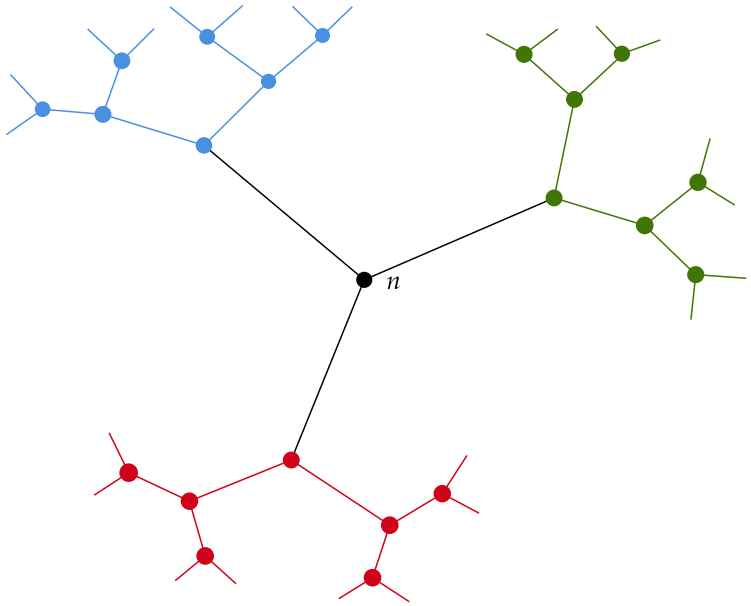

Figure 3.1: An excerpt of the Bethe lattice with coordination number $K+1=3$. The distinct site n, where the observable $K_{n,\varepsilon}$ is evaluated, is located at the center. Removing the site n disconnects the lattice into three independent subtrees (blue, green, red). On the infinite tree lattice, removing the root of one of these subtrees leaves $K=2$ isomorphic subtrees.

3.2.1 Retarded Green's function

To begin, we look at the first factor in $K_{n,\varepsilon}$, the retarded Green's function, $G = G(E+\mathrm{i}\varepsilon) \equiv G^{+}$. We remind the reader that for any real energy E, it is defined by

$$\sum_{n}(E+\mathrm{i}\varepsilon-h)_{n_1,n}\,G_{n,n_2} = \delta_{n_1 n_2}\,. \tag{3.6}$$

Here, as usual, ε is a positive real number shifting the Green's function poles into the lower half of the complex energy plane.

Schur complement

We first derive an equation which relates the diagonal element $G_{n,n} \equiv G_n$ of the retarded Green's function on the full lattice to the retarded Green's function on the lattice with the distinct site n omitted, $\mathbb{G}\setminus\{n\}$. This equation is a direct consequence

of the Schur complement formula for block matrices:

$$M = \begin{pmatrix} A & B \\ C & D \end{pmatrix}, \tag{3.7}$$

where A is a $p \times p$, B a $p \times q$, C a $q \times p$, and D a $q \times q$ matrix. We order

$$E + \mathrm{i}\varepsilon - h = \begin{pmatrix} E + \mathrm{i}\varepsilon - h_{n,n} & \tilde{h}^\dagger \\ \tilde{h} & E + \mathrm{i}\varepsilon - h' \end{pmatrix}, \tag{3.8}$$

where $\tilde{h}$ denotes the vector with entries $h_{n',n}$, $n' \neq n$, and h' denotes the Hamiltonian matrix restricted to the subspace $\ell^2(\mathbb{G} \setminus \{n\})$. The upper left entry of the inverse matrix, G_n, is given by the reciprocal of the Schur complement of the block $D = E + \mathrm{i}\varepsilon - h'$:

$$G_n = (A - BD^{-1}C)^{-1}, \tag{3.9}$$

or

$$\frac{1}{G_n} = A - BD^{-1}C = E + \mathrm{i}\varepsilon - h_{n,n} - \sum_{n_1,n_2(\neq n)} h_{n,n_1} G'_{n_1,n_2} h_{n_2,n}. \tag{3.10}$$

Eq. (3.10) thus follows from simple linear algebra and holds generally. Next, we focus on high dimensions and adopt an approximation.

AAT approximation

The following approximation scheme was introduced by Abou-Chacra, Anderson, and Thouless [1]. It is exact when loops are completely absent; in this case, the underlying lattice is the Bethe lattice $\mathbb{G} = \mathbb{B}$. In the following, we explain the "approximation" on the Bethe lattice, starting from Eq. (3.10). The rightmost term contains the restricted Green's function G'_{n_1,n_2}. Because h contains only diagonal and nearest neighbor interaction terms, the indices n_1, n_2 are restricted to the nearest neighbors of the distinct site n. From the absence of loops, it follows that for different nearest neighbors $n_1 \neq n_2$, the electron can only hop from n_1 to n_2 (or vice versa) by passing through the site n (see Fig. 3.1). Because the operator G' acts on the Hilbert space with site n removed, $G'_{n_1,n_2} = 0$ for different nearest neighbors $n_1 \neq n_2$. This observation reduces the right sum to

$$\sum_{n_1,n_2(\neq n)} h_{n,n_1} G'_{n_1,n_2} h_{n_2,n} \to \sum_{n'(\neq n)} |h_{n,n'}|^2 G'_{n'}. \tag{3.11}$$

Next, we repeat the Schur complement argument for the random variable $G'_{n'}$. While the sum on the right-hand side of Eq. (3.11) contains $K+1$ terms ($K+1$ is the coor-

dination number of the graph), the sum on the r.h.s. of the corresponding equation for $G'_{n'}$ contains only K terms. On the infinite lattice (in the thermodynamic limit), the tree section, disconnected from site n, with root at site n', and the one with root at site n'', disconnected from the site n', become indistinguishable. The corresponding subtrees are isomorphic. Here n'' denotes a nearest neighbor of the site n', except for the site n. In consequence, the probability laws of $G'_{n'}$ and $G''_{n''}$ (the Green's function on the Hilbert space with sites n, n' removed) are the same. In the thermodynamic limit, we thus obtain a fixed-point equation for the Green's function G':

$$\frac{1}{G'_{n'}} \stackrel{!}{=} E + \mathrm{i}\varepsilon - h_{n',n'} - \sum_{n''(\neq n')} |h_{n',n''}|^2 G'_{n''}. \tag{3.12}$$

Eq. (3.12) is called the AAT self-consistency equation. The notation $\stackrel{!}{=}$ is to say that both sides, as random variables, obey the same probability laws. In the final step, the solution of Eq. (3.12) is then plugged into the Schur complement equation for G_n:

$$\frac{1}{G_n} = E + \mathrm{i}\varepsilon - h_{n,n} - \sum_{n'(\neq n)} |h_{n,n'}|^2 G'_{n'}. \tag{3.13}$$

We remind the reader once more that on a cubic lattice $\mathbb{G} = \mathbb{Z}^d$, the AAT approximation becomes more and more accurate with increasing dimension d.

3.2.2 Generalized matrix Green's function

The goal now is to find the probability distribution of the complex variable G_n (for a fixed energy E and coordination number $K+1$) from the given distribution of the matrix elements $h_{n,n'}$, by assuming Eqs. (3.12) and (3.13). We proceed with a two-step process. First, we find the probability distribution of the variable $G'_{n'}$, i.e. the Green's function on the lattice with the distinct site n omitted. This step makes use of the AAT equation (3.12). In the second step, we find the distribution of the variable G_n by using Eq. (3.13).

We have already learned that the average local density of states (the disorder average of the imaginary part of the retarded Green's function) *does not* distinguish between the spectral types. We need to study the quadratic fluctuations of the distribution of the LDOS. For this purpose, both branches of the Green's function, retarded and advanced, must be brought into play. Indeed, the correlator $K_{n,\varepsilon}$ (3.5) contains both retarded and advanced Green's functions. Of course, the same two-step process as above can be repeated for the advanced Green's function, and for combinations of advanced and retarded Green's functions. In the following, we will focus on the first step (finding the distribution for the Green's functions on the

lattice with site n omitted) based on the AAT equation (3.12). To keep the notation and wording simple, we will omit the primes and will call the solutions of the AAT equation simply Green's function and write G_j (instead of G'_j) or $\mathcal{G}_j$ (instead of $\mathcal{G}'_j$) for its matrix-valued generalization which we will define below. The second step of finding the distribution of the Green's function $G_n(\mathcal{G}_n)$ on $\ell^2(\mathbb{G})$ from the Green's functions on the lattice with site n omitted (based on Eq. (3.13)) is explained in a later part, 3.3.3.

To bring both advanced and retarded Green's functions into play, we consider a matrix-valued generalization of the Green's function (still with $\varepsilon > 0$),

$$\mathcal{G} = \begin{pmatrix} E+\mathrm{i}\varepsilon - h & 0 \\ 0 & E-\mathrm{i}\varepsilon - h \end{pmatrix}^{-1} = \begin{pmatrix} G(E+\mathrm{i}\varepsilon) & 0 \\ 0 & G(E-\mathrm{i}\varepsilon) \end{pmatrix}. \tag{3.14}$$

We again focus on the local Green's function, $\mathcal{G}_j \equiv \mathcal{G}_{j,j}$, which is now a 2×2 matrix. The inverse matrix, $\mathcal{G}_j^{-1}$, has two real degrees of freedom, A_j, and D_j:

$$(\mathcal{G}_{j,j})^{-1} \equiv (\mathcal{G}_j)^{-1} = \begin{pmatrix} A_j + \mathrm{i}D_j & 0 \\ 0 & A_j - \mathrm{i}D_j \end{pmatrix}, \tag{3.15}$$

where

$$A_j = \frac{\mathrm{Re}(G_j(E-\mathrm{i}\varepsilon))}{|G_j(E+\mathrm{i}\varepsilon)|^2}, \quad D_j = \frac{\mathrm{Im}(G_j(E-\mathrm{i}\varepsilon))}{|G_j(E+\mathrm{i}\varepsilon)|^2}. \tag{3.16}$$

We observe that, while A_n multiplies unity $1_{2\times 2}$, D_n multiplies $\mathrm{i}\sigma_3$. Here σ_3 is the third Pauli matrix acting in retarded/advanced space. It turns out that $\mathrm{i}\sigma_3$ together with the other two Pauli matrices σ_1, σ_2 (also acting in retarded/advanced space) are the generators (over the real numbers) of the symmetry group of the theory, the non-compact Lie group SU(1,1):

$$\mathrm{su}(1,1) = \mathrm{span}_{\mathbb{R}}\{\mathrm{i}\sigma_3, \sigma_1, \sigma_2\}. \tag{3.17}$$

Next, let us offer an outlook on the conventional symmetry-breaking mechanism in (the field theory of) Anderson transitions. In the conventional symmetry-breaking picture, one identifies the regulator ε with the explicit symmetry-breaking parameter of the theory. Indeed, $\varepsilon \neq 0$ explicitly breaks the symmetries generated by the two Pauli matrices σ_1, σ_2, whereas it preserves the U(1) symmetry generated by $\mathrm{i}\sigma_3$. In the following, we will denote this U(1)-subgroup by $\mathrm{U}(1)_{\mathrm{i}\sigma_3}$. Due to the explicit symmetry-breaking by $\mathrm{i}\sigma_3$, the symmetry-breaking element D_n of the reciprocal Green's function $\mathcal{G}_j^{-1}$ is nonzero. When performing the limits carefully, i.e., when performing the infinite-volume limit first and performing the limit $\varepsilon \to 0$ af-

terwards (!), there exist two possibilites: (i) As we take ε to zero, the corresponding response D_n also goes to zero; this means the symmetries generated by the Pauli matrices σ_1, σ_2 are restored. (ii) The other possibility is that D_n remains nonzero for $\varepsilon \to 0$; in that case the symmetries generated by σ_1, σ_2 are spontaneously broken.

To end this subsection, let us offer a first glance at the novel mechanism advocated in this dissertation. It is based on the following observation: When identifying the regulator ε with the explicit symmetry-breaking term, the element $\mathrm{i}\sigma_3$ is singled out. Indeed, the U(1) symmetry generated by $\mathrm{i}\sigma_3$ is always intact when starting with the matrix-valued Green's function (3.14). Our goal is to generalize: From an algebraic viewpoint, it is not dictated to choose the element $\mathrm{i}\sigma_3$ as the symmetry-breaking point. The symmetry group naturally acts on its Lie algebra, and we can transform $\mathrm{i}\sigma_3$ to another point to obtain another explicit symmetry-breaking term. Indeed, the generalization of the AAT equation (3.12) for the matrix-valued Green's function (3.15) singling out $\mathrm{i}\sigma_3$ reads:

$$(\mathcal{G}_j)^{-1} \stackrel{!}{=} \begin{pmatrix} E + \mathrm{i}\varepsilon - h_{j,j} & 0 \\ 0 & E - \mathrm{i}\varepsilon - h_{j,j} \end{pmatrix} - \sum_{j'(\neq j)} |h_{j,j'}|^2 \, \mathcal{G}_{j'}. \tag{3.18}$$

Given a solution $\mathcal{G}_j$ of this equation, we obtain a related solution ${}^g\mathcal{G}_j$ which is defined via a symmetry transformation:

$$\mathcal{G}_j \to g \mathcal{G}_j g^{-1} \equiv {}^g\mathcal{G}_j, \;\; g \in \mathrm{SU}(1,1). \tag{3.19}$$

This related solution solves Eq. (3.18) with transformed explicit symmetry-breaking term:

$$\varepsilon \, \mathrm{i}\sigma_3 \to \varepsilon \, g \mathrm{i}\sigma_3 g^{-1}. \tag{3.20}$$

A preliminary motivation for also taking the symmetry-transformed solutions into account comes from an analogy to field theories with compact symmetry groups, such as the SO(3) Heisenberg antiferromagnet on $\mathbb{Z}^d$. Here the explicit symmetry-breaking term can single out an arbitrary point on the symmetry group orbit, S^2. In the symmetry-broken phase, different choices of points on S^2 select different symmetry-broken states, extremal Gibbs states, connected via a symmetry transformation. There is no reason to expect that the mechanism is different in spirit in the non-compact setting.

The above glance delivers a preliminary motivation for why we will analyze a

larger class of matrix Green's functions:

$$ {}^{g}\mathcal{G} = \left(\begin{pmatrix} E-h & 0 \\ 0 & E-h \end{pmatrix} + g \begin{pmatrix} \mathrm{i}\varepsilon & 0 \\ 0 & -\mathrm{i}\varepsilon \end{pmatrix} g^{-1} \right)^{-1}, \; g \in \mathrm{SU}(1,1). \tag{3.21} $$

For explicit calculations, we will restrict ourselves to a one-parameter subgroup

$$ g = g_s = \exp((s/2)\,\sigma_1), \quad s \in \mathbb{R}. \tag{3.22} $$

Of course, any other choice of generator in the linear span, $\mathrm{span}_{\mathbb{R}}\{\sigma_1, \sigma_2\}$, would work just as well. With the restriction (3.22) we obtain

$$ {}^{g_s}\mathcal{G} = \begin{pmatrix} E-h+\mathrm{i}\widetilde{\varepsilon} & -\mathrm{i}\widetilde{\delta} \\ \mathrm{i}\widetilde{\delta} & E-h-\mathrm{i}\widetilde{\varepsilon} \end{pmatrix}^{-1}, \quad \widetilde{\varepsilon} = \cosh(s)\,\varepsilon, \quad \widetilde{\delta} = \tanh(s)\,\widetilde{\varepsilon} < \widetilde{\varepsilon}. \tag{3.23} $$

Now in the inverse matrix $({}^{g_s}\mathcal{G}_j)^{-1}$ the off-diagonal parts are nonzero:

$$ ({}^{g_s}\mathcal{G}_j)^{-1} = \begin{pmatrix} A_j + \mathrm{i}\,{}^{g_s}D_j & -\mathrm{i}\,{}^{g_s}C_j \\ \mathrm{i}\,{}^{g_s}C_j & A_j - \mathrm{i}\,{}^{g_s}D_j \end{pmatrix}. \tag{3.24} $$

When ${}^{g_s}C_j$ remains nonzero for $\varepsilon \to 0$ the value of ${}^{g_s}C_j$ measures the deviation from the $\mathrm{U}(1)_{\mathrm{i}\sigma_3}$-invariant solution $(\mathcal{G}_j)^{-1}$. In some parts of the subsequent sections, we keep the notation more general. That is, we do not specify the explicit choice of one-parameter subgroup, and replace g_s by $g \in \mathrm{SU}(1,1)/\mathrm{U}(1)$ and accordingly ${}^{g_s}D_j$ (${}^{g_s}C_j$) by ${}^{g}D_j$ (${}^{g}C_j$). The subscript g_s will be reserved for the explicit choice, Eq. (3.22).

3.3 Fourier-Laplace transform Y and AAT integral equation

3.3.1 Definition

So far, our discussion has been focused on Green's functions that follow from the Wegner Hamiltonian H (3.1) and how they can, in principle, be calculated in high lattice dimensions. It is, however, still a very hard task to handle analytically the AAT equations for ${}^{g}\mathcal{G}$ (3.19) directly. As is often the case, it is fruitful to pass from the joint distribution of the random variables A_j,${}^{g}D_j$,${}^{g}C_j$ to its *characteristic function* (or *Fourier-Laplace transform*). The characteristic function is defined by

the transform

$$ {}^{g}Y(Q_j) := \mathbb{E}\Big(\mathrm{e}^{\mathrm{i}\mathrm{Tr}\, Q_j ({}^{g}\mathcal{G}_j)^{-1}}\Big), \tag{3.25} $$

where $\mathbb{E}(\bullet)$ is the expectation value with respect to the distribution of the random variables in the matrix $({}^{g}\mathcal{G}_j)^{-1}$, and the Fourier-conjugate variable Q_j is a 2×2 matrix

$$ Q_j = \begin{pmatrix} u_j\bar{u}_j & -u_j\bar{v}_j \\ v_j\bar{u}_j & -v_j\bar{v}_j \end{pmatrix} = \begin{pmatrix} u_j \\ v_j \end{pmatrix} \otimes \begin{pmatrix} \bar{u}_j & -\bar{v}_j \end{pmatrix} \qquad (u_j, v_j \in \mathbb{C}) \tag{3.26} $$

with the properties $Q_j = \sigma_3 Q_j^{\dagger}\sigma_3$ and $\mathrm{Det}(Q_j) = 0$. We note the special value

$$ {}^{g}Y(Q=0) = \mathbb{E}(\mathrm{e}^{0}) = 1 \tag{3.27} $$

due to normalization of the distribution for $\mathcal{G}_j^{-1}$. The variables Q_j (or supermatrices $\mathcal{Q}_j$ whose Bose-Bose sector is Q_j) will become the field variables of our field theory. We note that the minus sign on the r.h.s. of Eq. 3.26 is dictated due to convergence reasons.

3.3.2 Symmetry breaking on the level of ${}^{g}Y$

With the Fourier-Laplace transform ${}^{g}Y$ in hand, let us continue our heuristic discussion of symmetries and their breaking. For that purpose, we note that on an infinite graph $\mathbb{G}$ with translation invariance, the distribution of the random variables A_j, ${}^{g}D_j$, ${}^{g}C_j$ becomes independent of the site index j. We then simplify the notation: $A_j \equiv A$, ${}^{g}D_j \equiv {}^{g}D$, and ${}^{g}C_j \equiv {}^{g}C$. In the traditional approach, one only analyzes the $\mathrm{U}(1)_{\mathrm{i}\sigma_3}$-invariant $\mathcal{G}$ and thus sets $\widetilde{\delta} = 0$ (hence ${}^{g}C = 0$). One then encounters two alternatives for the distribution of ${}^{g=\mathrm{id}}D \equiv D$ to respond to the symmetry-breaking parameter ε. (The distribution of A carries information about the local density of states but is non-critical.)

(i) When the spectrum of H near the energy E is pure point, and the eigenfunctions of H are localized, the typical value of the LDOS

$$ \rho_j = \frac{1}{2\pi\mathrm{i}}\,\mathrm{Im}(G_j(E-\mathrm{i}\varepsilon)) \tag{3.28} $$

for small ε is small. Typically, the variable

$$ D_j = \frac{\mathrm{Im}(G_j(E-\mathrm{i}\varepsilon))}{|G_j(E+\mathrm{i}\varepsilon)|^2} \tag{3.29} $$

is then small too (the real part of the Green's function has a non-critical distribution). Furthermore, in the rare events where the LDOS is very large (this happens

when an eigenvalue lies in the window $[E-\mathrm{i}\varepsilon, E+\mathrm{i}\varepsilon]$), D is small because of the summand $\mathrm{Im}(G_j(E-\mathrm{i}\varepsilon))^2$ in the denominator. It is then plausible that the distribution of D in the limit of $\varepsilon \to 0$ shrinks to a Dirac-delta distribution supported at $D = 0$. The corresponding function Y has full symmetry

$$Y(Q) = Y(gQg^{-1}), \quad g \in \mathrm{SU}(1,1) \tag{3.30}$$

for $\varepsilon \to 0$.

(ii) In the case of ac spectrum near E, and extended eigenfunctions, the distribution of $\mathrm{Im}(G_j(E-\mathrm{i}\varepsilon))$ is narrowly supported around the nonzero mean. The distribution of D thus remains smooth for $\varepsilon \to 0$ with finite support on the positive real axis $D > 0$. The function Y satisfies the symmetry relation (3.30) only for g restricted to a maximal compact subgroup $\mathrm{U}(1)_{\mathrm{i}\sigma_3} \subset \mathrm{SU}(1,1)$.

So much for the conventional picture. Let us now motivate the unconventional scenario advocated in this work.

For concreteness, let us specify to the one-parameter subgroup (3.22) and assume that $\widetilde{\delta} > 0$, hence ${}^{g_s}C > 0$. (The opposite case is no different. In fact, rotating $\widetilde{\delta} \to \mathrm{e}^{\mathrm{i}\theta}\widetilde{\delta}$ we find that ${}^{g_s}C$ responds as ${}^{g_s}C \to \mathrm{e}^{\mathrm{i}\theta\,{}^{g_s}C}$.) We can then present ${}^{g_s}Y$ as

$${}^{g_s}Y(Q) = \mathbb{E}\left(\mathrm{e}^{\mathrm{i}A(|u|^2-|v|^2)}\,\mathrm{e}^{-({}^{g_s}D-{}^{g_s}C)(|u|^2+|v|^2)}\,\mathrm{e}^{-{}^{g_s}C|u-v|^2}\right). \tag{3.31}$$

What can we learn from this expression in the regime of strong disorder and high dimensions, i.e., the critical regime where the transition from the metallic to the insulating phase occurs? Strong disorder means that the random variable A has a very broad distribution. Hence, when the disorder average for A is carried out, the first factor under the expectation value effectively forces $|u| \approx |v|$. In the metallic phase (for $\varepsilon \to 0$, after taking the thermodynamic limit), the joint distribution of ${}^{g_s}D$ and ${}^{g_s}C$ has support when $0 <^{g_s} C <^{g_s} D$. For a fixed symmetry group element g_s, the support of the distribution for ${}^{g_s}D$, and accordingly the one for ${}^{g_s}C$, shrinks when tuning the system parameters to criticality from the metallic phase. At criticality, the support localizes at zero.

For the emergence of the novel critical solutions, it is essential that the symmetry group $\mathrm{SU}(1,1)$ is non-compact. We can think about what happens when the parameter s in g_s approaches $+\infty$ (or, equivalently $-\infty$, but we will stick to the first choice here). For this purpose, we first fix the parameter values to a point in the metallic phase. For large s (i.e., a large deviation from the $\mathrm{U}(1)_{\mathrm{i}\sigma_3}$-invariant solution), the support of the joint distributions of ${}^{g_s}D$ and ${}^{g_s}C$ grows. The positive random variable ${}^{g_s}C$ then acquires the role of a phase stiffness for $\overline{u}v$ (and

its complex conjugate $\overline{v}u$). Indeed, if ${}^{g_s}C$ is large, the third factor in (3.31) forces phase locking $u \approx v$ between the retarded and advanced variables. Furthermore, typically the difference between the random variables ${}^{g_s}D - {}^{g_s}C$ for increasing s becomes smaller and smaller. Thus the restriction on the fields u, v that comes from the second factor in (3.31) becomes weaker.

When combining both effects, i.e., tuning the system parameters to criticality from the metallic phase and a symmetry parameter s approaching infinity, the effects of decreasing support due to approaching criticality and increasing support due to increasing s balance. This results in the following situation: No restriction comes from the second factor in (3.31). This makes the support of ${}^{g_s}Y$ non-compact. However, since the second effect mentioned above induces a finite phase stiffness, the full SU(1, 1) symmetry is not restored. The resulting Y at criticality then takes the form

$$Y_{\mathrm{crit}}(Q) = \mathbb{E}\left(\mathrm{e}^{\mathrm{i}A(|u|^2-|v|^2)}\mathrm{e}^{-{}^{g_s}C|u-v|^2}\right). \tag{3.32}$$

The above explanation of the effects we are after, of course, only serves as a first heuristic argument. Our ongoing analysis in the following sections will show that the AAT self-consistency equation for ${}^{g_s}Y$, in fact, induces such behavior. We will furthermore argue that the critical solutions so obtained can quite naturally be related to sc spectrum: The non-compactness of the support together with the finite phase stiffness induces the sc-type behavior $\mathbb{E}(|G_n|^2) \sim \varepsilon^{1-\alpha}$. This concludes our first glimpse at the novel symmetry-breaking scenario at criticality, cast here in terms of the Fourier-Laplace transform ${}^{g_s}Y$.

3.3.3 AAT integral equation for ${}^{g}Y$

Let us first recall the (generalization of the) AAT equation (3.12) for the $\mathrm{U}(1)_{\mathrm{i}\sigma_3}$–broken matrix Green's function ${}^{g_s}\mathcal{G}$ (3.23):

$$({}^{g_s}\mathcal{G}_j)^{-1} \stackrel{!}{=} \begin{pmatrix} E + \mathrm{i}\widetilde{\varepsilon} - h_{n,n} & -\mathrm{i}\widetilde{\delta} \\ \mathrm{i}\widetilde{\delta} & E - \mathrm{i}\widetilde{\varepsilon} - h_{n,n} \end{pmatrix} - \sum_{j'(\neq j)} |h_{j,j'}|^2 \, {}^{g_s}\mathcal{G}_{j'}. \tag{3.33}$$

It should be understood as follows: (i) There exists a probability distribution for the random matrix ${}^{g_s}\mathcal{G}_j^{-1}$; (ii) if we draw K independent random matrices ${}^{g_s}\mathcal{G}_{j'}^{-1}$ from that same distribution, and (iii) we independently draw values for $h_{j,j}$ and $h_{j,j'}$ from their zero-centered Gaussian distributions with variances w_V^2 and w_T^2, then (iv) by forming the expression on the r.h.s. of Eq. (3.33) we obtain a random matrix that is statistically the same as a random matrix drawn directly from the distribution of ${}^{g_s}(\mathcal{G}_j)^{-1}$.

As announced above, instead of directly working with Eq. (3.33), we choose to reformulate it as an equivalent integral equation for the Fourier-Laplace transform ${}^{g_s}Y$. We will mostly call this integral equation AAT integral equation. It is the central equation and will be analyzed throughout the rest of this work. The information about the phase transition and the spectral types is encoded in the different symmetry properties of the solutions of the AAT integral equation in different parameter regimes. In the following, we present the derivation of this integral equation.

Recall that in the first introductory section, Section 2.1, we recapped some basic aspects of $\mathbb{Z}_2$-graded linear algebra and superanalysis. The reason was that our field theory (and the AAT integral equation) contains not only commuting, but also Grassmann variables. They enter the stage in the following first step of the derivation. We extend our Fourier Laplace transform ${}^{g}Y$ to a superanalytic continuation ${}^{g}\mathcal{Y}$

$$ {}^{g}\mathcal{Y} :=^{g} Y(Q_{\mathrm{BB}} - Q_{\mathrm{FF}}), \tag{3.34}$$

where BB stands for "Bose-Bose" and FF for "Fermi-Fermi". The matrix Q_{BB} is the one in (3.26) with index n omitted, while Q_{FF} is similar but composed of Grassmann variables $\zeta, \bar{\zeta}, \omega, \bar{\omega}$:

$$ Q_{\mathrm{BB}} = \begin{pmatrix} u\bar{u} & -u\bar{v} \\ v\bar{u} & -v\bar{v} \end{pmatrix}, \quad Q_{\mathrm{FF}} = \begin{pmatrix} \zeta\bar{\zeta} & \zeta\bar{\omega} \\ \omega\bar{\zeta} & \omega\bar{\omega} \end{pmatrix}. \tag{3.35}$$

The reason for introducing the Grassmann variables will become fully apparent in a later step of this derivation. In short, like in Efetov's standard supersymmetry method for the calculation of disorder averages of Green's functions [23], their purpose is to rewrite certain determinants that come from complex Gaussian integrals as Gaussian "integrals" over Grassmann variables.

Note that the superfunction ${}^{g}\mathcal{Y}$ inherits from ${}^{g}Y$ the important property

$$ {}^{g}\mathcal{Y}\big|_{Q_{\mathrm{BB}}=0=Q_{\mathrm{FF}}} = {}^{g}Y(0) = 1. \tag{3.36}$$

As a superfunction, ${}^{g}\mathcal{Y}$ is to be integrated against some kind of Berezin integration form, which we denote by $\mathcal{DQ}$. The form with the translation invariance appropriate to the present context is

$$ \mathcal{DQ} = \frac{d^2u}{\pi}\frac{d^2v}{\pi} \times \left(- \frac{\partial^2}{\partial\zeta\partial\bar{\zeta}} \frac{\partial^2}{\partial\omega\partial\bar{\omega}} \right). \tag{3.37}$$

We see that $\mathcal{DQ}$ is proportional to the usual Lebesgue measure for $(u, v) \in \mathbb{C}^2$ multiplied by the product of partial derivatives for all the Grassmann variables at hand.

For present use, we mention a characteristic property of the superfunction ${}^{g}\mathcal{Y}$. By its definition (3.34), ${}^{g}\mathcal{Y}$ is expressed in terms of the matrix entries of $Q_{\mathrm{BB}} - Q_{\mathrm{FF}}$, which are $u\bar{u} - \zeta\bar{\zeta}$ and three analogous combinations. All of these vanish upon the action of two odd vector fields:

$$\begin{aligned} K^{+} &= -\overline{u}\frac{\partial}{\partial\overline{\zeta}} + \zeta\frac{\partial}{\partial u} + \overline{v}\frac{\partial}{\partial\overline{\omega}} + \omega\frac{\partial}{\partial v}, \\ K^{-} &= u\frac{\partial}{\partial\zeta} + \overline{\zeta}\frac{\partial}{\partial\overline{u}} + v\frac{\partial}{\partial\omega} - \overline{\omega}\frac{\partial}{\partial\overline{v}}. \end{aligned} \tag{3.38}$$

Thus ${}^{g}\mathcal{Y}$ has two supersymmetries, $K^{\pm}$. Moreover, the vector fields $K^{\pm}$ are Killing vector fields for the Berezin integration form (3.37). In the final part of the introductory section, Section (2.1), we explained how supersymmetries can lead to the localization of Berezin integrals. Such a localization theorem goes into effect here: the integral of ${}^{g}\mathcal{Y}$ against $\mathcal{D}\mathcal{Q}$ localizes at $Q_{\mathrm{BB}} = Q_{\mathrm{FF}} = 0$, the (super-)point distinguished as the sole common zero locus of the vector fields (3.38):

$$\int \mathcal{D}\mathcal{Q}\, {}^{g}\mathcal{Y} = {}^{g}\mathcal{Y}\Big|_{Q_{\mathrm{BB}}=Q_{\mathrm{FF}}=0} = 1. \tag{3.39}$$

The identity (3.39) ensures that the property (3.36) is preserved under iteration with the AAT integral equation. Going beyond the AAT approximation, in the field theory on $\mathbb{Z}^d$, the supersymmetric localization theorem ensures the normalization of the partition sum.

Derivation of the AAT integral equation

Now we finally present the derivation for the AAT integral equation for ${}^{g_s}\mathcal{Y}$. [We remind the reader that for explicit calculations, a restriction to the one-parameter subgroup (3.22), i.e., $g \equiv g_s$ is sufficient. It will be evident how to generalize to other choices of one-parameter subgroups.] We begin by inserting the r.h.s. of the AAT equation for the matrix Green's function (3.33) into the definition of ${}^{g_s}\mathcal{Y}$ that follows immediately from (3.25) :

$$\begin{aligned} {}^{g_s}\mathcal{Y}(\mathcal{Q}_j) &:= \mathbb{E}\left(\mathrm{e}^{\mathrm{i}\mathrm{Tr}(Q_{\mathrm{BB}_j} - Q_{\mathrm{FF}_j})({}^{g_s}\mathcal{G}_j)^{-1}}\right) \\ &= \mathrm{e}^{\mathrm{i}\mathrm{Tr}\,(Q_{\mathrm{BB}_j} - Q_{\mathrm{FF}_j})(E + \mathrm{i}\widetilde{\varepsilon}\sigma_3 + \widetilde{\delta}\sigma_2)}\, \mathbb{E}\left(\mathrm{e}^{-\mathrm{i}\mathrm{Tr}\,(Q_{\mathrm{BB}_j} - Q_{\mathrm{FF}_j})h_{j,j} - \mathrm{i}\sum \mathrm{Tr}\,(Q_{\mathrm{BB}_j} - Q_{\mathrm{FF}_j})^{g_s}\mathcal{G}_{j'}|h_{j,j'}|^2}\right). \end{aligned} \tag{3.40}$$

Here we have omitted the sum subscript $j'(\neq j)$ to avoid cluttering of notation. Next, we recall the notion of supertrace in $\mathbb{Z}_2$-graded linear algebra:

$$\mathrm{STr}\, Q = \mathrm{Tr}\, Q_{\mathrm{BB}} - \mathrm{Tr}\, Q_{\mathrm{FF}} \tag{3.41}$$

and abbreviate:

$$^{g_s}\mathcal{Y}(\mathcal{Q}_j) = \mathrm{e}^{\mathrm{i}\,\mathrm{STr}\,\mathcal{Q}_j(E+\mathrm{i}\widetilde{\varepsilon}\Sigma_3+\widetilde{\delta}\Sigma_2)}\,\mathbb{E}\left(\mathrm{e}^{-\mathrm{i}h_{j,j}\,\mathrm{STr}\,\mathcal{Q}_j - \mathrm{i}\sum|h_{j,j'}|^2\,\mathrm{STr}\,\mathcal{Q}_j(^{g_s}\mathcal{G}_{j'})}\right). \tag{3.42}$$

In (3.42) we have extended

$$\sigma_3 \to \Sigma_3 = \sigma_3 \otimes \mathbf{1},\ \sigma_2 \to \Sigma_2 = \sigma_2 \otimes \mathbf{1},\ ^{g_s}\mathcal{G}_{j'} \to {}^{g_s}\mathcal{G}_{j'} \otimes \mathbf{1} \equiv {}^{g_s}\mathcal{G}_{j'} \tag{3.43}$$

from the space $\mathbb{C}^2$ to the $\mathbb{Z}_2$ graded space $\mathbb{C}^{2|2}$ by tensoring with the identity $\mathbf{1}$ on $\mathbb{C}^{1|1}$. Next we observe that the entries of the Hamiltonian matrix $h_{j,j}$ and $h_{j,j'}$ in Eq. (3.42) occur in an exponential to at most quadratic order. Because they are Gaussian-distributed, their disorder-average can be computed. We begin with the disorder-average over the diagonal elements $h_{j,j}$. Furthermore, to prepare the second step of averaging over the off-diagonal elements $h_{j,j'}$, we observe that the K terms ($K+1$ is the coordination number of the underlying lattice) in the sum on the r.h.s. over j' are all statistically independent and identical. We obtain:

$$^{g_s}\mathcal{Y}(\mathcal{Q}_j) = \mathrm{e}^{\mathrm{i}\,\mathrm{STr}\,\mathcal{Q}_j(E\mathbf{1}+\mathrm{i}\widetilde{\varepsilon}\Sigma_3+\widetilde{\delta}\Sigma_2) - \frac{w_V^2}{2}(\mathrm{STr}\,\mathcal{Q}_j)^2}\mathbb{E}\left(\mathrm{e}^{-\mathrm{i}|h_{j,j'}|^2\,\mathrm{STr}\,\mathcal{Q}_j\,{}^{g_s}\mathcal{G}_{j'}}\right)^K, \tag{3.44}$$

where j' now labels one of the K nearest neighbors of site j. Next we introduce an auxiliary supermatrix $\mathcal{Q}_{j'}$ (the field values on the neighboring sites) by

$$\mathcal{Q}_{j'} \equiv \Phi_{j'} \otimes \widetilde{\Phi}_{j'}, \quad \Phi_{j'} = \begin{pmatrix} u_{j'} \\ v_{j'} \\ \zeta_{j'} \\ \omega_{j'} \end{pmatrix}, \quad \widetilde{\Phi}_{j'} = (\bar{u}_{j'} \ \ -\bar{v}_{j'} \ \ \bar{\zeta}_{j'} \ \ \bar{\omega}_{j'}) \quad (u_{j'}, v_{j'} \in \mathbb{C}). \tag{3.45}$$

We then process the exponential under the expectation by a Gaussian Berezin integral:

$$\begin{aligned} \mathrm{e}^{-\mathrm{i}|h_{j,j'}|^2\,\mathrm{STr}\,\mathcal{Q}_j\,{}^{g_s}\mathcal{G}_{j'}} &= \mathrm{e}^{-\mathrm{i}|h_{j,j'}|^2\widetilde{\Phi}_j\,{}^{g_s}\mathcal{G}_{j'}\Phi_j} \\ = -\pi^{-2}\int_{\mathbb{C}} d^2u_{j'}\int_{\mathbb{C}} d^2v_{j'}\,&\frac{\partial^2}{\partial\zeta_{j'}\partial\bar{\zeta}_{j'}}\frac{\partial^2}{\partial\omega_{j'}\partial\bar{\omega}_{j'}}\,\mathrm{e}^{\mathrm{i}\widetilde{\Phi}_{j'}\,{}^{g_s}\mathcal{G}_{j'}^{-1}\Phi_{j'}+\mathrm{i}h_{j,j'}\tilde{\Phi}_j\Phi_{j'}+\mathrm{i}h_{j',j}\widetilde{\Phi}_{j'}\Phi_j}. \end{aligned} \tag{3.46}$$

The integral converges because the real part of the exponent is negative by our choice of $\Phi_{j'}, \widetilde{\Phi}_{j'}$:

$$\mathrm{Re}\Big(\mathrm{i}\widetilde{\Phi}_{j'}{}^{g_s}\mathcal{G}_{j'}^{-1}\Phi_{j'}\Big)_{\mathrm{BB}} = -{}^{g_s}D_{j'}\,(|u|^2+|v|^2)+2\,{}^{g_s}C_{j'}\,|uv|\,\cos(\arg(\overline{u}v)) < 0 \qquad (3.47)$$

[Recall ${}^{g_s}D_{j'} > 0$ from Eq. (3.16) and $|{}^{g_s}C_{j'}| < {}^{g_s}D_{j'}$ by construction.] Now the reason for introducing Grassmann variables and continuing ${}^{g_s}Y$ to the superfunction ${}^{g_s}\mathcal{Y}$ (3.34) is transparent: The Gaussian integration over the complex variables $u_{j'}, v_{j'}$ produces a determinant $\mathrm{Det}({}^{g_s}\mathcal{G}_{j'})$. To recover the l.h.s. of Eq. (3.46), this determinant has to cancel out. The introduction of Grassmann variables does this job: indeed, the Grassmann derivatives in (3.46) yield the inverse determinant $\mathrm{Det}({}^{g_s}\mathcal{G}_{j'})^{-1}$. Also, the integrand in Eq. (3.46) is Gaussian, and the disorder-average over the Gaussian disorder can easily be performed. In summary, with the Grassmann variables, we recover the l.h.s. while retaining a simple form of the integrand. We are now in a position to perform the average over the Gaussian-distributed off-diagonal elements $h_{j,j'} = \overline{h_{j',j}}$:

$$\mathbb{E}\left(\mathrm{e}^{\mathrm{i}h_{j,j'}\widetilde{\Phi}_j\Phi_{j'}+\mathrm{i}h_{j',j}\widetilde{\Phi}_{j'}\Phi_j}\right) = \mathrm{e}^{-w_T^2\widetilde{\Phi}_j\Phi_{j'}\widetilde{\Phi}_{j'}\Phi_j} = \mathrm{e}^{-w_T^2\,\mathrm{STr}\,\mathcal{Q}_j\mathcal{Q}_{j'}}. \qquad (3.48)$$

Assembling the various pieces yields

$$\begin{aligned}&\mathbb{E}\left(\mathrm{e}^{-\mathrm{i}|h_{j,j'}|^2\,\mathrm{STr}\,\mathcal{Q}_j{}^{g_s}\mathcal{G}_{j'}}\right)\\ &= -\pi^{-2}\int_{\mathbb{C}}d^2u_{j'}\int_{\mathbb{C}}d^2v_{j'}\,\frac{\partial^2}{\partial\zeta_{j'}\partial\bar{\zeta}_{j'}}\frac{\partial^2}{\partial\omega_{j'}\partial\bar{\omega}_{j'}}\,\mathrm{e}^{-w_T^2\,\mathrm{STr}\,\mathcal{Q}_j\mathcal{Q}_{j'}}\,\mathbb{E}\left(\mathrm{e}^{\mathrm{i}\widetilde{\Phi}_{j'}({}^{g_s}\mathcal{G}_{j'})^{-1}\Phi_{j'}}\right).\end{aligned} \qquad (3.49)$$

Finally, we notice that $\mathbb{E}\Big(\mathrm{e}^{\mathrm{i}\widetilde{\Phi}_{j'}({}^{g_s}\mathcal{G}_{j'})^{-1}\Phi_{j'}}\Big) = {}^{g_s}\mathcal{Y}(\mathcal{Q}_{j'})$, and we recall the intermediate result (3.44). We then arrive at the AAT integral equation for the Fourier-Laplace transform ${}^{g_s}\mathcal{Y}$:

$${}^{g_s}\mathcal{Y}(\mathcal{Q}) = \mathrm{e}^{\mathrm{i}\,\mathrm{STr}\,\mathcal{Q}(E+\mathrm{i}\widetilde{\epsilon}\Sigma_3+\widetilde{\delta}\Sigma_2)-\frac{1}{2}w_V^2\,\mathrm{STr}\,\mathcal{Q}^2}\left(\int\mathcal{D}\mathcal{Q}'\,\mathrm{e}^{-w_T^2\mathrm{STr}\,\mathcal{Q}\mathcal{Q}'}\;{}^{g_s}\mathcal{Y}(\mathcal{Q}')\right)^K, \qquad (3.50)$$

where $\mathcal{Q}$ denotes the 4×4 supermatrix

$$\mathcal{Q} := \begin{pmatrix} u \\ v \\ \zeta \\ \omega \end{pmatrix} \otimes \begin{pmatrix} \bar{u} & -\bar{v} & \bar{\zeta} & \bar{\omega} \end{pmatrix} \equiv \begin{pmatrix} Q_{\mathrm{BB}} & Q_{\mathrm{BF}} \\ Q_{\mathrm{FB}} & Q_{\mathrm{FF}} \end{pmatrix}, \qquad (3.51)$$

which coincides with Q_{BB} in the Bose-Bose sector and Q_{FF} in the Fermi-Fermi

sector. Note that ${}^{g_s}\mathcal{Y} \equiv {}^{g_s}\mathcal{Y}(\mathcal{Q})$ remains a function of $Q_{\mathrm{BB}} - Q_{\mathrm{FF}}$, the difference of the diagonal blocks.

Eq. (3.50) constitutes the central object of our analysis and provides the starting point for the symmetry-breaking mechanisms studied in the Chapters 4, 5. In Section 3.5, we will eliminate the Grassmann variables from Eq. (3.50) to arrive at an equivalent formulation involving only the Bose-Bose matrix Q_{BB}. This step turns out to be somewhat delicate, as we intend to avoid the usual assumption of $\mathrm{i}\sigma_3$-generated $\mathrm{U}(1)_{\mathrm{i}\sigma_3}$-symmetry. We will see that the solutions of this "bosonic" equation lead to the different $\varepsilon-$scalings of the observable $K_{n,\varepsilon}$.

How to obtain the Fourier-Laplace transform on the distinct site n?

We recall that finding the solutions of the AAT integral equation (3.50) is only one step of the two-step process of calculating local observables, like $\mathbb{E}(|G_n|^2)$. Indeed, as explained in Sections 3.2.1 and 3.2.2, the AAT equation delivers the distribution of the matrix Green's functions on the lattice with the distinct site n omitted. [Recall that n is the site where the operator is inserted.] So, having found the fixed points ${}^{g_s}\mathcal{Y}(\mathcal{Q})$ of Eq. (3.50), we repeat the above derivation for the Schur-complement equation for $({}^{g_s}\mathcal{G}_n)^{-1}$ (the generalization of Eq. (3.13)):

$$({}^{g_s}\mathcal{G}_n)^{-1} \stackrel{!}{=} \begin{pmatrix} E + \mathrm{i}\varepsilon - h_{n,n} & 0 \\ 0 & E - \mathrm{i}\varepsilon - h_{n,n} \end{pmatrix} - \sum_{j(\neq n)} |h_{n,j}|^2 \, {}^{g_s}\mathcal{G}'_j. \tag{3.52}$$

Here again ${}^{g_s}\mathcal{G}'_j$ denotes the matrix Green's function of the lattice with site n omitted. [For notational simplicity in the derivation of the AAT integral equation and before, the prime was omitted.] We also comment on why in Eq. (3.52) in the first matrix on the r.h.s. there is the ε term instead of the symmetry-transformed $\widetilde{\varepsilon}, \widetilde{\delta}$ term. The reason is that $\widetilde{\varepsilon}, \widetilde{\delta}$, besides their regulating nature, have the interpretation of the explicit symmetry-breaking parameters of the theory. Symmetry breaking is a phenomenon in infinite-volume. It corresponds to a parameter regime where the integral equation 3.50 has different symmetry-broken fixed point solutions. The equation for step two, Eq. (3.52), only knows about the infinite volume due to the rightmost term, ${}^{g_s}\mathcal{G}'_j$ (which can undergo spontaneous symmetry breaking). In the middle matrix, ε serves only as a regulator (the shift of the energy away from the real axis), instead of an explicit symmetry-breaking term. As such, it is always $\mathrm{U}(1)_{\mathrm{i}\sigma_3}$-invariant.

Again, we can translate the matrix equation (3.52) to an integral equation over

the supermatrix $\mathcal{Q}$ by repeating the steps of the derivation (3.3.3). We end up with:

$$\begin{aligned} \mathbb{E}\left(\mathrm{e}^{\mathrm{i}\mathrm{STr}\mathcal{Q}_n((^{g_s}\mathcal{G}_n)^{-1})}\right) &\equiv {}^{g_s}\mathcal{Y}(\mathcal{Q}_n) \\ = \mathrm{e}^{\mathrm{i}\mathrm{STr}\mathcal{Q}_n(E+\mathrm{i}\varepsilon\Sigma_3)-\frac{1}{2}w_V^2\mathrm{STr}\mathcal{Q}_n{}^2}&\left(\int\mathcal{D}\mathcal{Q}'\ \mathrm{e}^{-w_T^2\mathrm{STr}\mathcal{Q}_n\mathcal{Q}'}\ {}^{g_s}\mathcal{Y}(\mathcal{Q}')\right)^{K+1}, \end{aligned} \tag{3.53}$$

where ${}^{g_s}\mathcal{Y}(\mathcal{Q}')$ is a solution of Eq. (3.50).

We now summarize the two-step process we plan to follow in our analysis:

- **Step 1**: Study the (symmetry-broken) solutions ${}^{g_s}\mathcal{Y}$ of the AAT integral equation (3.50) for different values of the system parameters. The explicit symmetry-breaking term containing $\widetilde{\varepsilon},\widetilde{\delta}$ serves as a tool to select different symmetry-broken solutions when spontaneous symmetry breaking occurs.

- **Step 2**: Eq. (3.53) tells us how to compute the Fourier-Laplace transform of the matrix Green's function at the distinct site n with the solutions ${}^{g_s}\mathcal{Y}$ of the AAT integral equation. We will see soon how ${}^{g_s}\mathcal{Y}(\mathcal{Q}_n)$ is connected to the observables we are after (such as $\mathbb{E}(|G_n|^2)$). We first calculate them for regulator $\varepsilon > 0$ and finally send $\varepsilon \to 0$.

In the following section, we pursue two goals. First, we will see how our Fourier-Laplace transform is related to the observable we are after, the quadratic fluctuations of the LDOS at site n and energy E, $\mathbb{E}(|G_n|^2)$. Second, we deliver further motivation for leaving behind the assumption of $\mathrm{U}(1)_{\mathrm{i}\sigma_3}$ symmetry.

3.4 Connecting ${}^{g}Y$ to extremal Gibbs states

We now have developed enough theory to continue our discussion of why we choose to enlarge the solution space of the AAT equation and analyze $\mathrm{U}(1)_{\mathrm{i}\sigma_3}$–symmetry–broken functions. We first give a short outline of the argument: While in the preceding sections we immediately used the AAT approximation for the retarded Green's function (3.6) to arrive at the AAT integral equation, there is an alternative path which we will follow here: Using the standard Wegner-Efetov supersymmetry method we can express the observable $K_{n,\varepsilon}$ as a field-theoretical expectation value of a local field observable, i.e., a local field operator, localized at site n. The field variables of the field theory are the supermatrices $\mathcal{Q}_j$, or, after elimination of the Grassmann variables, their Bose-Bose sectors.

The Fourier-Laplace transform ${}^{g}\mathcal{Y}(\mathcal{Q}_n)$ (3.34) (which, of course, can be defined on arbitrary lattices $\mathbb{G}$) can then be identified with the field integral of the statistical weight over all lattice sites except for the site n of the operator insertion

(the insertion point of the observable). Now, in the thermodynamic limit, spontaneous symmetry breaking can occur: The state in which the observable is calculated can become non-unique. When restricted to observables localized at site n, the symmetry-broken states can be identified with symmetry-broken AAT solutions ${}^g\mathcal{Y}$ in high lattice dimension.

The Wegner-Efetov supersymmetry method connects the different scalings of $K_{n,\varepsilon}$ in the regulator ε, i.e., the three different spectral types –pp, ac, and, if existing, sc– to different classes of (extremal) Gibbs states. In the AAT approximation, we obtain a further connection to the solutions ${}^g\mathcal{Y}$.

This section is based on the theory developed in the introductory section on Gibbs states 2.3. In the spirit of the introductory section, it makes the ensuing discussion more transparent to fix an arbitrary finite sublattice $\Gamma \subset \mathbb{G}$. We assume that the distinct site n lies in Γ: $n \in \Gamma$. In the following, we consider the observable $K^\Gamma_{n,\varepsilon}$, i.e., the restriction of $K_{n,\varepsilon}$ to the finite lattice Γ with boundary conditions. To every site $i \in \mathbb{G}$, we attach a supermatrix $\mathcal{Q}_i$, defined in (3.51). As a boundary condition, we fix the configurations $\mathcal{Q}_i$ on the complement Γ^c. Since our model only has nearest neighbor interactions, it is actually sufficient to fix the fields $\mathcal{Q}_i$ immediately adjacent to Γ.

3.4.1 Relating $K_{n,\varepsilon}$ to ${}^gY(Q_n)$

Recall the definition (3.25) of the Fourier-Laplace transform ${}^gY(Q)$ and its superanalytic extension (3.34) by ${}^g\mathcal{Y} = {}^gY(Q_{\mathrm{BB}} - Q_{\mathrm{FF}})$. On the finite lattice, no spontaneous symmetry breaking can occur for $\varepsilon \to 0$; ε here only serves as a regulator. It is then a simple task to relate the correlator $K^\Gamma_{n,\varepsilon}$ to $\mathcal{Y}_\Gamma$:

$$K^\Gamma_{n,\varepsilon} = \int \mathcal{D}\mathcal{Q}_n \, (-\bar{\zeta}_n \zeta_n \bar{\omega}_n \omega_n) \, \mathcal{Y}_\Gamma(\mathcal{Q}_n). \tag{3.54}$$

The proof is very short: Since the Berezin integral on the r.h.s. of Eq. (3.54) is Gaussian in the complex variables $u_n, v_n, \zeta_n, \omega_n$ with flat Berezin integration form (3.37), and by Wick's principle for Gaussian integrals, we get

$$\int \mathcal{D}\mathcal{Q}_n \, (-\bar{\zeta}_n \zeta_n \bar{\omega}_n \omega_n) \, \mathrm{e}^{\mathrm{i}\mathrm{Tr}\,(\mathcal{G}^\Gamma_n)^{-1}(Q_{\mathrm{BB}\,n} - Q_{\mathrm{FF}\,n})} = G^\Gamma_{n,n}(E + \mathrm{i}\varepsilon)\, G^\Gamma_{n,n}(E - \mathrm{i}\varepsilon), \tag{3.55}$$

where $G^\Gamma_{n,n}(E \pm \mathrm{i}\varepsilon)$ are the diagonal entries of the matrix Green's function $\mathcal{G}^\Gamma_n$. Our claim then follows immediately by taking the expectation value $\mathbb{E}(\bullet)$ on both sides.

By noting $\bar{\zeta}_n \zeta_n \bar{\omega}_n \omega_n \, \mathcal{Y}_\Gamma = \bar{\zeta}_n \zeta_n \bar{\omega}_n \omega_n \, Y_\Gamma$ to simplify the integrand of the Berezin

integral, we now arrive at a formula for $K^{\Gamma}_{n,\varepsilon} = \mathbb{E}\Big(G^{\Gamma}_{n,n}(E+\mathrm{i}\varepsilon)\, G^{\Gamma}_{n,n}(E-\mathrm{i}\varepsilon)\Big)$:

$$K^{\Gamma}_{n,\varepsilon} = \int \mathrm{d}Q_n \; Y_{\Gamma}(Q_n \equiv Q_{\mathrm{BB}n}), \quad \mathrm{d}Q_n = \pi^{-2}\mathrm{d}^2u_n\,\mathrm{d}^2v_n, \tag{3.56}$$

which will be useful in the following. [In due course, we will push the Lebesgue measure $\mathrm{d}Q$ forward to a measure on the 3-dimensional cone, C^3, of the matrices Q in Eq. (3.35).]

3.4.2 Field theory on arbitrary infinite lattices $\mathbb{G}$

In the preceding sections, we have explained that the function ${}^{g}\mathcal{Y}$ within the AAT approach in the thermodynamic limit is the solution of a fixed-point equation, the AAT integral equation. To make the connection to Gibbs states apparent, we now leave this approximation aside for a moment. Instead, we set up the general field theory to calculate observables like $K^{\Gamma}_{n,\varepsilon}$. This is a standard exercise in applying the Wegner-Efetov supersymmetry method. The derivation can be found in an Appendix 8.1. The finite volume action reads:

$$\begin{aligned} &S_{\Gamma} = S_{\mathrm{reg}\Gamma} + S_{V\Gamma} + S_{T\Gamma}, \quad S_{\mathrm{reg}\Gamma} = \sum_{j\in\Gamma} \mathrm{STr}\,(\varepsilon\Sigma_3)\mathcal{Q}_j\,, \\ &S_{V\Gamma} = \sum_{j\in\Gamma} \mathrm{STr}\left(-\mathrm{i}E\mathcal{Q}_j + \tfrac{1}{2}w_V^2\mathcal{Q}_j^2\right), \quad S_{T\Gamma} = w_T^2 \sum_{jj'\in\overline{\Gamma}} A_{jj'}\,\mathrm{STr}\,\mathcal{Q}_j\mathcal{Q}_{j'}. \end{aligned} \tag{3.57}$$

Here the sum over $\overline{\Gamma}$ is a shorthand notation for the hopping terms in Γ and the interaction with the fields adjacent to Γ, which are fixed by the boundary condition. We emphasize that (3.57) is well-defined on any finite sublattice. On the full infinite lattice $\mathbb{G}$, it is merely a symbolic expression; it diverges for almost all field configurations. The observable $K^{\Gamma}_{n,\varepsilon}$ on the field theory side is the expectation value of a local field operator:

$$K^{\Gamma}_{n,\varepsilon} = \langle -\overline{\zeta_n}\zeta_n\overline{\omega_n}\omega_n\rangle_{\Gamma}, \tag{3.58}$$

where

$$\langle \bullet_n\rangle_{\Gamma} = \int \prod_{j\in\Gamma} \mathcal{D}\mathcal{Q}_j \;\; \bullet_n \;\; \mathrm{e}^{-S_{\Gamma}}. \tag{3.59}$$

$\bullet_n$ emphasizes that in this work, we look at an observable (a field operator) localized at site n. Recalling the identity (3.56), we can identify $\mathcal{Y}_{\Gamma}$ with the following field integral:

$$\begin{aligned} \mathcal{Y}_{\Gamma}(\mathcal{Q}_n) = \mathrm{e}^{-\mathrm{STr}(\varepsilon\Sigma_3)\mathcal{Q}_n} \;\mathrm{e}^{\mathrm{i}E\mathrm{STr}\mathcal{Q}_n - \frac{1}{2}w_V^2\mathrm{STr}\mathcal{Q}_n^2}\times \\ \times \int \prod_{j\in\Gamma\setminus\{n\}} \mathcal{D}\mathcal{Q}_j \;\mathrm{e}^{-S_{\mathrm{reg}_{\Gamma\setminus\{n\}}} - S_{V_{\Gamma\setminus\{n\}}} - S_{T_{\Gamma}}}, \end{aligned} \tag{3.60}$$

and obtain

$$\langle \bullet_n \rangle_\Gamma = \int \mathcal{D}\mathcal{Q}_n \ \bullet_n \mathcal{Y}_\Gamma(\mathcal{Q}_n). \tag{3.61}$$

The distribution $\langle \bullet_n \rangle_\Gamma$, or equivalently, its representing function $\mathcal{Y}_\Gamma$, should be viewed as a superanalytic analogue of a finite-volume Gibbs state, restricted on observables localized at site n, with fixed boundary conditions on the complement Γ^c. To keep the wording short, we will sometimes omit the fact that the Gibbs state is restricted to observables localized at site n and simply call it the Gibbs state.

We note that due to the supersymmetries, a localization theorem goes into effect, which guarantees the normalization of the field theory.

3.4.3 Selection of extremal Gibbs states

Of course, the finite-volume Gibbs state (3.59) is unique for all parameter values (i.e., energies E, (off-)diagonal disorder (w_T) w_V, and branching numbers K). We are now interested in the convex set of infinite volume Gibbs states corresponding to (3.59), in particular, the extremal ones. To answer how we can select them, we recall the introductory section on the general theory of Gibbs states 2.3. One option is to turn on an infinitesimal symmetry-breaking term and send it to zero after the thermodynamic limit $\Gamma \to \mathbb{G}$. In expression (3.60), symmetry breaking can occur in the rightmost factor, the field integral over all lattice sites except for the site n. [In the thermodynamic limit, this expression formally contains an infinite product of integrals]. In the derivation in finite volume, the regulator term

$$S_{\mathrm{reg}_{\Gamma\setminus\{n\}}} = \sum_{j\in\Gamma\setminus\{n\}} \mathrm{STr}(\varepsilon\Sigma_3)\mathcal{Q}_j \tag{3.62}$$

occurs. It explicitly breaks non-compact symmetries but preserves the $\mathrm{i}\sigma_3$-generated U(1) symmetry, $\mathrm{U}(1)_{\mathrm{i}\sigma_3}$. Its purpose, however, is to regulate the field theory, not to select a certain Gibbs state, because in finite volume the symmetry is restored for $\varepsilon \to 0$ and the Gibbs state is unique. It is now tempting (and in the standard field-theoretical approach to Anderson transitions usual) to identify this regulator term with the selector of Gibbs states in the thermodynamic limit:

$$S_{\mathrm{reg}_{\Gamma\setminus\{n\}}} \to S^{\mathrm{sym}}_{\Gamma\setminus\{n\}}, \tag{3.63}$$

where we identify the $\mathrm{U}(1)_{\mathrm{i}\sigma_3}$-invariant selector term of extremal Gibbs states with $S^{\mathrm{sym}}_{\Gamma\setminus\{n\}}$. As such, it can distinguish between presence and absence of non-compact symmetry breaking: In the metallic phase (ac spectrum), the limit $\lim_{\varepsilon\to 0}\lim_{\Lambda\to\mathbb{G}}$ of the field integral in (3.60) spontaneously breaks the non-compact symmetry. In

the insulating phase (pp spectrum), the same limit yields a fully symmetric state.

One key insight of the present work is that the identification of the finite-volume regulator term with the selector term of extremal Gibbs states in the thermodynamic limit is not dictated. As we have learned in the introductory section, Section 2.3, when spontaneous symmetry breaking occurs, there are several extremal Gibbs states, connected via the action of the symmetry group. Consequently, the identification (3.63) is only one out of a class of choices. We can select other extremal Gibbs states by symmetry-transforming the symmetry-breaking term with a fixed element from the symmetry group. We then end up with a modified, explicitly symmetry-broken field integral in comparison to Eq. (3.60):

$$S_{\mathrm{reg}_{\Gamma\setminus\{n\}}} \to {}^g S^{\mathrm{sym}}_{\Gamma\setminus\{n\}} \equiv \sum_{j\in\Gamma\setminus\{n\}} \mathrm{STr}(\varepsilon g \Sigma_3 g^{-1}) \mathcal{Q}_j \tag{3.64}$$

where g is an element of the symmetry group. [We remind the reader that in the reduction of the field theory to the bosonic sector, which will be carried out in Section 3.5, this symmetry group is the non-compact group $\mathrm{SU}(1,1)$.]

Interlude: an objection and its invalidation

At this point, the attentive reader might object that the generalization (3.64) does not lead to new consequences as the observable $K_{n,\varepsilon}$ itself is invariant under the symmetry group. Indeed, the expression (3.56) connecting $K_{n,\varepsilon}$ with the Fourier-Laplace transform Y does not change under symmetry transformations $Y \to {}^gY$ because the integral measure $\mathrm{d}Q_n$ is invariant (symmetries act as isometries on the field target space). We can invalidate this objection with two arguments: First, the observable $K_{n,\varepsilon}$ is only one out of several observables that can be calculated within our field-theoretical approach. For instance, higher moments of the distribution of the LDOS do break the symmetry and thus are sensitive to which extremal Gibbs state is spontaneously selected by the system. Second, the above objection ($K_{n,\varepsilon}$ being insensitive to which extremal Gibbs state is selected) is only true in a fixed phase of the system with a fixed symmetry-breaking mechanism. Indeed, in the metallic phase of the Wegner model, the non-compact symmetries are broken, while a compact residual symmetry $\mathrm{U}(1)_{\mathrm{i}g\sigma_3 g^{-1}}$ is preserved (which one, i.e., which extremal Gibbs state is chosen, is encoded in the symmetry group element g). The observable $K_{n,\varepsilon}$ then yields the same result independent of g for $\varepsilon \to 0$. However, in this work, we propose that at criticality, the symmetry-breaking mechanism is different! The solutions ${}^gY$ of metallic type restore the full symmetry for $\varepsilon \to 0$, but new solutions, that undergo a different kind of symmetry-breaking mechanism

(a new class of extremal Gibbs states), arise. To detect them, it is indispensable to work with the generalization (3.64). In short, the typical field configurations in these critical extremal Gibbs states concentrate around an arbitrary boundary point of the symmetry group orbits (the Goldstone manifold), $\mathrm{SU}(1,1)/\mathrm{U}(1)_{\mathrm{i}\sigma_3}$. Hence, to access these states, one needs to probe the boundary of the orbits via an appropriately transformed symmetry-breaking term in Eq. (3.64). One can anticipate that, since the boundary is at infinity, the procedure of sending the symmetry-breaking term to the boundary is subtle. The main analysis in Chapter 5 will suggest that one should think of the critical extremal Gibbs states, and their selection via a symmetry-breaking term, as a limit of near-to-critical metallic extremal Gibbs states. These are selected by well-defined symmetry-breaking terms (selecting points near but not on the boundary of the Goldstone manifold), for fixed elements g. Chapter 5 will show that this limit yields to a well-defined critical solution which naturally leads to an sc-type scaling of the correlator $K_{n,\varepsilon}$.

Interim summary

We now quickly summarize what we have discussed in the present section. The term S_{reg_Γ} is present in the finite-volume derivation of the field theory (3.59) and serves as a regulator term. As such, it breaks the non-compact symmetry of the field target space down to the compact subgroup $\mathrm{U}(1)_{\mathrm{i}\sigma_3}$. In the traditional field-theoretical approach, it is identified with the extremal Gibbs state selector in the thermodynamic limit. This selects the extremal Gibbs state that is invariant under the compact subgroup generated by $\mathrm{i}\sigma_3$. In this work, we extend to a larger class of extremal Gibbs states by also allowing for symmetry-transformed regulator terms, i.e., symmetry-transformed Gibbs state selector terms. Symmetry breaking may occur in the field integral in (3.60) when sending the selector term to zero after the thermodynamic limit. Additionally, in the second step of the calculation of local observables, the result of this field integral is integrated against the terms localized at site n, i.e.:

$$\mathrm{e}^{-\mathrm{STr}(\varepsilon\Sigma_3)\mathcal{Q}_n}\ \mathrm{e}^{\mathrm{i}E\mathrm{STr}\mathcal{Q}_n-\frac{1}{2}w_V^2\mathrm{STr}\mathcal{Q}_n^2} \tag{3.65}$$

in expression (3.60).

In parallel with preceding sections, without loss, we will now restrict ourselves to a one-parameter subgroup:

$$g_s=\exp\left(\frac{s}{2}\sigma_1\right),\ s\in\mathbb{R} \tag{3.66}$$

until the end of Subsection 3.4.4. The selector term of extremal Gibbs states then

becomes:

$$ {}^{g_s}S^{\mathrm{sym}}_{\Gamma\setminus\{n\}} \equiv \sum_{j\in\Gamma\setminus\{n\}} \mathrm{STr}(\widetilde{\varepsilon}\Sigma_3 - \mathrm{i}\widetilde{\delta}\Sigma_2)\mathcal{Q}_j, \quad \widetilde{\varepsilon} = \cosh(s)\,\varepsilon, \quad \widetilde{\delta} = \tanh(s)\,\widetilde{\varepsilon}. \tag{3.67} $$

3.4.4 Closing the circle-Going back to AAT approximation

Finally, we close the circle back to the AAT approximation. In the present field-theoretical setting, the AAT approximation enters in the field integral in expression (3.60):

$$ {}^{g_s}\mathcal{I}(\mathcal{Q}_n) = \int \prod_{j\in\Gamma\setminus\{n\}} \mathcal{D}\mathcal{Q}_j \; \mathrm{e}^{-w_T^2 \sum_{j\in\Gamma} A_{nj}\mathrm{STr}\mathcal{Q}_n\mathcal{Q}_j} \mathrm{e}^{-{}^{g_s}S^{\mathrm{sym}}{}_{\Gamma\setminus\{n\}} - S_{V_{\Gamma\setminus\{n\}}} - S_{T_{\Gamma\setminus\{n\}}}}. \tag{3.68} $$

The rightmost exponential in (3.68) is the statistical weight of the field theory on the restricted lattice $\Gamma\setminus\{n\}$ (or, in the thermodynamic limit, $\mathbb{G}\setminus\{n\}$). Obviously, the argument of the AAT approach, which leads to the AAT equation for the retarded Green's function in Section (3.2.1), also holds here. We write ${}^{g_s}\mathcal{Y}(\mathcal{Q}_j)$ for the result of integrating the statistical weight on the lattice $\mathbb{G}\setminus\{n\}$ from the treetop to a certain site $j \neq n$. In the AAT approximation, the calculation of the field integral then reduces to a recursive equation. In the thermodynamic limit, we look for fixed points of this equation. It reads:

$$ {}^{g_s}\mathcal{Y}(\mathcal{Q}) = \mathrm{e}^{\mathrm{iSTr}\mathcal{Q}(E+\mathrm{i}\widetilde{\varepsilon}\Sigma_3+\widetilde{\delta}\Sigma_2)-\frac{1}{2}w_V^2\mathrm{STr}\mathcal{Q}^2} \left(\int \mathcal{D}\mathcal{Q}' \; \mathrm{e}^{-w_T^2\mathrm{STr}\mathcal{Q}\mathcal{Q}'} \; {}^{g_s}\mathcal{Y}(\mathcal{Q}') \right)^K. \tag{3.69} $$

As expected, it is identical to the AAT integral equation, Eq. (3.50), derived in the preceding sections.

Discussion

To summarize, the present section makes it more transparent why in Section 3.2.2 we generalized the matrix Green's function (3.14) to symmetry-transformed matrix Green's functions (3.23). The generalization stems from the fact that in the field theory, there is more than one extremal Gibbs state when spontaneous symmetry breaking occurs. On the level of the AAT integral equation, the stable solutions of that equation are a continuum of symmetry-broken functions ${}^{g_s}\mathcal{Y}$ when spontaneous symmetry breaking occurs. A particular one is selected by symmetry-transforming the regulator term on infinitely many lattice sites (in our case we do so on $\mathbb{G}\setminus\{n\}$). Invoking Eqs. (3.60) and (3.61), the symmetry-broken solutions of the AAT integral equation (3.50) correspond to extremal Gibbs states of the field theory on

high-dimensional lattices $\mathbb{G}$, restricted to local observables. To finish this part, we now write down the central formula which connects the (symmetry-broken) fixed points ${}^{g_s}\mathcal{Y}$ of the AAT integral equation (3.50) with the detection tool of spectral types, the correlator $K_{n,\varepsilon}$:

$$K_{n,\varepsilon} \stackrel{!}{=} \lim_{\Lambda\to\mathbb{G}} {}^{g_s}\langle -\overline{\zeta_n}\zeta_n\overline{\omega_n}\omega_n\rangle_\Gamma = \lim_{\Lambda\to\mathbb{G}} \int \mathcal{D}\mathcal{Q}_n \ (-\overline{\zeta_n}\zeta_n\overline{\omega_n}\omega_n) \ {}^{g_s}\mathcal{Y}_\Gamma(\mathcal{Q}_n), \tag{3.70}$$

where the notation $\stackrel{!}{=}$ means that we calculate the observable in an extremal Gibbs state specified by g_s. By inserting expression (3.60), the AAT approximation, and by performing the thermodynamic limit, we get

$$\begin{aligned} K_{n,\varepsilon} \stackrel{!}{=} \int \mathcal{D}\mathcal{Q}_n \ (-\overline{\zeta_n}\zeta_n\overline{\omega_n}\omega_n) \ \mathrm{e}^{-\mathrm{STr}(\varepsilon\Sigma_3)\mathcal{Q}_n} \ \mathrm{e}^{\mathrm{i}E\mathrm{STr}\mathcal{Q}_n - \frac{1}{2}w_V^2\mathrm{STr}\mathcal{Q}_n^2} \times \\ \times \left(\int \mathcal{D}\mathcal{Q}' \mathrm{e}^{-w_T^2\mathrm{STr}\mathcal{Q}_n\mathcal{Q}'} \ {}^{g_s}\mathcal{Y}(\mathcal{Q}') \right)^{K+1}, \end{aligned} \tag{3.71}$$

where ${}^{g_s}\mathcal{Y}(\mathcal{Q}')$ denotes a stable fixed point of the AAT integral equation (selected by a certain Gibbs state selector term).

In the ensuing analysis in Chapters 4, 5, when discussing the metallic and critical solutions, we will work with a slightly modified version of Eq. (3.71). The reason is that in these cases, spontaneous symmetry breaking occurs, and the term ${}^{g_s}S^{\mathrm{sym}}_{\Gamma\setminus\{n\}}$ only serves as the selector of different symmetry-broken extremal Gibbs states, not as a regulator of the involved field integrals (in the metallic phase, no regularization is needed because the metallic solutions ${}^{g}Y_{\mathrm{ac}}$ remain integrable for $\widetilde{\varepsilon},\widetilde{\delta}\to 0$). In the insulating phase, the solutions of the AAT integral equation for $\widetilde{\varepsilon}=\widetilde{\delta}=0$ have full non-compact symmetry, and the term ${}^{g_s}S^{\mathrm{sym}}_{\Gamma\setminus\{n\}}$ instead serves as the regulator term, distributed over all lattice sites.

Hence, as we are interested in the whole family of extremal Gibbs states that potentially can be selected, in the metallic phase and at criticality, we take a shortcut and study the AAT integral equation with symmetry-breaking term set to zero ($\widetilde{\varepsilon}=\widetilde{\delta}=0$) right from the beginning. The resulting equation has a large solution space; the equation is equivariant under the symmetry group: Given a solution $\mathcal{Y}(\mathcal{Q})$, the transformed solution

$${}^{g}\mathcal{Y}(\mathcal{Q}) \equiv \mathcal{Y}(g^{-1}\mathcal{Q}g), \tag{3.72}$$

is also a solution. The different stable solutions of the equivariant equation then represent the different extremal Gibbs states. With stability, we mean linear stability, i.e., the linearized integral equation around the corresponding solution has eigenval-

ues with magnitude < 1. We remark that the above shortcut comes with a subtlety at criticality. As announced above, and portrayed in more detail in the subsequent subsection, Subsection 3.4.5, the critical solutions, which are to be understood as a suitable limit of near-to-critical metallic solutions, concentrate around a boundary point of the symmetry orbits. As their support is non-compact, integrals over these solutions need to be regulated to be finite. Rescue comes from the fact that in Eq. (3.71) the selector term only enters in ${}^{g}\mathcal{Y}(\mathcal{Q}')$. In the final integration over $\mathcal{Q}_n$, the critical solutions are integrated against the regulator term at site n, so that the expression on the r.h.s. of Eq. (3.71) is well-defined for $\varepsilon > 0$.

Next, we observe that when the selector term is sent to zero the $\mathcal{Q}'$ integral in Eq. (3.71) with the ensuing multiplication of the exponentials involving the energy E and the diagonal disorder w_V is simply another iteration step of the AAT integral equation (up to the minor issue that K is replaced by $K+1$; this does not change the scaling of $K_{n,\varepsilon}$). As a result, we can replace the $\mathcal{Q}'$ integration, the raising to the power of $K+1$ and the ensuing multiplication with the exponential involving E and w_V with the expression ${}^{g_s}\mathcal{Y}(\mathcal{Q}_n)$, the fixed point function of the AAT integral equation. Finally, we perform the differentiation with respect to the Grassmann variables at site n and obtain a purely "bosonic" equation:

$$K_{n,\varepsilon} \stackrel{!}{=} \int \mathrm{d}Q_n \; \mathrm{e}^{-\mathrm{Tr}(\varepsilon\sigma_3)Q_n \; {}^{g_s}Y(Q_n)}, \tag{3.73}$$

where ${}^{g_s}Y(Q_n)$ in the metallic phase (and at criticality) denotes one of the stable solutions of the equivariant ($\widetilde{\varepsilon} = \widetilde{\delta} = 0$) AAT integral equation with Grassmann variables eliminated ("bosonic"). In the insulating phase (absence of symmetry breaking), $\mathrm{e}^{-\mathrm{Tr}(\varepsilon\sigma_3)Q_n \, {}^{g_s}Y(Q_n)} \equiv Y_{\mathrm{pp}}(Q_n)$ is a solution of the "bosonic" AAT integral equation with $\mathrm{U}(1)_{\mathrm{i}\sigma_3}$-invariant regulator term.

Eq. (3.73) is the central equation that connects our objects of analysis, the functions ${}^{g_s}Y(Q_n)$, with the observable we are interested in. In the following, we will often call the integral 3.73 "spectral integral".

It should be clear that our quest now is to find the (symmetry-broken) solutions of the AAT integral equation (3.50). Before doing so, we give an outlook on the structure of the solutions and the extremal Gibbs states.

3.4.5 Outlook: Classes of extremal Gibbs states and spectral types

After eliminating the Grassmann variables, we can reduce the supersymmetric equation (3.50) to a purely "bosonic" one. This is explained in depth in the following

section, Section 3.5. The reduction has the symmetry group $G = \mathrm{SU}(1,1)$ for vanishing symmetry-breaking term ($\widetilde{\varepsilon} = \widetilde{\delta} = 0$). We will explain later that we can actually reduce G to the Lorentz group $\mathrm{SO}(1,2)$. We now define the ratio

$$w \equiv \frac{w_V}{w_T} \tag{3.74}$$

and simply call it the disorder. Definition (3.74) will be used throughout the rest of this work. We now give an outlook on the different classes of solutions of the AAT integral equation. Shedding light on the claims made in the present subsection is the goal of the subsequent chapters, Chapters 4, 5, 6.

1. **insulating phase:** For strong disorder $K \ll w$, the Wegner model is in the insulating phase. For fixed parameter values, the solution $Y_{\mathrm{pp}}(Q)$ is unique and restores the $\mathrm{SU}(1,1)$ symmetry for $\widetilde{\varepsilon}, \widetilde{\delta} \to 0$. Consequently, there is only one Gibbs state (the symmetric one); it is obviously extremal. $K_{n,\varepsilon}$ diverges like ε^{-1} for $\varepsilon \to 0$. This is a signal for a pp spectrum as discussed in the introductory section, Section 2.2. Similar to the examples of the Ising model and the Heisenberg antiferromagnet in the framework section, Section 2.3, also here, to an extremal Gibbs state one can associate a corresponding typical field configuration. We anticipate that in the present case, the field target space is a three-dimensional cone, C^3. It is a foliation by $\mathrm{SU}(1,1)$ symmetry orbits, two-dimensional hyperboloids. Because the extremal Gibbs states in the insulating phase are symmetric, the field fluctuates over the whole of the symmetry orbit.

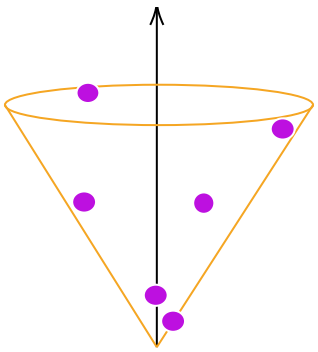

Figure 3.2: Sketch of a typical field configuration in the pp phase: The field fluctuates near the boundary (orange) of the target cone C^3, but explores the whole of the corresponding symmetry group orbits.

2. **metallic phase:** For the opposite case of weak disorder $K \gg w$ and energies E not too far from the band center, the Wegner model is in the metallic phase. The stable solutions ${}^{g}Y_{\mathrm{ac}}(Q)$ remain symmetry-broken for $\widetilde{\varepsilon}, \widetilde{\delta} \to 0$. The set of

stable solutions can be identified with the two-hyperboloid:

$$H^2 \cong \mathrm{SU}(1,1)/\mathrm{U}(1), \tag{3.75}$$

which we will often identify with the Poincaré disk $H^2 \cong D^2$. The fact that the space of ac-type solutions for fixed parameter values can be identified with H^2 can be understood quite quickly: One ac-type solution is given by a $\mathrm{U}(1)_{\mathrm{i}\sigma_3}$-invariant function $Y_{\mathrm{ac}}(Q)$. It is of an ac-type because it rapidly decays in the non-compact directions of the field target space. By G-equivariance of the AAT integral equation for $\widetilde{\varepsilon} = \widetilde{\delta} = 0$, other solutions are obtained by operating with the symmetry group G. Nevertheless, due to the $\mathrm{U}(1)_{\mathrm{i}\sigma_3}$ invariance of Y_{ac}, there is a redundancy which is modded out in Eq. (3.75).

Using the correspondence between the space of stable fixed points of the AAT equation and extremal Gibbs states, the space of extremal Gibbs states can be identified with D^2. Due to the breaking of non-compact symmetry, in the rightmost integral in Eq. (3.73), we can use the dominated convergence theorem and exchange limit and integral. $K_{n,\varepsilon}$ remains finite for $\varepsilon \to 0$, which is a signal for ac spectrum. General Gibbs states arise from averaging the extremal Gibbs states with respect to different probability measures on H^2.

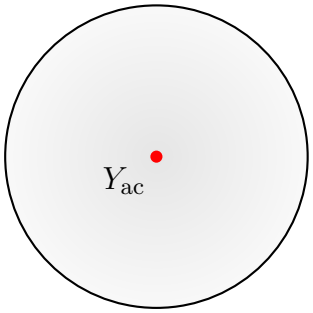

Figure 3.3: Moduli space $H^2 \cong D^2$ of ac-type solutions ${}^gY_{\mathrm{ac}}$. The $\mathrm{U}(1)_{\mathrm{i}\sigma_3}$-invariant solution Y_{ac} (red dot) sits at the center of the disk. Other solutions ${}^gY_{\mathrm{ac}}$ are obtained by transforming Y_{ac} with $g \in \mathrm{SU}(1,1)$.

The typical field configuration in the $\mathrm{U}(1)_{\mathrm{i}\sigma_3}$-invariant extremal Gibbs state (red dot in the Fig. 6.2) is centered around the center half-axes of C^3.

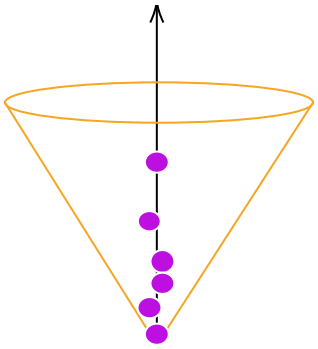

Figure 3.4: Sketch of a typical field configuration in the $\mathrm{U}(1)_{\mathrm{i}\sigma_3}$-invariant extremal Gibbs state in the metallic phase. The field clusters around the center half-axes (the black arrow is the positive one).

3. **Criticality** On the critical manifold in parameter space, which sits in the regime $K \sim w$ for energies $E \ll w_V$, we find solutions that undergo a distinct symmetry-breaking pattern that naturally corresponds to a local sc spectrum at energy E. The solutions $Y_{\mathrm{sc}}(Q)$, as opposed to the ac case, have non-compact support but do not possess the full $\mathrm{SU}(1,1)$ symmetry; they are invariant under a nilpotent subgroup $N \subset \mathrm{SU}(1,1)$. The set of solutions ${}^gY_{\mathrm{sc}}(Q)$ can now be identified with rays $\cong \mathbb{R}^+$ that are characterized by a U(1)-angle, or, more concretely, a boundary point $p \in \partial H^2 \cong \partial D^2$. The family of rays can then be identified with the punctured Poincaré disk $D^2 \setminus \{o\}$, where o denotes the center of the disk. The reason for excluding the center is that it corresponds to the metallic solutions ${}^gY_{\mathrm{ac}}$ with $\mathrm{U}(1)_{\mathrm{i}g\sigma_3 g^{-1}}$ symmetry. These solutions become fully symmetric on the critical manifold (they turn into the solution of pp-type). Again, general sc-type Gibbs states are obtained by averaging over the extremal ones.

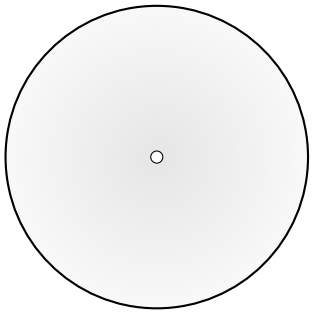

Figure 3.5: Moduli space $D^2 \setminus \{o\}$ of sc-type solutions Y_{sc}. The center is excluded because it corresponds to the fully symmetric solution.

Now the field configurations corresponding to the extremal Gibbs states are non-compact as opposed to the ac phase, but do not restore the full symmetry. They are centered around an arbitrary ray from the tip of the cone C^3 to a boundary point at infinity. For better illustration, in the following figure, the target space is projected to the Poincaré disk.

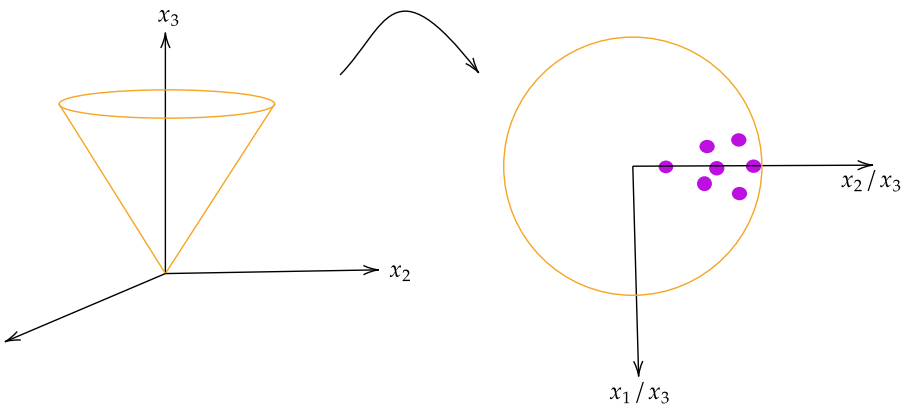

Figure 3.6: Sketch of a typical field configuration in an extremal Gibbs state at criticality. Now the field clusters around a ray ending at a certain boundary point on the boundary of the Poincaré disk.

In the remainder of this work, our goal is to substantiate the claims made in this section. Particularly in the final section, Section 6.3 of Chapter 6, we close the circle to the present section by shedding more light on the ac and sc moduli space from an algebraic perspective.

After this motivational section and the discussion of the connection to our observable of interest, we now continue the analysis of the AAT integral equation (3.50). To begin, we go back to the spectral integral (3.73). It involves only the "bosonic" function ${}^{g_s}Y(Q)$. A natural first step of the analysis is to eliminate the Grassmann variables and reduce the integral equation (3.50) to a purely "bosonic" equation.

3.5 Reduction of the AAT integral equation to a "bosonic" equation

With the understanding that now we also analyze $\mathrm{U}(1)_{\mathrm{i}\sigma_3}$ symmetry-broken solutions of the AAT integral equation, we will omit the superscript g in front of Y in the present section, Section 3.5. Only when we explicitly restrict to the one-parameter subgroup g_s (3.22), we write the superscript.

We wish to convert Eq. (3.50) to a reduced equation no longer featuring the Grassmann variables $\zeta,\bar{\zeta},\omega,\bar{\omega}$ of Q_{FF}. The naive initial step in this quest is to simply set $Q_{\mathrm{FF}} \equiv 0$ on the left-hand side, thereby restricting $\mathcal{Y}(\mathcal{Q})$ to $Y(Q_{\mathrm{BB}} \equiv Q)$. In this way, however, one does not arrive at a closed equation for the restricted

function $Y(Q)$, as the integration (actually, differentiation) over the Grassmann variables on the right-hand side introduces derivatives of $Y(Q)$. Some effort has to be invested to account for those derivatives. To better understand how the Grassmann derivatives lead to usual derivatives of the "bosonic" function $Y(Q)$ and on what manifold these derivatives are defined, in the following, we investigate the geometric structure underlying the supermatrix $\mathcal{Q}$. Not only will this discussion be of technical use, but it will also be essential in the ensuing analysis of the symmetry-breaking mechanisms and the phase transition.

3.5.1 Three-dimensional cone C^3

We begin by recalling the definition of the supermatrix $\mathcal{Q}$ (which we state once more for better readability):

$$\mathcal{Q} = \Phi \otimes \widetilde{\Phi},\ \Phi = \begin{pmatrix} u \\ v \\ \zeta \\ \omega \end{pmatrix},\ \widetilde{\Phi} = \begin{pmatrix} \overline{u} & -\overline{v} & \overline{\zeta} & \overline{\omega} \end{pmatrix}. \tag{3.76}$$

Let P be a positive Hermitian 2×2 matrix. The space of such matrices has real dimension 4 and is in bijection with $\mathrm{GL}(2,\mathbb{C})/\mathrm{U}(2)$ by the mapping $g \cdot \mathrm{U}(2) \mapsto gg^\dagger = P$; we denote it by $\mathrm{Herm}^+(2)$. Our interest is in its 3-dimensional boundary,

$$C^3 = \partial\left(\mathrm{Herm}^+(2)\right) := \{P \in \overline{\mathrm{Herm}^+(2)} \mid \mathrm{Det}P = 0\}, \tag{3.77}$$

where at least one of the two eigenvalues of P has gone to zero. The manifold C^3 is relevant here because our matrices $Q\sigma_3$ (Q is the Bose-Bose sector of $\mathcal{Q}$), with Q parameterized according to Eq. (3.76) by $(u, v) \in \mathbb{C}^2$, constitute C^3. In the sequel, we will make good use of the inclusion mapping

$$i:\ C^3 \to \overline{\mathrm{Herm}^+(2)}, \tag{3.78}$$

interpreting the matrices $Q\sigma_3$ (or, equivalently, Q) as points in the closure of the open set $\mathrm{Herm}^+(2)$.

Why is the inclusion map (3.78) useful? The short answer is that our function Y, by its formal definition in Eq. (3.25), extends from C^3 to $\overline{\mathrm{Herm}^+(2)}$. As a matter of fact, if we were analyzing the Wegner model with $N \geq 2$ orbitals, we would simply

replace the parametrization (3.26) of Q by a sum over orbitals:

$$Q\sigma_3 = \sum_{\alpha=1}^{N} \begin{pmatrix} u_\alpha \bar{u}_\alpha & u_\alpha \bar{v}_\alpha \\ v_\alpha \bar{u}_\alpha & v_\alpha \bar{v}_\alpha \end{pmatrix} \in \overline{\mathrm{Herm}^+(2)} \qquad (u_\alpha, v_\alpha \in \mathbb{C}). \tag{3.79}$$

Next we recall that our superfunction $\mathcal{Y}$ depends only on $Q_{\mathrm{BB}} - Q_{\mathrm{FF}}$. We express that difference as

$$\mathrm{i}(Q_{\mathrm{BB}} - Q_{\mathrm{FF}}) = \hat{x}_0 \mathrm{i}\mathbf{1} + \hat{x}_3 \mathrm{i}\sigma_3 + \hat{x}_1 \sigma_1 + \hat{x}_2 \sigma_2 \tag{3.80}$$

in terms of basic superfunctions $\hat{x}_\mu$ ($\mu = 0,1,2,3$). By inverting this expression, we get (with $\sigma_0 \equiv \mathbf{1}$)

$$\hat{x}_j = \frac{1}{2}\mathrm{Tr}\,(Q_{\mathrm{BB}} - Q_{\mathrm{FF}})\,\sigma_j \quad (j = 0,3), \quad \hat{x}_k = \frac{\mathrm{i}}{2}\mathrm{Tr}\,(Q_{\mathrm{BB}} - Q_{\mathrm{FF}})\,\sigma_k \quad (k = 1,2). \tag{3.81}$$

Next we want to insert (3.80) into $\mathcal{Y}$ and expand at all points $Q_{\mathrm{BB}} \equiv Q$ (with $Q\sigma_3 \in C^3$) with respect to the nilpotent parts (i.e., the Grassmann variables) in the $\hat{x}_\mu$. This plan runs into a complication: since the number parts of the four functions $\hat{x}_\mu$ ($\mu = 0,1,2,3$) cannot be linearly independent as functions on the 3-dimensional space C^3, the operation of taking partial derivatives with respect to them is not well-defined.

There exist two fixes for this complication. The first one already acted in the background in the definition (3.23) of ${}^{g_s}\mathcal{G}$. Recall that we restricted ourselves to a one-parameter subgroup $g_s = \exp((s/2)\sigma_1),\ s \in \mathbb{R}$. The resulting function ${}^{g_s}\mathcal{Y}(\mathcal{Q})$ effectively only depends on the three superfunctions $\hat{x}_0, \hat{x}_3, \hat{x}_2$. The operation of taking partial derivatives with respect to the three functions x_μ on C^3 is well-defined. [Of course, the explicit choice of the one-parameter subgroup does not matter: For instance, we could instead choose $\widetilde{g}_s = \exp((s/2)\sigma_2),\ s \in \mathbb{R}$ and would obtain functions ${}^{g_s}\mathcal{Y}(\mathcal{Q})$ that now effectively depend on $\hat{x}_0, \hat{x}_3, \hat{x}_1$.] So, in principle, we could simply work with the restricted functions ${}^{g_s}\mathcal{Y}$, expand in the Grassmann variables, and obtain a closed equation for ${}^{g_s}Y(Q)$. Nevertheless, in order to gain a more general overview, we here develop the full theory without a priori restrictions to certain one-parameter subgroups. In the subsequent analysis in Chapters 4 and 5, we will then deduce the expressions for the restriction from the more general ones obtained here. This brings us to the second fix: Recall that the function Y naturally extends to the ambient space $\overline{\mathrm{Herm}^+(2)}$. Taking the cue from (3.80), we introduce four $\mathbb{R}$-valued functions x_μ (without hat) by

$$\mathrm{i}P\sigma_3 = x_0 \mathrm{i}\mathbf{1} + x_3 \mathrm{i}\sigma_3 + x_1 \sigma_1 + x_2 \sigma_2\,. \tag{3.82}$$

These may serve as coordinate functions for the 4-dimensional ambient space. As such, they are subject to the conditions

$$x_3 > 0, \quad x_3^2 > x_0^2 + x_1^2 + x_2^2. \tag{3.83}$$

The boundary $C^3 \subset \overline{\mathrm{Herm}^+(2)}$ is reached by allowing (and demanding, respectively) equality:

$$C^3: \quad x_3 \geq 0, \quad x_3^2 = x_0^2 + x_1^2 + x_2^2. \tag{3.84}$$

Indeed, the last equality is the coordinate expression for the equation $\mathrm{Det}\, Q = 0$, singling out the subspace C^3. We note that under pullback $i^* x_\mu \equiv x_\mu \circ i$ by the inclusion map (3.78) we have

$$i^*x_0 = \frac{1}{2}(\bar{u}u - \bar{v}v), \quad i^*x_1 = \frac{\mathrm{i}}{2}(\bar{u}v - \bar{v}u), \quad i^*x_2 = \frac{1}{2}(\bar{u}v + \bar{v}u), \quad i^*x_3 = \frac{1}{2}(\bar{u}u + \bar{v}v). \tag{3.85}$$

Now by invoking the second equation of Eqs. (3.35), we extend the superfunctions $\hat{x}_\mu$ to the 4-dimensional space $\overline{\mathrm{Herm}^+(2)}$ as

$$\begin{aligned} \hat{x}_0 &= x_0 + \frac{1}{2}(\bar{\zeta}\zeta + \bar{\omega}\omega), \quad \hat{x}_1 = x_1 + \frac{\mathrm{i}}{2}(\bar{\zeta}\omega + \bar{\omega}\zeta), \\ \hat{x}_2 &= x_2 + \frac{1}{2}(\bar{\zeta}\omega - \bar{\omega}\zeta), \quad \hat{x}_3 = x_3 + \frac{1}{2}(\bar{\zeta}\zeta - \bar{\omega}\omega). \end{aligned} \tag{3.86}$$

3.5.2 Expanding the superfunction $\mathcal{Y}$: enter the Laplacian

We are finally in a position to execute our plan of expanding the full superfunction $\mathcal{Y}$ (without a priori restrictions) with respect to the Grassmann variables:

$$\begin{aligned} \mathcal{Y} = Y(Q) &+ \frac{1}{2}(\bar{\zeta}\zeta + \bar{\omega}\omega)\frac{\partial Y}{\partial x_0}(Q) + \frac{1}{2}(\bar{\zeta}\zeta - \bar{\omega}\omega)\frac{\partial Y}{\partial x_3}(Q) \\ &+ \frac{\mathrm{i}}{2}(\bar{\zeta}\omega + \bar{\omega}\zeta)\frac{\partial Y}{\partial x_1}(Q) + \frac{1}{2}(\bar{\zeta}\omega - \bar{\omega}\zeta)\frac{\partial Y}{\partial x_2}(Q) - \bar{\zeta}\zeta\bar{\omega}\omega\Delta Y(Q), \qquad Q \in C^3 \cdot \sigma_3. \end{aligned} \tag{3.87}$$

The second-order differential operator Δ in the last summand is of Laplace-type:

$$\Delta = \frac{1}{4}\left(\frac{\partial^2}{\partial x_3^2} - \frac{\partial^2}{\partial x_0^2} - \frac{\partial^2}{\partial x_1^2} - \frac{\partial^2}{\partial x_2^2}\right). \tag{3.88}$$

We recall that $Y(Q)$ has been extended from C^3 to $\mathrm{Herm}^+(2)$ by the formal definition (3.25). Thus ΔY and all partial derivatives $\partial Y/\partial x_\mu$ are now well-defined. They still exist as one-sided derivatives in the limit of approaching the boundary points $Q\sigma_3 \in C^3 \subset \overline{\mathrm{Herm}^+(2)}$.

Next we set $Q_{\mathrm{FF}} = 0$ in Eq. (3.50) and observe that

$$\mathrm{e}^{-w_T^2 \mathrm{STr}\, \mathcal{Q}\mathcal{Q}'}\Big|_{Q_{\mathrm{FF}} \equiv 0} = \mathrm{e}^{-w_T^2 \mathrm{Tr}\, Q_{\mathrm{BB}} Q'_{\mathrm{BB}}}, \tag{3.89}$$

which tells us (in the case of $Q_{\mathrm{FF}} = 0$) that all dependence on the Grassmann variables of Q'_{FF} in the integrand on the right-hand side of Eq. (3.50) resides in $\mathcal{Y}(\mathcal{Q}')$. Consequently, integration over those Grassmann variables picks up nothing but the last term on the r.h.s. of (3.87). Thus we obtain for $Y(Q) = \mathcal{Y}\big|_{Q_{\mathrm{FF}=0}}$ the equation

$$Y(Q) = \mathrm{e}^{\mathrm{i}\,\mathrm{Tr}\, Q(E + \mathrm{i}\widetilde{\varepsilon}\sigma_3 + \widetilde{\delta}\sigma_2) - \frac{1}{2} w_V^2 \mathrm{Tr}\, Q^2} \left(\int d\mu(Q')\, \mathrm{e}^{-w_T^2 \mathrm{Tr}\, QQ'} (\Delta Y)(Q') \right)^K, \tag{3.90}$$

where both $Q\sigma_3$ and $Q'\sigma_3$ run through C^3. For the measure of integration $d\mu(Q)$, we may take $\pi^{-2} d^2u\, d^2v$ from Eq. (3.37) or, even better, the push forward of this measure to C^3. Note that for the rank-one matrix Q (on C^3) one has the identity $(\mathrm{Tr}\, Q)^2 = \mathrm{Tr}\,(Q^2)$.

As it stands, Eq. (3.90) fails to be closed for Y as a function on C^3. The reason is that ΔY is *not* determined by the values that Y takes on C^3; some information on its directional derivatives *normal* to C^3 is needed. What is the minimal information that has to be added? To answer this question, consider the first-order differential operators

$$\begin{aligned} K_1 &= x_2 \frac{\partial}{\partial x_3} + x_3 \frac{\partial}{\partial x_2}, \quad & K_2 &= x_3 \frac{\partial}{\partial x_1} + x_1 \frac{\partial}{\partial x_3}, \\ K_3 &= x_1 \frac{\partial}{\partial x_2} - x_2 \frac{\partial}{\partial x_1}, \quad & D &= \sum_{\mu=0}^{3} x_\mu \frac{\partial}{\partial x_\mu}. \end{aligned} \tag{3.91}$$

All of these annihilate the function $\mathrm{Det}\, Q = x_0^2 + x_1^2 + x_2^2 - x_3^2$ (in the case of D this holds after restriction to C^3, which is good enough for our purposes). Since C^3 is defined by $\mathrm{Det}\, Q = 0$, this means that each of D and K_j $(j = 1, 2, 3)$ corresponds to a vector field *tangential* to C^3. Armed with this information, one does a straightforward calculation to show that Δ operating on functions on $\mathrm{Herm}^+(2)$ has the expression

$$\Delta = \frac{1}{4}(x_3^2 - x_2^2 - x_1^2)^{-1} \left(\Delta^\flat - 2D \circ x_0 \frac{\partial}{\partial x_0} + (x_0^2 + x_1^2 + x_2^2 - x_3^2) \frac{\partial^2}{\partial x_0^2} \right), \tag{3.92}$$

where $\Delta^\flat$ is a second-order differential operator that will appear repeatedly in the

following:

$$\Delta^\flat = K_3^2 - K_2^2 - K_1^2 + D^2 + D. \tag{3.93}$$

The calculation can be found in the Appendix 8.2. We will need $(\Delta Y)(Q)$ only in the limit of taking $Q\sigma_3$ to C^3, in which case the expression (3.92) simplifies to

$$(\Delta Y)(Q) = \frac{1}{4x_0^2}(\Delta^\flat Y)(Q) - \frac{1}{2x_0}(D+1)\frac{\partial Y}{\partial x_0}(Q), \tag{3.94}$$

where we have used $i^*(x_0^2 + x_1^2 + x_2^2 - x_3^2) = 0$ and the commutation relation $D \circ x_0 = x_0(D+1)$. It is clear from the definition (3.88) that the operator Δ commutes with the group action $Q \mapsto gQg^{-1}$ by $g \in \mathrm{SU}(1,1)$. As a check on the C^3-restricted Laplacian (3.94), one verifies that this commutation law still holds.

3.5.3 Closing the system of equations

What can we learn from the formula (3.94)? The first summand on the right-hand side is expressed in terms of the C^3-tangential operators D and K_j, which restrict to first-order differential operators on C^3. If this were the only summand, the equation for $Y(Q)$ would already be closed. However, the second summand involves the partial derivative $\partial Y/\partial x_0$, which is not tangential to C^3. Therefore, in order to close the equation, we must carry along $\partial Y/\partial x_0$ and augment the equation for $Y(Q)$ by an equation for $(\partial Y/\partial x_0)(Q)$.

To obtain an equation for $\partial Y/\partial x_0$, we return to Eq. (3.50) and apply $\partial/\partial x_0$ on both sides. Having done so, we proceed as before: we set $Q_{\mathrm{FF}} = 0$ and carry out the Grassmann integration on the right-hand side. The resulting equation is somewhat cumbersome; to present it in a manageable form, we introduce the abbreviation

$$X(Q) \equiv \int d\mu(Q')\, \mathrm{e}^{-w_T^2 \operatorname{Tr} QQ'} \left(\frac{1}{4{x_0'}^2}(\Delta^\flat Y)(Q') - \frac{1}{2x_0'}(D+1)\frac{\partial Y}{\partial x_0}(Q') \right). \tag{3.95}$$

The equation for $\partial Y/\partial x_0$ then reads

$$\begin{aligned} \frac{\partial Y}{\partial x_0}(Q) = \mathrm{e}^{\mathrm{i}\operatorname{Tr} Q(E + \mathrm{i}\widetilde{\varepsilon}\sigma_3 + \widetilde{\delta}\sigma_2) - \frac{1}{2}w_V^2 \operatorname{Tr} Q^2} \Big(& 2(\mathrm{i}E - w_V^2 \operatorname{Tr} Q)\, X(Q)^K \\ & + K X(Q)^{K-1} \int d\mu(Q')\, \mathrm{e}^{-w_T^2 \operatorname{Tr} QQ'} w_T^2 (1 - w_T^2 \operatorname{Tr} QQ') \frac{\partial Y}{\partial x_0}(Q') \Big). \end{aligned} \tag{3.96}$$

We observe that our system of equations is now closed, as no further unknowns enter on the right-hand side. Note that with the abbreviation (3.95), the equation (3.90)

for Y takes the shortened form

$$Y(Q) = \mathrm{e}^{\mathrm{i}\,\mathrm{Tr}\,Q(E+\mathrm{i}\widetilde{\varepsilon}\sigma_3+\widetilde{\delta}\sigma_2)-\frac{1}{2}w_V^2\,\mathrm{Tr}\,Q^2} X(Q)^K. \tag{3.97}$$

In summary, we have derived a system of two equations, (3.97) and (3.96), for two functions, Y and $\partial Y/\partial x_0$. A distinctive feature of this system (in the limit of vanishing symmetry-breaking parameters $\widetilde{\varepsilon}$ and $\widetilde{\delta}$) is its SU(1,1)-equivariance: if $Y(Q)$ and $(\partial Y/\partial x_0)(Q)$ form a solution of the system, then so do the transformed functions $Y(gQg^{-1})$ and $(\partial Y/\partial x_0)(gQg^{-1})$ for any $g \in \mathrm{SU}(1,1)$.

Once more, we remark that in the main analysis we will restrict to functions that only depend on x_3, x_0, x_2 (but not on x_1). After this restriction, the equation for Y (3.90) is already closed without the extra information in $\partial/\partial x_0 Y$. However, the resulting Laplace operator $\widetilde{\Delta}$ that fulfills

$$i^*\Delta Y = \widetilde{\Delta} i^* Y \tag{3.98}$$

breaks the full SU(1,1)-invariance.

4 Analysis of the AAT integral equation I: pp and ac phase

4.1 Target space of the field theory: a closer inspection

The unusual features of the Anderson transition can be attributed to the fact that the symmetry group $\mathrm{SU}(1,1) \equiv G$ is non-compact and the space C^3 of our matrices Q carries a G-invariant hyperbolic geometry. To prepare the ensuing analysis, we recall the material from Section 3.5.1 and delve a little deeper into the structure of C^3.

The three-dimensional space C^3 is diffeomorphic to $\mathbb{R}^3$ by

$$\mathbb{R}^3 \to C^3, \quad (x_0, x_1, x_2) \mapsto \left(x_0, x_1, x_2, x_3 = +\sqrt{x_0^2 + x_1^2 + x_2^2} \right), \tag{4.1}$$

where the x_μ ($\mu = 0,1,2,3$) were introduced in Eq. (3.82) as quasi-Cartesian coordinates for the space of positive Hermitian 2×2-matrices, $\mathrm{Herm}^+(2)$. We recall the characterization of C^3 as a boundary, $C^3 = \partial \overline{\mathrm{Herm}^+(2)}$. We also recall that our function ${}^g Y(Q)$ extends from C^3 into $\mathrm{Herm}^+(2)$.

Geometrically speaking, C^3 is a convex cone foliated by two-dimensional hyperboloids, $H^2_{x_0}$. Each of the latter is given as the solution set of a quadratic equation,

$$H^2_{x_0} : \; x_3^2 - x_1^2 - x_2^2 = x_0^2 \quad (x_3 \geq |x_0|), \tag{4.2}$$

for the variables x_j ($j = 1,2,3$) with the parameter $x_0 \in \mathbb{R}$ held fixed. [Invoking the language of special relativity, we might say that x_3 is a positive energy, x_1 and x_2 are momentum components, and $|x_0|$ is the invariant mass of a relativistic particle.] The non-compact group G acts transitively on each of the hyperboloids $H^2_{x_0}$, by conjugation $Q \mapsto gQg^{-1}$. In consequence, the target space C^3 is a foliation by symmetry group orbits, with foliation parameter given by the $\mathrm{SU}(1,1)$-invariant x_0. Since the subgroup $\mathbb{Z}_2 \subset G$ of elements $\pm\mathbf{1}$ acts trivially on Q, we may replace $G = \mathrm{SU}(1,1)$ by the Lorentz group $\mathrm{SU}(1,1)/\mathbb{Z}_2 \cong \mathrm{SO}(1,2) \equiv G'$. Doing so, we may

refer to G-invariant objects as "Lorentz invariants".

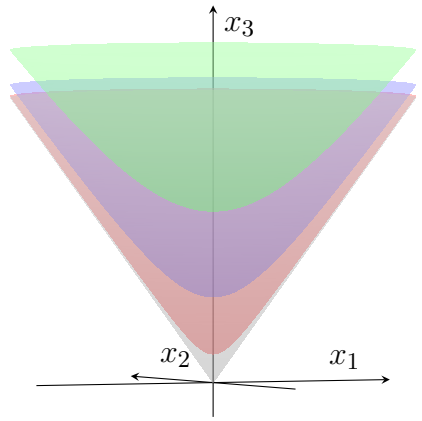

Figure 4.1: Picture of four members of the family $C^3 = \bigcup_{x_0 \in \mathbb{R}} H^2_{x_0}$: The boundary orbit H^2_0 (a.k.a. light cone in special relativity) in gray, and three other hyperboloids $H^2_{x_0>0}$.

4.2 $\mathrm{U}(1)_{\mathrm{i}\sigma_3}$-symmetry reduction

A good starting point for the analysis of the AAT integral equation (3.90) is the inspection of the $\mathrm{U}(1)_{\mathrm{i}\sigma_3}$-invariant solution, i.e., the function ${}^{g=\mathrm{id}}Y \equiv Y$. This corresponds to turning off the symmetry-breaking parameter $\widetilde{\delta}$, $\widetilde{\delta} = 0$. We remind the reader that the $\mathrm{U}(1)_{\mathrm{i}\sigma_3}$-invariant solution corresponds to the $\mathrm{U}(1)_{\mathrm{i}\sigma_3}$-invariant (extremal) Gibbs state. The present discussion will yield expressions for the mean local density of states $\mathbb{E}(\rho_{n,\varepsilon})$ and explicit expressions for the pp-type solution Y_{pp} for weak and strong disorder at large dimension parameter K. Additionally, properties of the $\mathrm{U}(1)_{\mathrm{i}\sigma_3}$-invariant ac-type solution Y_{ac} are discussed, and we derive an explicit expression for Y_{ac} in the deep metallic limit $w_V^2 = 0$, and $K \to \infty$. (Of course, the expression is expected to hold to a good approximation for $w_V \ll 1$, $K \gg 1$).

4.2.1 Restricted Laplacian

With $\widetilde{\delta}$ absent, the symmetry-breaking response ${}^{g_s}C$ in Eq. (3.24) is also absent, and the expression (3.25) for Y simplifies to

$$Y = \mathbb{E}\Big(\mathrm{e}^{2\mathrm{i}x_0 A - 2x_3 D}\Big). \tag{4.3}$$

Thus Y depends now on two variables only, the Lorentz-invariant function x_0 and the $\mathrm{U}(1)_{\mathrm{i}\sigma_3}$-invariant function x_3, both defined as Cartesian coordinates on $\mathrm{Herm}^+(2)$ by Eq. (3.82).

To pull back the analysis from $\mathrm{Herm}^+(2)$, we introduce two restricted coordinate

functions p, q on C^3 by

$$p = i^*(x_3 + x_0), \quad q = i^*(x_3 - x_0), \tag{4.4}$$

and define their partial derivatives $\partial/\partial p$ and $\partial/\partial q$ by the convention that i^*x_1 is held fixed. [The special choice of x_1 is made in anticipation of Y becoming x_2-dependent when $\widetilde{\delta}$ (hence ${}^{g_s}C$) is turned back on.] Now for functions Y on $\mathrm{Herm}^+(2)$ that depend on x_3, x_0 (but not on x_1, x_2) the result ΔY of applying the Laplacian (3.88) restricts to

$$i^*(\Delta Y) = i^* \frac{1}{4} \left(\frac{\partial^2}{\partial x_3^2} - \frac{\partial^2}{\partial x_0^2} \right) Y = \frac{\partial^2}{\partial p \, \partial q} i^* Y \equiv \frac{\partial^2}{\partial p \, \partial q} Y. \tag{4.5}$$

[Here and in the following, we abuse the notation by simply writing Y instead of i^*Y (as the meaning will always be clear from the context).] We see that $i^*\Delta Y$ is now expressed by C^3-data alone. Hence the equation (3.90) for Y is already closed (when $\widetilde{\delta} = 0$), and there is no need to carry along the extra information in $\partial Y/\partial x_0$.

4.2.2 $\mathrm{U}(1)_{\mathrm{i}\sigma_3}$-reduced AAT integral equation

Let us then make the closed equation (3.90) explicit in p and q. Another view of Eq. (4.4) is $p = |u|^2 \geq 0$ and $q = |v|^2 \geq 0$, where u, v appeared in the early going of Section 3.3. To complete the coordinate system for C^3, we augment p, q by an angular variable, $\phi = \arg(\bar{u}v)$. The integration measure $d\mu(Q)$ on C^3 is then expressed as

$$d\mu(Q) = dp \, dq \, \frac{d\phi}{2\pi}, \tag{4.6}$$

and the exponent of the integral kernel $\mathrm{e}^{-w_T^2 \mathrm{Tr}\, QQ'}$ becomes

$$\mathrm{Tr}\, QQ' = pp' + qq' - 2\sqrt{pqp'q'} \cos(\phi - \phi'). \tag{4.7}$$

Since the $\mathrm{U}(1)_{\mathrm{i}\sigma_3}$-invariant function Y does not depend on ϕ, we may average the kernel over angles to arrive at

$$\begin{gathered} Y(p,q) = \mathrm{e}^{\mathrm{i}E(p-q) - \varepsilon(p+q) - \frac{1}{2}w_V^2 (p-q)^2} \times \ldots \\ \ldots \times \left(\int_{\mathbb{R}_+^2} dp' dq' \, \mathrm{e}^{-w_T^2(pp'+qq')} I_0(2w_T^2 \sqrt{pqp'q'}) \, \frac{\partial^2}{\partial p' \partial q'} Y(p', q') \right)^K , \end{gathered} \tag{4.8}$$

with I_0 a modified Bessel function of the first kind. The $\mathrm{U}(1)_{\mathrm{i}\sigma_3}$-reduced equation, Eq. (4.8), already contains information about the transition. In the metallic phase, the linearly stable solution of this equation (for $\varepsilon = 0$), Y_{ac}, breaks the $\mathrm{SU}(1,1)$

symmetry by remaining dependent on both variables p, q (or $p-q$ and $p+q$). When tuning the system parameters to the transition point, the scale where the stable fixed point Y_{ac} becomes effectively dependent on the Lorentz-symmetry-breaking coordinate $p+q$, moves to infinity. At the transition itself, the stable fixed point becomes independent of $p+q$ (for $\varepsilon = 0$) and turns into a fully symmetric pp solution Y_{pp} which only depends on the invariant mass $p-q$.

4.2.3 Dimensional reduction

It turns out that some special values of the solutions Y of Eq. (4.8) are already determined by a dimensionally reduced equation – these are the function values on the two subspaces

$$H^{\pm}: \; x_3 \pm x_0 = 0, \quad x_1 = x_2 = 0, \tag{4.9}$$

which are central half-axes in C^3. To see how the reduction works, set $q \equiv 0$ in Eq. (4.8). The integral kernel then becomes independent of q', so that the derivative with respect to q' is a total one and can be integrated. Using that $Y(p', \infty) = 0$, and abbreviating $Y(p, 0) \equiv Z_\varepsilon(p)$, we obtain the reduced equation

$$Z_\varepsilon(p) = \mathrm{e}^{\mathrm{i}(E+\mathrm{i}\varepsilon)p - \frac{1}{2}w_V^2 p^2} \left(-\int_0^\infty dp' \mathrm{e}^{-w_T^2 p p'} \frac{\partial}{\partial p'} Z_\varepsilon(p') \right)^K, \tag{4.10}$$

which determines $Z_\varepsilon(p)$ for $p \geq 0$. To extend Z_ε to the negative real axis, we vary the blueprint above: we set $p = 0$ and $Y(0, q) = Z_\varepsilon(-q)$ and so on, to obtain the variant of Eq. (4.10) which determines the second branch of Z_ε, where its argument is negative. That branch glues continuously to the first one because $Z_\varepsilon(0+) = Z_\varepsilon(0-) = 1$. The finished product of the construction is a smooth function $\mathbb{R} \ni r \mapsto Z_\varepsilon(r)$ with the property $Z_\varepsilon(-r) = \overline{Z_\varepsilon(r)}$.

Eq. (4.10) is relatively easy to analyze. Its solution interpolates between $Z_\varepsilon(r = 0) = 1$ and $Z_\varepsilon(r \to \pm\infty) = 0$. For the special energy $E = 0$, the function $Z_\varepsilon(r)$ is real-valued, even, positive, and monotonically decreasing on $\mathbb{R}_+$. The dimensional reduction (4.10) has lost information about the non-compact symmetry group (it only depends on a single coordinate function) and, as such, cannot show critical behavior. Physically speaking, this equation still contains information about the average local density of states. However, we have already argued in the introductory chapter, Chapter 2.2.6, that the average local density of states is uncritical; the fluctuations of the distribution of the local density of states have to be analyzed. Nevertheless, it is still worth analyzing the average local density of states in the weak- and strong-disorder limit. This can be put into practice with Eq. (4.10).

4.2.4 Mean local density of states in high dimensions

We recall that in the present work, we are mainly interested in the regime of high dimensions and strong disorder. For a large dimension parameter $K \gg 1$, the analysis of Eq. (4.10) simplifies due to

$$\lim_{K\to\infty}(1-y/K)^K = \mathrm{e}^{-y}. \tag{4.11}$$

In order to exploit that limit law, we change variables by $y = p\sqrt{K}w_T$, $y' = p'\sqrt{K}w_T$, and we introduce the dimensionless parameters $w^2/K = w_V^2/Kw_T^2$, $w = w_V/w_T$ and $\eta = (E+\mathrm{i}\varepsilon)/\sqrt{K}w_T$, which are to be kept fixed as K grows large. By partially integrating in Eq. (4.10), we are then led to the scaled equation (let $Z_\varepsilon \equiv Z$ for now)

$$Z(\cdot) = \mathrm{e}^{\mathrm{i}\eta y - \frac{1}{2}\frac{w^2}{K}y^2}\left(1 - \frac{y}{K}\int_0^\infty dy' Z(\cdot')\,\mathrm{e}^{-yy'/K}\right)^K. \tag{4.12}$$

As will be seen presently, the integral of Z over $\mathbb{R}_+$ remains finite in the proposed scaling limit for large K. In anticipation of that, we take $K\to\infty$ in (4.12) to obtain the equation

$$Z(\cdot) = \exp\left(\mathrm{i}\eta y - \frac{1}{2}\frac{w^2}{K}y^2 - y\int_0^\infty Z(\cdot')\,dy'\right) \quad (K\to\infty). \tag{4.13}$$

Its solution for $w^2 = 0$, the limit of vanishing disorder potential (referred to as the "weak-disorder limit" for short), is exponential in $y = p\sqrt{K}w_T$:

$$Z = \mathrm{e}^{-\left(\sqrt{1-(\eta/2)^2}-\mathrm{i}\eta/2\right)y}. \tag{4.14}$$

Next we relate the expression for the average local density of states, $\mathbb{E}(\rho_n(E))$, to the function Z. From the introductory section on spectral theory, Section 2.2, we recall that the average local density of states is connected with the Green's function:

$$\mathbb{E}(\rho_n(E)) = \frac{1}{\pi}\mathbb{E}\left(\mathrm{Im}(G_n(E-\mathrm{i}\varepsilon))\right). \tag{4.15}$$

By recalling the identity (4.3), $Z(p) = Y(p,0)$, and

$$A_n = \frac{\mathrm{Re}(G_n(E-\mathrm{i}\varepsilon))}{|G_n(E-\mathrm{i}\varepsilon)|^2}, \quad D_n = \frac{\mathrm{Im}(G_n(E-\mathrm{i}\varepsilon))}{|G_n(E-\mathrm{i}\varepsilon)|^2}, \tag{4.16}$$

Eq. (3.16), we obtain

$$Z(p) = \mathbb{E}\left(\mathrm{e}^{\mathrm{i}p\frac{1}{G_n(E+\mathrm{i}\varepsilon)}}\right), \tag{4.17}$$

and

$$\mathbb{E}(\rho_n(E)) = \frac{1}{\pi}\mathrm{Re}\left(\int_0^\infty \mathrm{d}p\ Z(p)\right). \tag{4.18}$$

With the result for Z in the weak-disorder limit, Eq. (4.14), we see that the mean local density of states $\mathbb{E}(\rho_n(E))$ obeys Wigner's semicircle law [98, 99]:

$$\mathbb{E}(\rho_n(E))\,dE = \frac{1}{\pi}\sqrt{1 - E^2/(4Kw_T^2)}\,\frac{dE}{\sqrt{K}w_T}, \tag{4.19}$$

in the form of an energy band $-2\sqrt{K}w_T \le E \le 2\sqrt{K}w_T$ of width set by the random hopping with strength w_T.

Our interest, however, is in the opposite limit of large $w^2/K = w_V^2/Kw_T^2$ ("strong disorder"). In that case, the solution for Z is a Gaussian with offset:

$$Z = \mathrm{e}^{-\frac{1}{2}\frac{w^2}{K}y^2 - \mathrm{i}\eta y}. \tag{4.20}$$

By returning to the variable p and integrating as before, we obtain a result that one would expect:

$$\mathbb{E}(\rho_n(E))\,dE = \frac{dE}{\pi}\,\mathrm{Re}\int_0^\infty Z(p)\,dp = \exp\left(-\frac{E^2}{2w_V^2}\right)\frac{dE}{\sqrt{2\pi}\,w_V}. \tag{4.21}$$

Indeed, by simple reasoning, the mean local density of states in the strong-disorder limit is given by the distribution of the on-site potential disorder.

4.3 Solution of pp-type

We now communicate that Eq. (4.8) for $\varepsilon \to 0$ always has a solution, Y_{pp}, which possesses the full Lorentz symmetry. (As a disclaimer, we must caution that, while this solution always exists, it is linearly unstable outside the pp-phase.)

Taking Lorentz invariance for granted, the solution $Q \mapsto Y_{\mathrm{pp}}(Q)$ is uniquely determined as follows. First, assume $\mathrm{Tr}\,\sigma_3 Q > 0$. In that case, there exists a Lorentz transformation $Q \mapsto gQg^{-1}$ that conjugates Q to $\mathrm{diag}(p, 0)$ with $p > 0$, and we must have $Y_{\mathrm{pp}}(Q) = Z_{\varepsilon=0}(p)$ as explained at the end of Section 4.2. Second, if $\mathrm{Tr}\,\sigma_3 Q < 0$, then we Lorentz-conjugate to $\mathrm{diag}(0, -q)$ (still with $q > 0$) and set $Y_{\mathrm{pp}}(Q) = Z_0(-q)$. Third, the values of $Y_{\mathrm{pp}}(Q)$ for $\mathrm{Tr}\,\sigma_3 Q = 0$ (in which case Q typically fails to be diagonalizable) are given by continuous extension. The outcome of the whole procedure can be succinctly summarized as

$$Y_{\mathrm{pp}}(Q) = Z_0(\mathrm{Tr}\,Q). \tag{4.22}$$

By construction, the function Y_{pp} so defined is the unique Lorentz-invariant function that satisfies the requirement of taking the boundary values prescribed by Eq. (4.10) on the two half-axes $H^{\pm} \subset C^3$.

4.3.1 Y_{pp} describes pp spectrum

We now go back to the spectral integral Eq. (3.73) from Section 3.4, which we state again (for the pp case):

$$K_{n,\varepsilon}^{\mathrm{pp}} \stackrel{!}{=} \int \mathrm{d}Q_n \, \mathrm{e}^{-\mathrm{Tr}(\varepsilon\sigma_3)Q_n} Y_{\mathrm{pp}}(Q_n). \tag{4.23}$$

As a consequence of Lorentz invariance, and the infinite volume of the Lorentz-group orbits in C^3, the spectral integral for zero regulator $\varepsilon = 0$, $\int Y_{\mathrm{pp}}(Q)\, d\mu(Q)$ is divergent. From expression (4.23 it then follows immediately that the observable $K_{n,\varepsilon}$ diverges like ε^{-1}, when the regulator ε is sent to zero. Such a divergence is characteristic of spectral measures of pp-type, as we have learned in the introductory section, Section 2.2. Now on physical and mathematical grounds, the pp-phase exists and is thermodynamically stable for strong enough disorder. Therefore, the solution Y_{pp} is expected to be stable with respect to generic perturbations in the strong-disorder regime ($w_V^2 \gg K w_T^2$). The corresponding extremal Gibbs state is unique (for fixed system parameters) and obviously Lorentz-invariant; its restriction on observables localized at the distinct site n is given by the Lorentz-invariant function Y_{pp}. Hence we have substantiated the claims made about the pp phase in the Outlook 3.4.5.

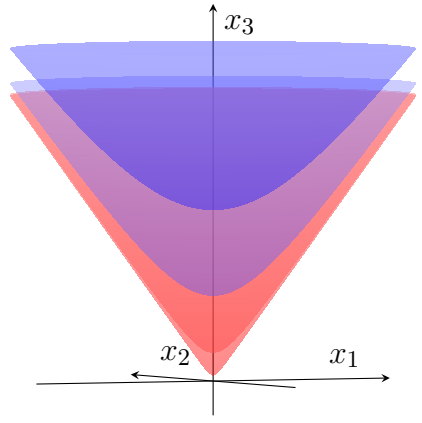

Figure 4.2: Sketch of the solution of pp-type for $x_0 \geq 0$: It is constant on every fixed hyperboloid $H^2_{x_0=m}$ and decays in m direction. The decay is indicated by the change of color from red to blue.

4.4 Solutions of ac-type

4.4.1 $\mathrm{U}(1)_{\mathrm{i}\sigma_3}$-invariant solutions of ac-type

In the opposite limit of weak disorder ($w_V^2 \ll w_T^2$), K large and energy E not too far from the band center, the solution Y_{pp} is certain to be unstable with respect to generic perturbations. A different type of stable solution, Y_{ac}, describing metallic behavior, emerges. That solution exhibits fast decay in the variables p and q, thereby spontaneously breaking the non-compact one-parameter subgroups generated by σ_1 and σ_2 in the symmetry group $\mathrm{SO}(1,2) \cong \mathrm{SU}(1,1)/\mathbb{Z}_2$. By virtue of that decay, the expectation $\mathbb{E}(|G_n|^{2r})$ is finite for any $r \in \mathbb{C}$ with positive real part, which is the hallmark of absolutely continuous spectral measures and ergodic eigenfunctions of the Hamiltonian.

As a demonstration of principle, let us present the solution Y_{ac} in the deep-metallic limit of $w_V^2 = 0$ and $K \to \infty$. Invoking the large-K scaling of Section 4.2.4, we see that the Bessel function I_0 in Eq. (4.8) can be approximated as $I_0 \approx 1$ in that limit. The integral over p', q' then separates, and so does the solution:

$$Y_{\mathrm{ac}}(p,q) = Z_0(p)\,\overline{Z_0(q)} = \mathrm{e}^{-\sqrt{Kw_T^2-(E/2)^2}(p+q)+\mathrm{i}(E/2)(p-q)} \qquad (w_V^2 = 0, \quad K \gg 1). \tag{4.24}$$

This expression illustrates the qualitative features stated above, most notably the finiteness of the spectral integral (3.73) for regulator $\varepsilon = 0$:

$$\mathbb{E}\left(|G_n(E)|^2\right) = \int_{\mathbb{R}_+^{\not\varepsilon}} \mathrm{d}p\,\mathrm{d}q\, Y_{\mathrm{ac}}(p,q) < \infty. \tag{4.25}$$

We remark that, similar to the derivation at the beginning of Section (3.4.1), one can also relate higher moments of the distribution of the local density of states, $\mathbb{E}(|G_n|^{2r})$, to the solutions ${}^gY$. For the ac-type solutions Y_{ac} also the higher moments stay finite for regulator $\varepsilon \to 0$:

$$\mathbb{E}\Big(|G_n(E)|^{2r}\Big) = \int_{\mathbb{R}_+^2} dp\,dq\, Y_{\mathrm{ac}}(p,q)\,(pq)^{r-1} < \infty \tag{4.26}$$

for all r with $\mathrm{Re}(r) > 0$. The finiteness of $\mathbb{E}(|G_n|^2)$ (and higher moments) is characteristic of an absolutely continuous spectral measure. Note that due to the fast decay of Y_{ac}, the limit of sending the regulator to zero, $\varepsilon \to 0$, and integral can be exchanged in the expression (3.73) for $K_{n,\varepsilon}$ or in the corresponding expression for the higher moments. This is consistent with our earlier discussion in Subsection 3.4.4 in Chapter 3, where we explained that in the metallic phase the corresponding

integrals do not require regularization.

For the related case of the Anderson model, a solution of the type of Eq. (4.24) was exhibited in the work of [60] using methods similar to ours.

4.4.2 Lorentz-transformed solutions of ac-type, space of ac-type solutions and corresponding extremal Gibbs states

In this section, we delve deeper into the geometry of the spontaneous symmetry breaking mechanism in the metallic phase. Furthermore, the observations of this subsection pave the way for a full understanding of the critical regime and especially the construction of sc type-solutions. The critical regime will be the subject of the following sections.

To start, we recall the central observation from Section (3.4) and translate what it means on the level of the "bosonic" equations (3.97) and (3.96): The $\mathrm{U}(1)_{\mathrm{i}\sigma_3}$-invariant solution Y_{ac} is just one of a two-dimensional continuum of stable solutions. Indeed, as was pointed out at the very end of Section 3.5.3, the system of equations (3.97) and (3.96) for $\widetilde{\varepsilon} = \widetilde{\delta} = 0$ is Lorentz-equivariant and given any solution Y_{ac} (augmented by $\partial Y_{\mathrm{ac}}/\partial x_0$) we can obtain another solution ${}^{g}Y_{\mathrm{ac}}$ [augmented by $\partial({}^{g}Y_{\mathrm{ac}})/\partial x_0$] by making a symmetry transformation

$$ {}^{g}Y_{\mathrm{ac}}(Q) = Y_{\mathrm{ac}}(g^{-1}Qg), \quad g \in \mathrm{SU}(1,1). \tag{4.27} $$

The moduli space of solutions thus obtained is the coset space $\mathrm{SU}(1,1)/\mathrm{U}(1)$, which may be interpreted as the order-parameter space of the metallic phase. We will sometimes call it the metallic moduli space. We recall from Section 3.4 that a strategy to select one of them is to Lorentz transform the explicit symmetry-breaking term

$$ \mathrm{e}^{-\varepsilon \operatorname{Tr}\sigma_3 Q} \to \mathrm{e}^{-\varepsilon \operatorname{Tr}\sigma_3 g^{-1}Qg} \tag{4.28} $$

and sending ε to zero after performing the thermodynamic limit.

We now delve a little deeper into the structure of the transformed metallic solutions. In light of the observations in Section 3.3, we expect that the non-compact nature of the Lorentz group has interesting consequences. In short, in comparison to compact moduli spaces, like the two-sphere S^2, the metallic moduli space (the Poincaré disk D^2) has an asymptotic boundary, the circle S^1. Under a finite Lorentz transformation, the solution (4.27) can be thought of as one point inside the disk D^2. It is the result of Lorentz transforming the center of the disk, i.e., the $\mathrm{U}(1)_{\mathrm{i}\sigma_3}$-invariant solution Y_{ac}, to a different point ${}^{g}Y_{\mathrm{ac}}$ in D^2. But when we take

the non-compact nature seriously, we can ask the question, what happens when we let the symmetry group transformation approach the asymptotic boundary of D^2?

Example

To answer this question, we will here consider an example at band center $E = 0$. While this example mainly serves as a demonstration of how Lorentz transformations act on the metallic solution Y_{ac}, it also introduces an important new coordinate system that will be used throughout the rest of this dissertation. As in previous sections, here we restrict ourselves to certain Lorentz transformations, namely the one-parameter subgroup $g_s = \exp((s/2)\sigma_1)$. The action of these transformations becomes very transparent in so-called *horospherical* coordinates:

$$\begin{aligned} i^*x_0 = m, \quad i^*x_1 = b, \quad i^*x_2 = \frac{1}{2}(\mathrm{e}^{\varphi} - (m^2+b^2)\mathrm{e}^{-\varphi}), \\ i^*x_3 = \frac{1}{2}(\mathrm{e}^{\varphi} + (m^2+b^2)\mathrm{e}^{-\varphi}), \end{aligned} \tag{4.29}$$

where $m, b, \varphi : C^3 \to \mathbb{R}$. m is the Lorentz invariant $m = 1/2\ \mathrm{Tr}Q$. The coordinate lines of b are horocycles on a fixed hyperboloid $H^2_{x_0}$ and φ is the coordinate of the Lorentz-boost geodesics in the x_2x_3 plane. The coordinates b, φ are symmetry degrees of freedom. This coordinate system is useful because the above one-parameter subgroup with elements g_s simply acts as a translation in the φ coordinate. Indeed,

$$\begin{aligned} \mathrm{e}^{\frac{s}{2}\sigma_1}\, i^*x_3\, \mathrm{i}\sigma_3\, \mathrm{e}^{-\frac{s}{2}\sigma_1} &= \cosh(s)\, i^*x_3\, \mathrm{i}\sigma_3 + \sinh(s)\, i^*x_3\, \sigma_2, \\ \mathrm{e}^{\frac{s}{2}\sigma_1}\, i^*x_2\, \sigma_2\, \mathrm{e}^{-\frac{s}{2}\sigma_1} &= \cosh(s)\, i^*x_2\, \sigma_2 + \sinh(s)\, i^*x_2\, \mathrm{i}\sigma_3. \end{aligned} \tag{4.30}$$

Hence the two coordinate functions i^*x_3, i^*x_2, under the above transformations, are mapped to

$$\begin{aligned} i^*x_3 \to \cosh(s)\, i^*x_3 + \sinh(s)\, i^*x_2 &= \frac{1}{2}(\mathrm{e}^{\varphi+s} + (m^2+b^2)\,\mathrm{e}^{-\varphi-s}), \\ i^*x_2 \to \cosh(s)\, i^*x_2 + \sinh(s)\, i^*x_3 &= \frac{1}{2}(\mathrm{e}^{\varphi+s} - (m^2+b^2)\,\mathrm{e}^{-\varphi-s}). \end{aligned} \tag{4.31}$$

It can be verified that for functions on $\mathrm{Herm}^+(2)$ that depend on x_3, x_0, x_2 (but not on x_1) the result $\Delta^{g_s}Y$ of applying the Laplacian (3.94) restricts to:

$$i^*(\Delta^{g_s}Y) = i^*\frac{1}{4}\left(\frac{\partial^2}{\partial x_3^2} - \frac{\partial^2}{\partial x_0^2} - \frac{\partial^2}{\partial x_2^2}\right){}^{g_s}Y = \left(-\frac{1}{4}\left(\frac{\partial^2}{\partial m^2} + \frac{\partial^2}{\partial b^2}\right) + \frac{1}{2b}\frac{\partial}{\partial b} \circ D\right) i^*\,{}^{g_s}Y. \tag{4.32}$$

Again, from now on, we will omit the pullback $i^{*g_s}Y \equiv {}^{g_s}Y$. Under the above

restriction, the equation (3.90) for ${}^{g_s}Y$ is already closed, and again there is no need to carry the extra information in $\partial {}^{g_s}Y/\partial x_0$. The above restricted Laplacian (4.32) is translation-invariant in φ. Consequently, the restricted AAT equation (3.90) is equivariant under the Lorentz boost $\varphi \to \varphi - s,\ s \in \mathbb{R}$.

In the deep ac regime $w \ll w_c$ and in high dimensions $K \gg 1$, the $\mathrm{U}(1)_{\mathrm{i}\sigma_3}$-invariant solution Y_{ac} can be approximated by a Gaussian in the mass m and the horospherical coordinate b. Indeed, the extreme case $w_V^2 = 0$ and $K \to \infty$ has been discussed in the previous section 4.4.1, and it has been shown that the $\mathrm{U}(1)_{\mathrm{i}\sigma_3}$-invariant solution takes the form

$$\begin{gathered} Y_{\mathrm{ac}}(Q) = Z_0(p)\,\overline{Z_0(q)} = \exp(-2\beta\, x_3) = \exp\left(-\beta\,(\mathrm{e}^{\varphi} + (m^2+b^2)\mathrm{e}^{-\varphi})\right), \\ \beta = \sqrt{K w_T^2} \in \mathbb{R}^+. \end{gathered} \tag{4.33}$$

Next we act on Y_{ac} with the one-parameter subgroup $g_s = \exp((s/2)\,\sigma_1)$, $s \in \mathbb{R}$ to obtain the transformed metallic solutions ${}^{g_s}Y_{\mathrm{ac}}$. [They are also solutions by equivariance of the "bosonic" AAT integral equation (3.90) under the one-parameter subgroup for $\widetilde{\varepsilon} = \widetilde{\delta} = 0$.] The result is:

$${}^{g_s}Y_{\mathrm{ac}}(Q) = \exp\left(-\beta\left(\mathrm{e}^{\varphi - s} + (m^2+b^2)\mathrm{e}^{-\varphi+s}\right)\right). \tag{4.34}$$

What happens for large parameters $s \gg 0$? [Of course, we could equivalently look for small parameters $s \ll 0$. Here and in the following, we will nevertheless concentrate on the large parameter limit. Only in Section 6.3 of the last chapter, Chapter 6, we will comment on the opposite limit.] As Eq. (4.34) shows, the support of ${}^{g_s}Y_{\mathrm{ac}}$ becomes elongated in a neighborhood of the φ geodesic for $m = b = 0$ and narrowed in other directions: For $(m,b) \neq (0,0)$ the rightmost term in Eq. (4.34) causes rapid decay of Y with increasing s. Only for $(m,b) = (0,0)$ this term is identically zero. The decay due to $\exp\left(-\beta \mathrm{e}^{\varphi - s}\right)$ is weakened for large s. For $s \to \infty$, the support eventually coincides with the ray

$$L_0 = \{(m,b) = (0,0),\, \varphi \in \mathbb{R}\}. \tag{4.35}$$

Note that, strictly speaking, the limit $s \to \infty$ does not yield a continuous function anymore (but a distribution, supported on the asymptotic boundary of the hyperboloids). Hence we can make the group parameter s arbitrarily large but not strictly infinite when allowing for classical (continuous) solutions of the AAT integral equation only. This observation explains the fact that the moduli space of ac-type solutions is H^2 and not its closure $\overline{H^2}$. [Later, we will see that there is an instance

of a continuous solution ${}^{g_s}Y$ when s goes to infinity. It happens at criticality; the result will be an sc-type (critical) solution.]

Clearly, we could $\mathrm{U}(1)_{\mathrm{i}\sigma_3}$-rotate the ray L_0 so that it ends at a different boundary point on $\partial H^2_{m=0}$ and obtain solutions supported on the rotated ray. This would correspond to restricting the analysis to a different class of functions (not depending on x_0, x_3, x_2, but on another combination). However, with the present observation in mind, in the following we will continue to restrict to functions that depend on x_0, x_3, x_2 and to the one-parameter subgroup $\exp((s/2)\sigma_1)$.

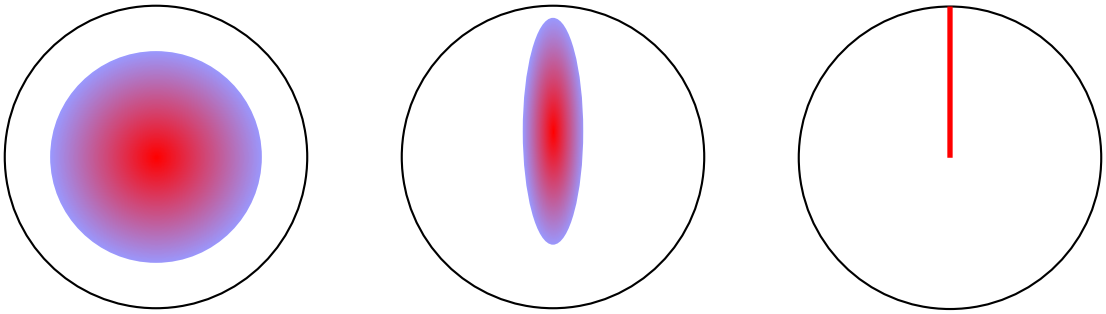

Figure 4.3: Support of three members of the metallic moduli space: The disks are the Poincaré disk model of $H^2_{x_0=0}$. The solutions are maximal in the red regions, decay in the blue regions, and are (almost) zero in the white regions. The $\mathrm{U}(1)_{\mathrm{i}\sigma_3}$-invariant solution Y_{ac} is on the left. In the middle and on the right, one sees symmetry-transformed solutions ${}^{g_s}Y$ with different parameters $s > 0$. In the middle picture, a moderate s and on the right picture a large s is shown.

We summarize what we know about the pp and ac solutions in a table:

spectrum	diagnostic	moduli space of Y
pp	$K_{n,\varepsilon} \sim \varepsilon^{-1}$	single point
ac	$K_{n,\varepsilon} < \infty$	H^2
sc	$K_{n,\varepsilon} \sim \varepsilon^{-\alpha}$	?

After analyzing the pp and deep ac phase, we now want to shed light on the remaining red question mark in Table (4.4.2). This is done in the remainder of this work. In the final paragraph of the present section, we motivate why the novel type of solutions with a different symmetry-breaking pattern and a correspondence to an sc spectrum are expected in this regime.

Heuristic argument for sc solution

The concept of symmetry-transformed ac-type solutions for large parameters s helps in understanding how the sc-type solutions emerge at criticality. The reason is that

this emergence relies on two effects. The first one is the one explained here: Under large s, ${}^{g_s}Y_{\mathrm{ac}}$ is elongated along the ray L_0 on the lightcone $H^2_{x_0=0}$ until its support coincides with this ray. But this process does not change the spectral integral (3.73) over ${}^{g_s}Y$ and alone cannot lead to new spectral behavior. Indeed, g_s is an isometry of the integral measure for all $s \in \mathbb{R}$ and, of course, the transformation $Y_{\mathrm{ac}} \to {}^{g_s}Y_{\mathrm{ac}}$ does not change the scaling of $K_{n,\varepsilon}$.

The second relevant effect becomes visible when tuning the parameters from the metallic phase to the critical manifold (in the parameter space spanned by K, w, w_V, E). In this process, the weight M of Y_{ac}, $M = \int \mathrm{d}\mu(Q)\, Y_{\mathrm{ac}}(Q)$, increases and eventually goes to infinity on the critical manifold (we will calculate the location of the critical manifold in the next section). This is because on the critical manifold the $\mathrm{U}(1)_{\mathrm{i}\sigma_3}$-invariant solution Y_{ac} turns into the pp solution Y_{pp} which has non-compact support.

The result of the combination of both effects is a function that has non-compact support but still breaks the hyperbolic symmetry. It is constant along horocycles centered around certain boundary points on the hyperboloids $H^2_{x_0}$. We thus expect sc solutions to arise from the coupled limit (for fixed K)

$$w \nearrow w_c, \quad s(w_c - w) \to \infty, \tag{4.36}$$

where s is again the symmetry parameter from the one-parameter subgroup with generator σ_1.

5 Analysis of the AAT integral equation II: critical behavior and sc type solutions

With the help of the geometric ideas from the last section, Section 4.4.2, in Chapter 4, we now have a clear agenda for the remainder of this work, especially the present chapter, Chapter 5. This chapter contains the central result of this work. It suggests that the critical regime of the Anderson transition is governed by a qualitatively new symmetry-breaking mechanism, namely symmetry breaking to a nilpotent rather than compact group. We will now explain the strategy to detect the novel symmetry-breaking mechanism.

First, we want to find the location of the critical manifold, i.e., the set in parameter space where the pp solution Y_{pp} becomes linearly unstable with respect to generic perturbations δY. Instability with respect to these perturbations is a signal that now the stable solutions of the AAT integral equation (3.90) are symmetry-broken. In other words, the critical manifold separates the insulating and metallic phases. However, it is not clear a priori which spectral type is realized on the critical manifold itself. For the purpose of locating the critical manifold, we will use harmonic analysis to find the eigenfunctions of the Lorentz-invariant linearized AAT operator, i.e., the linearized AAT equation around the Lorentz-symmetric, pp-type solution Y_{pp}. This happens in Section 5.1. Harmonic analysis is a strong tool: With it, we are able to derive an explicit formula for the location of the critical manifold in high dimensions $K \gg 1$, exact in the limit $K \to \infty$, and this formula is in good accordance with numerical data for small K (already $K = 3$). Nevertheless, even more valuable is the fact that we can write down the full eigenfunctions of the linearized AAT operator. We can do so not only in asymptotic regimes but in the whole field-theory target space C^3. We recall that we have discussed the basic tools and necessary formulas of harmonic analysis on the symmetric space H^2 in an introductory section, Section 2.4. The knowledge of the eigenfunctions is the base for the analysis of the $\mathrm{U}(1)_{\mathrm{i}\sigma_3}$-invariant ac type solutions Y_{ac} when approaching the critical manifold. In

this work, we do so by fixing the other parameters and sending $w \nearrow w_c$. This will be the subject of Section 5.2. We will end up with an analytical expression for Y_{ac} for $w \nearrow w_c$, and we will find its scaling with $w_c - w$. This scaling determines the divergence of the weight $M = \int \mathrm{d}\mu(Q)\, Y_{\mathrm{ac}}(Q)$ on the way to the critical manifold. Afterwards, in the light of the heuristics presented in Subsection 4.4.2, we symmetry-transform the solution Y_{ac} to ${}^{g_s}Y_{\mathrm{ac}}$. We will see that a certain scaling relation

$$s = s(w_c - w) \to \infty, \quad w_c \nearrow w, \tag{5.1}$$

leads to a continuous functions Y_{sc} with a nilpotent symmetry rather than a compact or a full Lorentz symmetry on the critical manifold. In more geometrical terms, the critical solutions are constant on horocycles centered around a certain boundary point on C^3. This is done in Section 5.3. Finally, we will complete Table 4.4.2 by inserting the expression so obtained for the critical solutions Y_{sc} into the spectral integral (3.73). We show that integrating Y_{sc} against the regulator term $\exp(-\varepsilon \operatorname{Tr} Q\sigma_3)$ leads to sc-type scaling of the correlator $K_{n,\varepsilon}$. Heuristically, this scaling comes from the fact that Y_{sc} possesses a non-compact symmetry but is not fully Lorentz-invariant.

5.1 Harmonic analysis and location of critical manifold

In this section, we derive an exact expression for the critical manifold in high dimensions $K \to \infty$:

$$K(w_c) = \frac{1}{\sqrt{2}} \frac{w_c}{\ln(w_c)} \exp\left(\frac{E^2}{2w_V^2}\right). \tag{5.2}$$

Note that, up to a logarithmic correction, K is proportional to the critical disorder strength w_c.

The critical manifold denotes the set of points in the (K, w, w_V, E) parameter space, where the pp solution (4.22) becomes linearly unstable against perturbations δY. To derive Eq. (5.2), it suffices to restrict to perturbations invariant under the $\mathrm{U}(1)_{\mathrm{i}\sigma_3}$ subgroup. (In-)stability against Lorentz-transformed perturbations follows from Lorentz-equivariance. We linearize the "bosonic" AAT integral equation (3.90) around the pp solution Y_{pp} and compute the eigenfunctions of the corresponding linear operator. The fundamental observation that makes this goal realistic is the fact that Y_{pp} and $(\partial Y/\partial x_0)_{\mathrm{pp}}$ have full Lorentz symmetry. This opens the door for the use of harmonic analysis on the field theory target space C^3. Its

purpose is to find the structure of the eigenfunctions in the symmetry degrees of freedom $g \in \mathrm{SU}(1,1)$. Having found it, we can integrate out the symmetry coordinates g and obtain a linear integral equation in the Lorentz-invariant mass m. It then remains to calculate the eigenvalues of this reduced equation. When the eigenvalue of maximal magnitude reaches magnitude one, the point of linear instability of the pp solution is reached. For arbitrary parameters K, w, w_v, E, we compute the maximal eigenvalue numerically. However, in the high-dimensional limit $K \to \infty$, and correspondingly strong disorder limit $w \to \infty$, we can determine the maximal eigenvalue and the related eigenfunction analytically. This yields the formula for the critical manifold given in (5.2). Nevertheless, already for small K, e.g., $K = 3$, the analytical formula is in good accordance with the numerical predictions.

5.1.1 Linearization

In the linear stability analysis around the pp solution pair $Y_{\mathrm{pp}}, (\partial Y/\partial x_0)_{\mathrm{pp}}$, instead of solving the full AAT equation, we study the differential of the corresponding nonlinear operator, which defines a linear operator. In other words, we perturb Y_{pp} by a function δY that has the general symmetry-broken form of ${}^{g_s}Y$ (3.25):

$$ {}^{g_s}Y(x_0, x_3, x_2; t) = Y_{\mathrm{pp}}(x_0) + t\,\delta Y(x_0, x_3, x_2), \quad t \in \mathbb{R}. \tag{5.3} $$

We then insert ${}^{g_s}Y(.;t)$ on both sides of the AAT equation, Eq. (3.90), and differentiate with respect to t at $t = 0$. The result is:

$$ \begin{aligned} \delta X^{\mathrm{new}}(Q) &= \int \mathrm{d}\mu(Q')\, e^{-w_T^2 \,\mathrm{Tr}\, QQ'}\, \Delta\, \delta Y(Q'), \\ \delta Y^{\mathrm{new}}(Q) &= K \frac{Y_{\mathrm{pp}}(Q)}{X_{\mathrm{pp}}(Q)}\, \delta X^{\mathrm{new}}(Q). \end{aligned} \tag{5.4} $$

The equation for δY (5.4) is a linear integro-differential equation, which is analytically much easier to handle than the full AAT equation.

5.1.2 Extracting the eigenfunctions

Choice of coordinates

To the subsequent calculation, we introduce *hyperbolic polar coordinates* as a convenient coordinate system:

$$ i^* x_0 = m, \quad i^* x_3 = |m| \cosh(\theta), \quad i^* x_1 = |m| \sinh(\theta) \cos(\phi), \quad i^* x_2 = |m| \sinh(\theta) \sin(\phi). \tag{5.5} $$

Here m is the Lorentz-invariant mass, and θ, ϕ parameterize the symmetry orbits, $H^2_{x_0}$, generated by the adjoint action $Q \to gQg^{-1}$. $\theta : H^2 \to \mathbb{R}^+$ is the hyperbolic radius and $\phi : H^2 \to (0, 2\pi)$ is the hyperbolic angle. Indeed, we can rewrite Q in the above coordinates as a result of the group action on a base point q_0: The base point sweeps continuously through the different hyperboloids $H^2_{x_0}$ foliating the convex cone C^3, as the mass m varies. For fixed m, $q_0 = q_0(m)$ is the base point of the fixed hyperboloid $H^2_{x_0=m}$. Because the G-action, parameterized by hyperbolic polar coordinates, is transitive, all the other points on the hyperboloid $H^2_{x_0=m}$ are then reached by acting with G on q_0. Formally, the above explanation boils down to:

$$i^*Q = gq_0g^{-1}, \quad q_0 = m\mathbf{1} + |m|\sigma_3, \quad g = \mathrm{e}^{\mathrm{i}\frac{\phi}{2}\sigma_3}\mathrm{e}^{\frac{\theta}{2}\sigma_1}. \tag{5.6}$$

The invariant measure $\mathrm{d}\mu(Q)$ is given by:

$$\mathrm{d}\mu(Q) = |m|\mathrm{d}m\,\sinh(\theta)\mathrm{d}\theta\,\frac{\mathrm{d}\phi}{\pi}. \tag{5.7}$$

The Laplace operator (3.94), when acting on functions which depend on x_3, x_0, x_2 (but not on x_1), in these coordinates reduces to:

$$\begin{aligned} i^*\Delta = \Bigg\{ \frac{1}{4m^2}\left(-\frac{1}{\sinh(\theta)}\frac{\partial}{\partial\theta}\sinh(\theta)\frac{\partial}{\partial\theta} - \frac{1}{\sinh(\theta)^2}\frac{\partial^2}{\partial\phi^2}\right) - \frac{1}{4}\frac{\partial^2}{\partial m^2} + \\ + \frac{1}{2m}\frac{\partial}{\partial m}\left(\frac{\cosh(\theta)}{\sinh(\theta)}\frac{\partial}{\partial\theta} - \frac{1}{\sinh(\theta)^2}\frac{\sin(\phi)}{\cos(\phi)}\frac{\partial}{\partial\phi}\right)\Bigg\} i^*. \end{aligned} \tag{5.8}$$

For better readability, we will henceforth avoid the pullback symbol i^*, with the understanding that all functions are now restricted to C^3.

Two ansatzes

A natural choice for the eigenfunctions is a product ansatz, separating the dependence on the symmetry group coordinates g from the dependence on the mass:

$$\delta Y(Q) = \sum_{n\in\mathbb{Z}} \delta Y_n(m,\theta)\,\omega_n(\phi), \quad \delta Y_n(m,\theta) = \sum_{\lambda} \delta y_{n,\lambda}(m)\,\Omega_{n,\lambda}(\theta). \tag{5.9}$$

In Eq. (5.9) n labels the angular eigenfunction $\omega_n(\phi)$, and λ is a number specifying the radial parts of the eigenfunctions, $\Omega_{n,\lambda}$. As announced above, we restrict ourselves to the $\mathrm{U}(1)_{\mathrm{i}\sigma_3}$-invariant mode $n = 0$:

$$\delta Y = \sum_{\lambda} \delta y_\lambda(m)\,\Omega_\lambda(\theta). \tag{5.10}$$

Our next step is to find the functions Ω_λ, and derive a reduced equation for the m-dependent perturbations $\delta y_\lambda(m)$. A plausible ansatz is that Ω_λ are given by ϕ-independent eigenfunctions of the Laplace-Beltrami operator, L_{H^2}, on $H^2 \cong \mathrm{SU}(1,1)/\mathrm{U}(1)$, the so called *zonal spherical functions* $\varphi_{0,\lambda}(\theta)$. An integral identity for these functions was derived in an introductory section, Section 2.4, Eq. (2.92).

This ansatz is motivated by the fact that the Laplace-Beltrami operator on H^2, L_{H^2}, appears in our Laplace operator Δ (3.88) (more concretely in $\Delta^\flat$, Eq. (3.93)). It is connected to $\Delta^\flat$ as follows:

$$-L_{H^2} = \Delta^\flat - (D^2 + D) = K_3^2 - K_2^2 - K_1^2. \tag{5.11}$$

Nonetheless, a closer inspection shows that zonal spherical functions on H^2 are <u>not</u> the right choice! One can see that they are not suitable by observing the following: When evaluated on the two center half-axes $H^\pm$, which in the above polar coordinate system (5.5) are given by $\theta = 0$, the zonal spherical functions equal one, $\varphi_{0,\lambda}(0) = 1$. Indeed, by invoking the integral representation (2.92):

$$\varphi_{0,\lambda}(\theta) = \int_0^{2\pi} \frac{\mathrm{d}\phi}{2\pi} \frac{1}{(\cosh(\theta) + \sinh(\theta)\cos(\phi))^{\frac{1}{2}+\mathrm{i}\lambda}}, \tag{5.12}$$

we see that the integrand becomes ϕ independent for $\theta = 0$. The ϕ integral then simply neutralizes the normalization factor $1/(2\pi)$.

The fact that the zonal spherical functions equal one on $H^\pm$ contradicts the boundary condition for the perturbations δY. The solutions of the $\mathrm{U}(1)_{\mathrm{i}\sigma_3}$ symmetry-reduced equation (4.8) are fixed along these two central half-axes. As explained in the preceding section, Section 4, they here for all system parameters coincide with the corresponding pp solution, Y_{pp}. [Note again that a pp solution exists for all parameters but is unstable outside the pp phase.] Consequently, the functions Ω_λ must vanish along the two central half-axes. It turns out that the correct functions are connected to (but not identical to) the spherical functions with angular quantum number ± 1, $\varphi_{\pm 1,\lambda}$. They are defined as follows: $\varphi_{\pm 1,\lambda}\, \mathrm{e}^{\pm \mathrm{i}\phi}$ is an eigenfunction of L_{H^2} with eigenvalue $-(\lambda^2 + \frac{1}{4})$, $\lambda \in \mathbb{R}$. We remind ourselves that we have derived an integral identity for the functions $\varphi_{\pm 1,\lambda}$ in the introductory section, Section (2.4), (the second of the two equations in (2.92):

$$\varphi_{\pm 1,\lambda}(\theta) = \int_0^{2\pi} \frac{\mathrm{d}\phi}{2\pi} \frac{\cos(\phi)}{(\cosh(\theta) + \sinh(\theta)\cos(\phi))^{\frac{1}{2}+\mathrm{i}\lambda}}. \tag{5.13}$$

This function equals zero for $\theta = 0$. Indeed,

$$\varphi_{\pm 1,\lambda}(0) = \int_0^{2\pi} \frac{\mathrm{d}\phi}{2\pi} \cos(\phi) = 0. \tag{5.14}$$

As we shall see below, the correct eigenfunctions of the linearized AAT operator around Y_{pp} (5.4) are given by:

$$\begin{aligned} \delta Y(m,\theta) &= \sum_\lambda \delta y_\lambda(m) \Omega_\lambda(\theta), \\ \Omega_\lambda(\theta) &\equiv \sinh(\theta) \varphi_{\pm 1,\lambda}(\theta). \end{aligned} \tag{5.15}$$

We will henceforth abbreviate $\varphi_{\pm 1,\lambda} \equiv \varphi_\lambda$.

5.1.3 Demonstration

In the $\mathrm{U}(1)_{\mathrm{i}\sigma_3}$-invariant sector the Laplace operator reduces to:

$$\Delta \delta Y(m,\theta) = \left(-\frac{1}{4m^2} \frac{1}{\sinh(\theta)} \frac{\partial}{\partial\theta} \sinh(\theta) \frac{\partial}{\partial\theta} - \frac{1}{4} \frac{\partial^2}{\partial m^2} + \frac{1}{2} \frac{\cosh(\theta)}{\sinh(\theta)} \frac{\partial}{\partial\theta} \frac{1}{m} \frac{\partial}{\partial m} \right) \delta Y(m,\theta), \tag{5.16}$$

and the first of the two equations in (5.4) becomes:

$$\begin{aligned} &\delta X^{\mathrm{new}}(m,\theta) = \\ &= \int \mathrm{d}\mu(Q') e^{-2w_T^2 mm' - 2w_T^2 |mm'| (\cosh(\theta)\cosh(\theta') - \sinh(\theta)\sinh(\theta')\cos(\phi-\phi'))} \Delta \delta Y(m',\theta') \\ &= 2 \int |m'| \mathrm{d}m' \int \sinh(\theta') \mathrm{d}\theta' e^{-2w_T^2 mm' - 2w_T^2 |mm'| \cosh(\theta)\cosh(\theta')} \times \\ &\times I_0(2w_T^2 |mm'| \sinh(\theta)\sinh(\theta')) \Delta \delta Y(m',\theta'). \end{aligned} \tag{5.17}$$

After ruling out the zonal spherical functions as eigenfunctions in θ, the correct eigenfunctions of Eq. (5.4) are not immediately obvious. The main difficulty is to make the role of the Laplacian more transparent. We do so by partially integrating so that it acts on the integral kernel in (5.17). For this purpose, we recall that the Laplacian Δ acting on $\mathrm{U}(1)_{\mathrm{i}\sigma_3}$-invariant functions has a particularly simple form in the coordinates (4.4):

$$m = \frac{p-q}{2}, \ |m| \cosh(\theta) = \frac{p+q}{2}, \tag{5.18}$$

and that Eq. (5.17) simplifies to:

$$\delta X^{\mathrm{new}}(p,q) = \int_{\mathbb{R}^+ \times \mathbb{R}^+} \mathrm{d}p' \mathrm{d}q' e^{-w_T^2 (pp' + qq')} I_0(2w_T^2 \sqrt{pqp'q'}) \Delta \delta Y(p',q'), \tag{5.19}$$

$$\Delta = \frac{\partial^2}{\partial p \partial q}. \tag{5.20}$$

We again emphasize that the perturbations δY vanish on the central half-axes $p = 0$ and $q = 0$. Consequently, the partial integration yields no boundary terms.

The result of the Laplacian acting on the kernel can be cast in the convenient form:

$$\begin{aligned} &\frac{\partial^2}{\partial p' \partial q'} \left(\mathrm{e}^{-w_T^2(pp'+qq')} I_0(2w_T^2 \sqrt{pqp'q'}) \right) = \\ &w_T^2 \sqrt{\frac{pq}{p'q'}} \left(1 + w_T^2 \frac{\partial}{\partial w_T^2} \right) \mathrm{e}^{-w_T^2(pp'+qq')} I_1(2w_T^2 \sqrt{pqp'q'}). \end{aligned} \tag{5.21}$$

Here $\partial/\partial w_T^2$ means partial derivative with respect to w_T^2 (while w_V^2, K, and E are held fixed). The corresponding calculation is straightforward. One uses standard identities for modified Bessel functions. Next we transform expression (5.21) back to hyperbolic polar coordinates and reinstall the polar angle integral. The result is:

$$\begin{aligned} \delta X^{\mathrm{new}}(m,\theta) = w_T^2 \int \mathrm{d}\mu(Q') \left| \frac{m}{m'} \right| \frac{\sinh(\theta)}{\sinh(\theta')} e^{\pm \mathrm{i}(\phi - \phi')} \times \\ \times \left(\left(1 + w_T^2 \frac{\partial}{\partial w_T^2} \right) e^{-w_T^2 \operatorname{Tr} QQ'} \right) \delta Y(m', \theta'). \end{aligned} \tag{5.22}$$

Note that the r.h.s. of Eq. (5.22) depends only on the difference $\phi - \phi'$ and thus is effectively independent of ϕ after ϕ' integration. Why is the version (5.22) of the linearized AAT integral equation useful? In short, the reason is that the integral kernel is separated into a Lorentz-invariant part (the integral measure and the factor in the big brackets) and the rest, which fails to be Lorentz-invariant. This version makes apparent which ansatz is the correct one for the eigenfunctions (5.15) of the linearized AAT integral operator (5.4):

$$\Omega_\lambda(\theta) = \sinh(\theta)\, \varphi_\lambda(\theta), \tag{5.23}$$

with the identification $\varphi_{\pm 1,\lambda}(\theta) \equiv \varphi_\lambda(\theta)$. Note that the functions Ω_γ satisfy the correct condition on the two center half-axes $H^\pm$:

$$\lim_{\theta \to 0} \Omega_\lambda(\theta) = 0. \tag{5.24}$$

Additionally, as opposed to the spherical functions on H^2, they diverge as $\sim \mathrm{e}^{\theta/2}$ for $\theta \to \infty$. In the following subsection, Subsection 5.1.4, we will see that with the choice (5.15), we can reduce the linearized equation (5.4) to a one-dimensional integral equation in the invariant mass m. Before doing so, there will be an interlude

on why the emergence of the functions Ω_λ, Eq. (5.23), is quite natural. They are zonal spherical functions on the hyperbolic supermanifold $H^{2|2}$.

Interlude: connecting spherical functions on H^2 and $H^{2|2}$

We here shed a bit more light on the geometric origin of the functions Ω_λ, Eq. 5.23. This interlude is not required for understanding the main line of the present argument. Because we want to keep it short, we refrain from defining the supermanifold $H^{2|2}$ and refer the reader to [103]. This article is the basis for the present observation. When equipping $H^{2|2}$ with the analogue of hyperbolic polar coordinates, the invariant metric tensor reads:

$$g = \mathrm{d}\theta^2 + \sinh(\theta)^2\,(1 - 2\overline{\eta}\eta)\,\mathrm{d}\phi^2 + 2\sinh(\theta)^2\,(1 - \overline{\eta}\eta)\,\mathrm{d}\overline{\eta}\,\mathrm{d}\eta. \tag{5.25}$$

Here $\theta \in (0, \infty)$ is the hyperbolic radius, $\phi \in (0, 2\pi)$ the hyperbolic angle, and $\overline{\eta}, \eta$ are Grassmann variables. To calculate the radial part of the Laplace-Beltrami operator, one can use the obvious generalization from the Riemannian setting:

$$L = \frac{1}{\sqrt{|\mathrm{SDet}(g)|}}(-1)^{|i|}\partial_i\left(\sqrt{|\mathrm{SDet}(g)|}g^{ij}\partial_j\right), \tag{5.26}$$

where $|\cdot|$ is the parity function and the summation over indices i, j is implicit. Plugging the expression for the metric tensor (5.25) in the formula (5.26) yields for the radial part of the Laplace Beltrami operator on $H^{2|2}$:

$$L^0_{H^{2|2}} = \frac{\partial^2}{\partial\theta^2} - \frac{\cosh(\theta)}{\sinh(\theta)}\frac{\partial}{\partial\theta}. \tag{5.27}$$

The superscript 0 means that it is the radial part of the full Laplacian.

Next we recall from the introductory section, Section 2.4, that the Laplacian on H^2 acting on functions with angular quantum number ± 1, such as $\varphi_\lambda(\theta)\mathrm{e}^{\pm\mathrm{i}\phi}$, reads

$$L^{\pm 1}_{H^2} = \frac{\partial^2}{\partial\theta^2} + \frac{\cosh(\theta}{\sinh(\theta)}\frac{\partial}{\partial\theta} - \frac{1}{\sinh(\theta)^2}. \tag{5.28}$$

It is easy to show that the two differential operators are related:

$$L^{\pm 1}_{H^2} = \frac{1}{\sinh(\theta)}L^0_{H^{2|2}} \circ \sinh(\theta). \tag{5.29}$$

Relation (5.29) shows that the radial eigenfunctions of the linearized AAT integral operator 5.4, $\Omega_\lambda(\theta)$ from Eq. 5.23, are eigenfunctions of the Laplace-Beltrami

operator on $H^{2|2}$, i.e., zonal spherical functions. Indeed,

$$\begin{aligned} L_{H^{2|2}}\,\Omega_\lambda(\theta) &= L^0_{H^{2|2}}\,\Omega_\lambda(\theta) = L^0_{H^{2|2}}\,\sinh(\theta)\,\varphi_\lambda(\theta) = \sinh(\theta)\,L^{\pm 1}_{H^2}\,\varphi_\lambda(\theta) \\ &= -\left(\lambda^2+\frac{1}{4}\right)\sinh(\theta)\,\varphi_\lambda(\theta) = -\left(\lambda^2+\frac{1}{4}\right)\Omega_\lambda(\theta). \end{aligned} \tag{5.30}$$

This already finishes the present interlude. The correct eigenfunctions $\Omega_\lambda(\theta)$ are in fact not eigenfunctions of L_{H^2} but of the Laplace-Beltrami operator of the supersymmetric analogue of H^2, $H^{2|2}$, $L_{H^{2|2}}$. Their emergence is quite natural because the original AAT integral equation (3.50) is supersymmetric. In the reduction to a bosonic equation (3.90), the supersymmetries, even if not immediately visible, are, in a sense, hidden in the Laplace operator Δ, Eq. (3.88).

After this interlude on the origin of the functions Ω_λ, let us continue with the main line of the present section, namely reducing the linearized equation, Eq. (5.4), to a one-dimensional integral equation in the invariant mass m.

5.1.4 Reduction to a one-dimensional integral equation

Integral identity for spherical functions on H^2

We begin by recalling an important identity from harmonic analysis on H^2 [44]: An eigenfunction f of the Laplace-Beltrami operator on H^2, L_{H^2}, which fulfills $L_{H^2} f = -(\lambda^2+\frac{1}{4})\,f$, satisfies the identity

$$\begin{aligned} &\int_{\mathrm{U}(1)_{\mathrm{i}\sigma_3}} \mathrm{d}k\, f(gk\cdot z) = f(g\cdot o)\,\varphi_{0,\lambda}(z), \\ &g\in \mathrm{SU}(1,1), \quad z\in H^2 \cong \mathrm{SU}(1,1)/\mathrm{U}(1)_{\mathrm{i}\sigma_3}. \end{aligned} \tag{5.31}$$

Here $o\sim \mathrm{i}\sigma_3$ is the base point of an arbitrary member of the foliation, $H^2_{x_0}$, $\cdot$ denotes the group action (the adjoint action), and, as above, $\varphi_{0,\lambda}(z)$ denotes the zonal spherical function with eigenvalue $-(\lambda^2+\frac{1}{4})$; $\mathrm{d}k$ is the Haar measure on $\mathrm{U}(1)_{\mathrm{i}\sigma_3}$.

Proof. The proof of this equation is short: Using the substitution rule, it follows that

$$z \to \int_{\mathrm{U}(1)_{\mathrm{i}\sigma_3}} \mathrm{d}k\, f(gk\cdot z) \tag{5.32}$$

is a $\mathrm{U}(1)_{\mathrm{i}\sigma_3}$-invariant eigenfunction of L_{H^2} with eigenvalue $-(\lambda^2+\frac{1}{4})$. Hence it is proportional to $\varphi_{0,\lambda}(z)$. The proportionality constant is determined by setting $z=0$ and using the normalization of the $\mathrm{U}(1)_{\mathrm{i}\sigma_3}$-Haar measure. □

To proceed, we insert only one summand from Eq. (5.15) in (5.22) by using lin-

earity. We obtain

$$\begin{aligned}\delta X^{\text{new}}(m,\theta) &= \sinh(\theta)\mathrm{e}^{\pm\mathrm{i}\phi}\int \mathrm{d}\mu(Q')\, w_T^2 \left|\frac{m}{m'}\right| \delta y_\lambda(m') \times \\ &\times \left(1 + w_T^2 \frac{\partial}{\partial w_T^2}\right) \mathrm{e}^{-w_T^2 \operatorname{Tr} QQ'} \varphi_\lambda(\theta')\, \mathrm{e}^{\mp\mathrm{i}\phi'}.\end{aligned} \tag{5.33}$$

In Eq. (5.33) on the r.h.s. the function $\varphi_\lambda(\theta')\mathrm{e}^{\mp\mathrm{i}\phi'} \equiv \Phi_\lambda(g'\cdot o)$ is an eigenfunction of L_{H^2} with eigenvalue $-(\lambda^2+\frac{1}{4})$. It follows that we can use theorem (5.31). As a preparation, we recall the conjugation action of $\mathrm{SU}(1,1)$ on Q (5.6), $Q = gq_0g^{-1}$. We substitute the integration variables $g' \to g^{-1}g'$ and exploit the $\mathrm{SU}(1,1)$-invariance of the measure. We end up with:

$$\begin{aligned}\delta X(m,\theta)^{\text{new}} &= \sinh(\theta) e^{\pm\mathrm{i}\phi}\int \mathrm{d}\mu(Q')\, w_T^2 \left|\frac{m}{m'}\right| \delta y_\lambda(m') \times \\ &\times \left(1 + w_T^2 \frac{\partial}{\partial w_T^2}\right) e^{-w_T^2 \operatorname{Tr} q_0 g' q_0' g'^{-1}} \Phi_\lambda(gg'\cdot o).\end{aligned} \tag{5.34}$$

Next we average transformations $g' \to k'g',\ k' \in \mathrm{U}(1)_{\mathrm{i}\sigma_3}$, over the $\mathrm{U}(1)_{\mathrm{i}\sigma_3}$ Haar measure. We use that k' commutes with the base point $q_0 \sim \mathrm{i}\sigma_3$ of Q:

$$\begin{aligned}\delta X(m,\theta)^{\text{new}} &= \sinh(\theta) e^{\pm\mathrm{i}\phi}\int \mathrm{d}\mu(Q')\, w_T^2 \left|\frac{m}{m'}\right| \delta y_\lambda(m') \times \\ &\times \left(1 + w_T^2 \frac{\partial}{\partial w_T^2}\right) e^{-w_T^2 \operatorname{Tr} q_0 g' q_0' g'^{-1}} \int_{\mathrm{U}(1)_{\mathrm{i}\sigma_3}} \mathrm{d}k'\ \Phi_\lambda(gk'g'\cdot o).\end{aligned} \tag{5.35}$$

Now we are ready to apply theorem (5.31) because Φ_λ is an eigenfunction of L_{H^2}. The result reads:

$$\begin{aligned}\delta X(m,\theta)^{\text{new}} &= \Omega_\lambda(\theta)\int \mathrm{d}\mu(Q')\, w_T^2 \left|\frac{m}{m'}\right| \delta y_\lambda(m') \times \\ &\times \left(1 + w_T^2 \frac{\partial}{\partial w_T^2}\right) e^{-w_T^2 \operatorname{Tr} q_0 Q'} \varphi_{0,\lambda}(\theta').\end{aligned} \tag{5.36}$$

Consequently, we have reproduced the function $\Omega_\lambda(\theta)$ and identified the correct eigenfunctions in the hyperbolic radius θ. The only degree of freedom that remains is the mass m and the corresponding functions $\delta y_\lambda(m)$. These functions satisfy a

one-dimensional integral equation which follows from (5.4), and (5.36):

$$\begin{aligned}\delta y_\lambda(m)^{\text{new}} &= K\frac{Y_{\text{pp}}(m)}{X_{\text{pp}}(m)}\int_{\mathbb{R}}|m'|\mathrm{d}m'\,w_T^2\left|\frac{m}{m'}\right|\delta y_\lambda(m')\times\\ &\times\int_{H^2}\mathrm{d}g'\left(1+w_T^2\frac{\partial}{\partial w_T^2}\right)e^{-w_T^2\,\mathrm{Tr}\,q_0Q'}\varphi_{0,\lambda}(\theta').\end{aligned}\tag{5.37}$$

We are left with performing the g' integration. The calculation can be found in an Appendix 8.3. After a rescaling $m\to\sqrt{w_T^2}m,\ m'\to\sqrt{w_T^2}m'$ the result reads

$$\begin{aligned}\delta y_\lambda(m)^{\text{new}} &= K\frac{Y_{\text{pp}}(m)}{X_{\text{pp}}(m)}\int_{\mathbb{R}}\frac{\mathrm{d}m'}{\sqrt{\pi}}e^{-2mm'}\sqrt{\left|\frac{m}{m'}\right|}\times\\ \times\Big(&(1-4mm')\,K_{i\lambda}(2|mm'|)-2|mm'|\,(K_{1+i\lambda}(2|mm'|)+K_{1-i\lambda}(2|mm'|))\Big)\,\delta y_\lambda(m'),\end{aligned}\tag{5.38}$$

where K_ν are modified Bessel functions of the second kind.

5.1.5 Strong coupling limit and exact formula for critical points

We now consider the strong coupling limit $K,w\to\infty$. We here investigate the case $\lambda=0$. The reason is that the eigenvalue with the maximum magnitude, which contains the information about the critical manifold, occurs for $\lambda=0$.

In the strong coupling limit, Eq. (5.38) for $\lambda=0$ (and also for $\lambda\neq0$) can be solved exactly. This means that we are able to determine its eigenvalues and eigenfunctions. The key step of this calculation is the following observation, which we show below: In the strong coupling limit, the integral operator in Eq. (5.38) undergoes a rank reduction. The rank of the strong coupling operator collapses from infinity to one. This observation reduces the determination of the eigenfunction and eigenvalue to a straightforward calculation. To start, we recall that, at strong disorder $w^2\gg K$, in the rescaled coordinates $m\to\sqrt{w_T^2}m,\ m'\to\sqrt{w_T^2}m'$, the pp solution takes the form

$$\frac{Y_{\text{pp}}(m)}{X_{\text{pp}}(m)}=\mathrm{e}^{-2w^2m^2-2\mathrm{i}\frac{E}{w_T}m}.\tag{5.39}$$

For the present purpose, we rescale once more: $m\to\sqrt{2}wm,\ m'\to\sqrt{2}wm'$, such that the typical scale for the rescaled m,m' variables is $m,m'\sim1$. The strong coupling

version of the rescaled form of Eq. (5.38) at $\lambda = 0$ is:

$$\begin{aligned}\delta y(m)^{\text{new}} &= \frac{K}{\sqrt{2w^2}} \mathrm{e}^{-m^2 - \sqrt{2}\mathrm{i}\frac{E}{w_V}m} \int_{\mathbb{R}} \frac{\mathrm{d}m'}{\sqrt{\pi}} e^{-\frac{mm'}{w^2}} \sqrt{\left|\frac{m}{m'}\right|} \times \\ \times \left(\left(1 - 2\frac{mm'}{w^2}\right) K_0\left(\frac{|mm'|}{w^2}\right) - 2\frac{|mm'|}{w^2} K_1\left(\frac{|mm'|}{w^2}\right) \right) &\delta y(m') \\ &\equiv \frac{K}{\sqrt{2w^2}} \mathrm{e}^{-m^2 - \sqrt{2}\mathrm{i}\frac{E}{w_V}m} \int_{\mathbb{R}} \frac{\mathrm{d}m'}{\sqrt{\pi}} \mathcal{K}_w\left(m, m'\right) \delta y(m').\end{aligned} \tag{5.40}$$

For $w \to \infty$, $\frac{mm'}{w^2}$ becomes small, allowing an expansion of the kernel $\mathcal{K}_w$. We use the small-argument expansion of the modified Bessel functions:

$$K_0(x) \sim -\ln(x), \quad K_1(x) \sim \frac{1}{x}. \tag{5.41}$$

For our purposes, it suffices to retain only the leading term in $1/w^2$:

$$\mathcal{K}_w\left(m, m'\right) \simeq \sqrt{\left|\frac{m}{m'}\right|} \ln\left(w^2\right). \tag{5.42}$$

In the strong coupling limit, the integral equation (5.40) takes the form:

$$\delta y(m)^{\text{new}} = \sqrt{2} K \frac{\ln(w)}{w} \sqrt{|m|} \mathrm{e}^{-m^2 - \sqrt{2}\mathrm{i}\frac{E}{w_V}m} \int \frac{\mathrm{d}m'}{\sqrt{\pi}} \frac{\delta y(m')}{\sqrt{|m'|}}. \tag{5.43}$$

Eq. (5.43) implies that in the strong coupling limit, the rank of the operator (5.40) collapses from infinity to one. An eigenfunction is:

$$\delta y(m) = \sqrt{|m|}\, \mathrm{e}^{-m^2 - \sqrt{2}\mathrm{i}\frac{E}{w_V}m}. \tag{5.44}$$

As a consistency check, we note that the required limiting behavior $\delta y \to 0,\ m \to 0$ is satisfied. The eigenvalue is

$$\nu = \sqrt{2} K \frac{\ln(w)}{w} \int \frac{\mathrm{d}m}{\sqrt{\pi}}\, \mathrm{e}^{-m^2 - \sqrt{2}\mathrm{i}\frac{E}{w_V}m} = \sqrt{2} K \frac{\ln(w)}{w} \exp\left(-\frac{E^2}{2w_V^2}\right). \tag{5.45}$$

The critical manifold is given by the requirement that ν reaches magnitude one. Consequently, the branching number K as a function of the critical disorder w_c, on-site disorder w_V, and energy E are given by:

$$K = \frac{1}{\sqrt{2}} \frac{w_c}{\ln(w_c)} \exp\left(\frac{E^2}{2w_V^2}\right) \tag{5.46}$$

in the limit of large branching number $K \to \infty$.

5.1.6 Location of critical points: numerical treatment at band center $E = 0$ and comparison to analytical results

In addition to the analytical treatment at strong coupling, Eq. (5.38) can also be analyzed numerically. To extract the critical points, we again calculate the eigenvalue maximal in magnitude (for $\lambda = 0$) using two recursive procedures. In the first procedure, we determine the pp solution $X^{\rm pp}, Y^{\rm pp}$. In the second one, we calculate the maximal eigenvalue of the linear integral equation (5.38), initializing with the strong coupling eigenfunction $\delta y_0^0(m) = \sqrt{|m|}\, e^{-2w^2 m^2}$. For $K = 3, 4, ...$ and at band center $E = 0$, the numerical results and the analytical predictions are summarized in the table below:

K	w_c^2 numerical	w_c^2 analytical
3	(88,89)	92
4	(240,241)	240
5	(479,480)	475
6	(818,819)	806
50	$(187 \times 10^3, 188 \times 10^3)$	184×10^3
100	$(959 \times 10^3, 960 \times 10^3)$	947×10^3

The intervals indicate that the actual value of $w_{\rm crit}^2$ lies within the specified range.

This finishes the section on the harmonic analysis. As announced in the preceding section, we will now use the eigenfunctions $\delta y_\gamma(m)\Omega_\gamma(\theta)$ to construct the $\mathrm{U}(1)_{\mathrm{i}\sigma_3}$-invariant metallic solution $Y_{\rm ac}$ near the critical manifold $w \nearrow w_c$.

5.2 $Y_{\rm ac}$ near the critical manifold

5.2.1 Scale of maximal decay Λ and equation for $Y_{\rm ac} - Y_{\rm pp}$

As opposed to Sections 4.4 and 4.4.2, where we used p, q coordinates (4.4) or horospherical coordinates (4.29) to describe $Y_{\rm ac}$, we now use hyperbolic polar coordinates (5.5). For $w \nearrow w_c$ the solution $Y_{\rm ac}$ turns into the pp solution $Y_{\rm pp}$. This means that the full G symmetry is restored for vanishing explicit symmetry-breaking term $\varepsilon = 0$.

Consequently, for $w_c - w \ll 1$ a large scale $\theta \sim \Lambda,\ \Lambda \gg 1$ emerges at which $Y_{\rm ac}$ decays and the difference between $Y_{\rm pp}$ and $Y_{\rm ac}$ becomes large. We expect that the

window of strong decay is small in high dimensions. The scale Λ goes to infinity at the critical point (for $w \nearrow w_c$). Since m is a massive degree of freedom, the scale for m in contrast remains finite, $m \sim 1$. How can we obtain an expression for the scale Λ? We now show that the key is the harmonic analysis from the preceding section.

Using the AAT integral Eq. (3.90), we can easily write down the equation for the difference $Y_{\mathrm{ac}} - Y_{\mathrm{pp}} \equiv \delta Y_{\mathrm{ac}}$:

$$\begin{aligned}\delta Y_{\mathrm{ac}}(Q) = Y_{\mathrm{pp}}(Q)\Bigg\{ \Big(\int \mathrm{d}\mu(Q')\ \mathrm{e}^{-w_T^2 \mathrm{Tr} QQ'} \Delta \left(Y_{\mathrm{pp}}(Q') + \delta Y_{\mathrm{ac}}(Q')\right)\Big)^K - \\ - \Big(\int \mathrm{d}\mu(Q')\ \mathrm{e}^{-w_T^2 \mathrm{Tr} QQ'} \Delta Y_{\mathrm{pp}}(Q')\Big)^K \Bigg\}.\end{aligned} \tag{5.47}$$

Here we used that for $K \gg 1$ and near the critical manifold

$$Y_{\mathrm{pp}}(Q) = \exp(-2w_V^2 m^2 - 2\mathrm{i}Em). \tag{5.48}$$

Eq. (5.48) is a direct consequence of the discussion in Subsection 4.2.4, Chapter 4.

By definition of the scale Λ, for $\theta \ll \Lambda$, the difference δY_{ac} is small and Eq. (5.47) can be linearized. The result is:

$$\delta Y_{\mathrm{ac}}(Q) = K Y_{\mathrm{pp}}(Q) \int \mathrm{d}\mu(Q') \mathrm{e}^{-w_T^2 \mathrm{Tr} QQ'} \Delta \delta Y_{\mathrm{ac}}(Q'). \tag{5.49}$$

Eq. (5.49) is simply the linear integral equation (5.4) from Section (5.1). We already know its eigenfunctions. On the metallic side of the transition, the maximal eigenvalue of the operator in (5.49) has already exceeded magnitude one. The fixed point of Eq. (5.49) is the eigenfunction $\delta Y_{\lambda^*}(Q)$, where λ^* labels the one with eigenvalue with magnitude one. When w approaches w_c, λ^* goes to zero. In a later part of this section, we will argue how λ^* scales with the disorder difference $w_c - w$.

5.2.2 Calculation of the scale Λ

The eigenfunctions δY_{λ^*} are given by:

$$\delta Y_{\lambda^*}(Q) = C(\lambda^*) \sinh(\theta)\, \varphi_{\lambda^*}(\theta)\, \delta y_{\lambda^*}(m) \tag{5.50}$$

where $C(\lambda^*)$ a priori is an arbitrary constant. It will be fixed later by the constraint that $Y_{\mathrm{ac}}, \partial_\theta Y_{\mathrm{ac}}$ should be continuous in the regime $\theta \sim \Lambda$. Once more, we recall that

$$\varphi_{\lambda^*}(\theta) = \int_0^{2\pi} \frac{\mathrm{d}\phi}{2\pi} \frac{\cos(\phi)}{(\cosh(\theta) + \sinh(\theta)\cos(\phi))^{\frac{1}{2}+\mathrm{i}\lambda^*}}. \tag{5.51}$$

We are now interested in the asymptotic regime $\theta \gg 1, \theta \ll \Lambda$, and $|\lambda^*| \ll 1$. The asymptotic expression of δY_{ac} follows from the asymptotic expression for φ_{λ^*}. It was derived in the final part of the introductory section, Section 2.4, Eq. (2.97):

$$\varphi_{\lambda^*}(\theta) \sim -\frac{1}{\lambda^*} \mathrm{e}^{-\frac{\theta}{2}} \sin(\lambda^*\theta - a\lambda^*), \tag{5.52}$$

where $a = 2 - 2\ln(2)$. Accordingly, the expression for δY_{ac} reads

$$\delta Y_{\mathrm{ac}}(Q) = -\frac{C(\lambda^*)}{\lambda^*} \mathrm{e}^{\frac{\theta}{2}} \sin(\lambda^*\theta - a\lambda^*)\, \delta y_{\lambda^*}(m). \tag{5.53}$$

To calculate the constant C and the scaling of the length scale Λ, we exploit that the ac-type solutions are sufficiently regular. In particular, Y_{ac}, and $\partial_\theta Y_{\mathrm{ac}}$ should be continuous in the regime $\theta \sim \Lambda$. This requirement is equivalent to the two conditions

$$\frac{\partial}{\partial\theta}\bigg|_{\theta=\Lambda} \delta Y_{\mathrm{ac}}(Q) \approx 0, \quad \delta Y_{\mathrm{ac}}(Q)\bigg|_{\theta=\Lambda} \approx -Y_{\mathrm{pp}}. \tag{5.54}$$

These two conditions lead to:

$$\Lambda \sim \frac{\pi}{|\lambda^*|}, \quad C \sim \mathrm{e}^{-\frac{\Lambda}{2}}. \tag{5.55}$$

Indeed, for $\lambda^* \ll 1$,

$$\delta y_{\lambda^*}(m) \approx \delta y_0(m) = \sqrt{|m|}\, Y_{\mathrm{pp}}(m), \tag{5.56}$$

and for $m \sim 1$ we can thus approximate

$$\delta y_{\lambda^*}(m) \approx Y_{\mathrm{pp}}(m). \tag{5.57}$$

The second of the two conditions in (5.54) yields

$$-2\lambda^* = \tan(\lambda^*\Lambda - a\lambda^*). \tag{5.58}$$

Expanding the r.h.s. in Eq. (5.58), we see that

$$\begin{aligned} \lambda^*\Lambda - a\lambda^* &= \pi - 2\lambda^*, \quad \lambda^* > 0 \\ \lambda^*\Lambda - a\lambda^* &= -\pi - 2\lambda^*, \quad \lambda^* < 0 \end{aligned} \tag{5.59}$$

or, when neglecting the small terms

$$\Lambda \sim \frac{\pi}{|\lambda^*|}. \tag{5.60}$$

[More generally, in Eq. (5.59) one may replace π by $l\pi$ and $-\pi$ by $-l\pi$, with $l \in \mathbb{N} \setminus \{0\}$. In the following, we restrict ourselves to the $l = 1$ branch.] Inserting Eq. (5.60) into the first condition then leads to

$$-\frac{C(\lambda^*)}{\lambda^*}\,\mathrm{e}^{\frac{\Lambda}{2}}\,\sin(\pi - a\lambda^*) \sim -C(\lambda^*)\,\mathrm{e}^{\frac{\Lambda}{2}} \stackrel{!}{=} -1, \tag{5.61}$$

and we end up with

$$\Lambda \sim \frac{\pi}{|\lambda^*|}, \quad C \sim \mathrm{e}^{-\frac{\Lambda}{2}} = \mathrm{e}^{-\frac{\pi}{2|\lambda^*|}}. \tag{5.62}$$

We note that relation (5.62) is in accordance with the corresponding result obtained for the Anderson model within the AAT approach; see [60]. The present derivation, however, is more transparent since it relies solely on the full eigenfunctions δY_{λ^*} of the harmonic analysis.

5.2.3 Formula for $Y_{\rm ac}$ at $w \nearrow w_c$

Now we are in a position to write down an approximation for the $\mathrm{U}(1)_{\mathrm{i}\sigma_3}$-invariant metallic solution $Y_{\rm ac}$ near the critical manifold. From the above construction, we know that for $\theta \ll \Lambda$, we have

$$Y_{\rm ac}(Q) = Y_{\rm pp}(Q) + C\,\sinh(\theta)\,\varphi_{\lambda^*}(\theta)\,\delta y_0(m), \quad C \sim \mathrm{e}^{-\frac{1}{2}\frac{\pi}{|\lambda^*|}}. \tag{5.63}$$

For $1 \ll \theta \ll \Lambda$ we can expand

$$\varphi_{\lambda^*}(\theta) \sim -\frac{1}{\lambda^*}\,\mathrm{e}^{-\frac{\theta}{2}}\,\sin(\lambda^*\theta - a\lambda^*) \sim -\theta\,\mathrm{e}^{-\frac{\theta}{2}} \sim \varphi_0(\theta). \tag{5.64}$$

The last identity in Eq. (5.64) follows from the introductory section 2.4, where we have also calculated the asymptotic expression for the function $\varphi_0(\theta)$ (Eq. (2.93)). It follows that in Eq. (5.63) we can replace φ_{λ^*} by φ_0

$$Y_{\rm ac}(Q) = Y_{\rm pp}(Q) + C\,\sinh(\theta)\,\varphi_0(\theta)\,\delta y_0(m), \quad C \sim \mathrm{e}^{-\frac{1}{2}\frac{\pi}{|\lambda^*|}}. \tag{5.65}$$

We remind ourselves that, with the above constructed δY_{ac} (Eq. (5.65)), at $\theta \sim \Lambda$, Y_{ac} is continuous and differentiable. For $\theta \gg \Lambda$ it is zero. In high dimensions K, the decay region $\theta \sim \Lambda$ is small, and the decay can be approximated by an exponential decay:

$$Y_{\mathrm{ac}}(Q) = Y_{\mathrm{pp}}(Q) \exp\left(C \sinh(\theta)\varphi_0(\theta)\sqrt{|m|}\right), \tag{5.66}$$

where we used that

$$\delta y_0(m) = \sqrt{|m|}\, Y_{\mathrm{pp}}(Q). \tag{5.67}$$

The approximation in (5.66) is quite flexible. The decay does not necessarily have to be exponential to obtain sc-type solutions at criticality in the subsequent section, Section 5.3. Finally, we need to understand how λ^* scales with the difference of disorder strengths $w_c - w$. The corresponding calculation is shown in the Appendix 8.4. For $w_c - w \ll 1$ we find

$$\lambda^* \sim \sqrt{w_c - w}, \quad w_c - w \ll 1. \tag{5.68}$$

The parameter C that determines the weight $M = \int \mathrm{d}\mu(Q) Y_{\mathrm{ac}}(Q)$ of Y_{ac} consequently fulfills:

$$C \sim \mathrm{e}^{-\frac{1}{2}\frac{\pi}{\sqrt{w_c - w}}}. \tag{5.69}$$

5.3 Construction of solutions of sc type

5.3.1 A refined heuristic argument

With all the geometric and analytic preliminary work from the last sections, we are now finally in a position to execute our main goal, namely, explicitly constructing the critical, sc-type solutions. To be as pedagogical as possible, before we delve into technical details, we present a refined heuristic argument for these solutions with a bit more technical knowledge from Sections 5.1 and 5.2. The construction relies on the combination of two fundamental observations that have been acquired throughout the preceding sections of this work:

- **Behavior of Y_{ac} when approaching criticality**: We have constructed the $\mathrm{U}(1)_{\mathrm{i}\sigma_3}$-invariant solutions Y_{ac} on the way to criticality $w \nearrow w_c$. Specifically, we have found the scaling of C for $w \nearrow w_c$, Eq. (5.69). The weight $M = \int \mathrm{d}\mu(Q)\, Y_{\mathrm{ac}}(Q)$ of these solutions diverges at the critical point $w = w_c$. This signals a divergent correlator $K_{n,\varepsilon}$ (for regulator $\varepsilon = 0$) by invoking the

spectral integral (3.73):

$$K_{n,\varepsilon} \stackrel{!}{=} \int \mathrm{d}Q_n \; \mathrm{e}^{-\mathrm{Tr}(\varepsilon\sigma_3)Q_n} \; {}^{g_s}Y(Q_n), \tag{5.70}$$

here for $s = 0$. How the weight diverges on the way to the critical point is fixed by the scaling of C.

- **Different ac type solutions in the ac phase for fixed parameter values**: Apart from the ac-type solution Y_{ac} there also exist $\mathrm{U}(1)_{\mathrm{i}\sigma_3}$ symmetry-broken ac-type solutions ${}^{g_s}Y_{\mathrm{ac}}$: They can be constructed from the solution Y_{ac} by symmetry transforming $Y_{\mathrm{ac}}(Q) \to {}^{g_s}Y_{\mathrm{ac}}(Q) \equiv Y_{\mathrm{ac}}(g_s^{-1} Q g_s)$, where for concreteness we restricted the discussion to a one-parameter-subgroup $g_s = \exp((s/2)\,\sigma_1)$. Due to the non-compactness of the Lorentz group, the "boost" parameter s can become arbitrarily large $s \gg 0$ (or arbitrarily small $s \ll 0$). As we have seen in the example (4.34) of Section 4.4.2 in Chapter 4, the support of Y_{ac} under this symmetry transformation becomes elongated along the ray L_0, (4.35), on H_0^2 and narrowed in the transverse directions until the support coincides with L_0. The transformation with a symmetry group element g_s, of course, does not change the weight: $\int \mathrm{d}\mu(Q)\, {}^{g_s}Y_{\mathrm{ac}}(Q) = \int \mathrm{d}\mu(Q)\, Y_{\mathrm{ac}}(Q)$ because all Lorentz transformations are isometries. In other words, the increase of weight in the direction of the ray L_0 is compensated by the decrease of weight in the transverse directions.

For fixed w with $w_c - w \ll 1$, the weight of Y_{ac} is large, but still finite. Up to the large scale Λ, Y_{ac} only slightly differs from the pp solution Y_{pp} and for $\theta \sim \Lambda$ it decays in θ direction, uniformly in the angular coordinate ϕ. When $w \nearrow w_c$, the argument that symmetry transformations with very large parameter $g_s,\ s \gg 1$ yield a "function" supported only on L_0 does not hold anymore because the weight of Y_{ac} diverges. What happens when we subject Y_{ac} to the coupled limit $C \to 0$ (i.e., we approach criticality from below by sending $w \nearrow w_c$ and fixing the other system parameters), and $s \to \infty$ (i.e., we select different $\mathrm{U}(1)_{\mathrm{i}\sigma_3}$-symmetry-broken ac-type solutions ${}^{g_s}Y_{\mathrm{ac}}$ for larger and larger s dynamically in $w \nearrow w_c$)? When coupling the two limits in a certain way (see below), we can arrange for the following situation: While the infinite Lorentz transformation $g_s,\ s \to \infty$ extends the support in C_0 but narrows the support in the transverse directions, the fact that the weight for $w \nearrow w_c$ increases, enlarges the support in the transverse directions. The balance of these two effects leads to a function that is not supported only on the ray L_0. It is a continuous function that is constant on horocycles centered around the boundary point where the ray L_0 ends. The $\mathrm{U}(1)_{\mathrm{i}\sigma_3}$ symmetry, however, remains broken. The fact that

the support of Y_{sc} is non-compact, even though Y_{sc} breaks the hyperbolic symmetry, results in a weaker divergence of the spectral integral (3.73) than in the pp case. Using the arguments from Sections 3.2, and 3.4 in Chapter 3 (symmetry breaking, spontaneous selection of extremal Gibbs states, etc.), this weaker divergence is rather naturally connected to sc spectrum of the Wegner Hamiltonian.

5.3.2 Construction

In the following, we will present the corresponding calculation. The idea is to take the $\mathrm{U}(1)_{\mathrm{i}\sigma_3}$-invariant solution (5.66) Y_{ac} for $w \nearrow w_c$ and transform them to ${}^{g_s}Y_{\mathrm{ac}}$ with a parameter s that scales with $w_c - w$. We isolate the part of Y_{ac} given by Eq. (5.66) that depends on the symmetry degrees of freedom:

$$\frac{\delta Y_0}{Y_{\mathrm{pp}}} = C\int_0^{2\pi}\frac{\mathrm{d}\phi}{2\pi}\frac{\sqrt{x_1^2+x_2^2}\cos(\phi)}{\left(x_3+\sqrt{x_1^2+x_2^2}\cos(\phi)\right)^{\frac{1}{2}}} = C\int_0^{2\pi}\frac{\mathrm{d}\phi}{2\pi}\frac{x_2\cos(\phi)+x_1\sin(\phi)}{(x_3+x_2\cos(\phi)+x_1\sin(\phi))^{\frac{1}{2}}}. \tag{5.71}$$

In Eq. (5.71) and also in the following, we again omit the pullback symbol i^*. The $x_i, \quad i=1,2,3$ are the quasi-Cartesian coordinates of the target space C^3 (defined in (3.82)). As a reminder, the connection to hyperbolic polar coordinates is given by:

$$\begin{gathered} x_3 = |m|\cosh(\theta), \quad x_1 = |m|\sinh(\theta)\cos(\alpha), \quad x_2 = |m|\sinh(\theta)\sin(\alpha), \\ \theta\in\mathbb{R}^+, \quad \alpha\in(0,2\pi). \end{gathered} \tag{5.72}$$

Additionally, to get from the l.h.s. to the r.h.s. in Eq. (5.71), we used translation invariance of integrals over S^1. Of course, due to the average over the angle ϕ, the r.h.s. of Eq. (5.71) is still $\mathrm{U}(1)_{\mathrm{i}\sigma_3}$-invariant. Now we use the equivariance of the "bosonic" AAT integral equation (3.90) for vanishing symmetry-breaking terms $\widetilde{\varepsilon}=\widetilde{\delta}=0$ under the one-parameter-subgroup $\{\exp((s/2)\,\sigma_1), s\in\mathbb{R}\}$ and construct $\mathrm{U}(1)_{\mathrm{i}\sigma_3}$-broken solutions, ${}^{g_s}Y_{\mathrm{ac}}$, via these Lorentz transformations. Again, we emphasize that for fixed $w<w_c$, they form a class of metallic solutions; they simply are different points of the metallic moduli space. How does the transformation g_s act on the r.h.s. of Eq. (5.71)? The action on the quasi-Cartesian coordinates is:

$$x_3+x_2 \equiv x_+ \to \mathrm{e}^{-s}x_+, \qquad x_3-x_2\equiv x_- \to \mathrm{e}^{s}x_-, \quad s\in\mathbb{R}. \tag{5.73}$$

Indeed, the identities (5.73) follow because the connection to the horospherical coordinates (4.29) is:

$$x_+ = \mathrm{e}^{\varphi}, \quad x_- = (m^2+b^2)\mathrm{e}^{-\varphi}. \tag{5.74}$$

Consequently, the integrand on the r.h.s. of (5.71) transforms as:

$$\begin{aligned} &x_2\cos(\phi)+x_1\sin(\phi) \to \frac{1}{2}\left(x_+\mathrm{e}^{-s}-x_-\mathrm{e}^{s}\right)\cos(\phi)+x_1\sin(\phi),\\ &x_3+x_2\cos(\phi)+x_1\sin(\phi) \to x_+\,\mathrm{e}^{-s}\,\frac{1}{2}\,(1+\cos(\phi))+x_-\,\mathrm{e}^{s}\,\frac{1}{2}\,(1-\cos(\phi))+x_1\sin(\phi). \end{aligned} \tag{5.75}$$

As motivated in the introductory paragraph of the present section, Section 5.3.1, to construct the novel type of solutions, we approach the critical point from below $w \nearrow w_c$ and send s to $+\infty$ in a coupled way, i.e., $s = s(w)$. It follows that we should look at the pointwise asymptotic expansion of the transformed version of the r.h.s. of (5.71), (5.75), for $s \gg 1$. After shifting the integration interval to $(-\pi,\pi)$, the leading contribution to the integral comes from ϕ near zero. By expanding the enumerator and nominator and ensuring the convergence of the integral, we end up with

$$g_s\left(\frac{\delta Y_0}{Y_{\mathrm{pp}}}\right) \approx -C\,x_-\,\mathrm{e}^{s}\int_0^{\pi}\frac{\mathrm{d}\phi}{2\pi}\frac{1}{\left(x_+\mathrm{e}^{-s}+x_-\mathrm{e}^{s}\frac{\phi^2}{4}\right)^{\frac{1}{2}}}. \tag{5.76}$$

Using standard manipulations and absorbing irrelevant constants into $\tilde{C}$, this integral can be brought to the standardized form:

$$g_s\left(\frac{\delta Y_0}{Y_{\mathrm{pp}}}\right) \approx -C\sqrt{x_-}\,\mathrm{e}^{\frac{s}{2}}\int_0^{\frac{\pi}{2}\sqrt{\frac{x_-}{x_+}}\mathrm{e}^{s}}\mathrm{d}x\,\frac{1}{\sqrt{1+x^2}} = -C\sqrt{x_-}\,\mathrm{e}^{\frac{s}{2}}\,\mathrm{arsinh}\left(\frac{\pi}{2}\sqrt{\frac{x_-}{x_+}}\mathrm{e}^{s}\right). \tag{5.77}$$

Finally, we use

$$\mathrm{arsinh}\left(\frac{x}{2}\right) \sim \ln(x), \quad x \gg 1, \tag{5.78}$$

and obtain:

$$g_s\left(\frac{\delta Y_0}{Y_{\mathrm{pp}}}\right) \approx -C\,s\,\mathrm{e}^{\frac{s}{2}}\sqrt{x_-}. \tag{5.79}$$

This already finishes the main calculation. We find that for large Lorentz boost parameter $s \gg 1$, the transformed ac solution of the AAT integral equation for $\widetilde{\varepsilon} = \widetilde{\delta} = 0$ equals:

$$g_{s\gg 1}Y_{\mathrm{ac}}(Q) = Y_{\mathrm{pp}}(Q)\,\exp\left(-C\,s\,\mathrm{e}^{\frac{s}{2}}\sqrt{x_-}\right). \tag{5.80}$$

Now we are in a position to identify the correct scaling

$$s = s(w), \quad w \nearrow w_c, \tag{5.81}$$

such that the result is a novel type of solution at criticality. In the case

$$C\,s\,\mathrm{e}^{\frac{s}{2}} \to \infty, \tag{5.82}$$

the limit is again only supported in $\{x_- = 0\}$. Thus this case does not lead to novel solutions. When

$$C\,s\,\mathrm{e}^{\frac{s}{2}} \to 0, \tag{5.83}$$

the function ${}^{g_s\to\infty}Y_{\mathrm{ac}}$ turns into the pp solution. The situation becomes nontrivial, and the procedure yields solutions of a novel type, when we require

$$C\,s\,\mathrm{e}^{\frac{s}{2}} \sim 1. \tag{5.84}$$

This requirement, together with the main result from Section 5.2, leads to a scaling relation for s. In that section, we have found how C scales with the disorder:

$$C \sim \exp\left(-\frac{1}{2}\frac{\pi}{\sqrt{w_c - w}}\right), \quad w \nearrow w_c. \tag{5.85}$$

Consequently, the requirement $Cs\mathrm{e}^{\frac{s}{2}} \sim 1$ leads to

$$s + 2\ln(s) \sim \Lambda \sim \frac{\pi}{\sqrt{w_c - w}}, \tag{5.86}$$

or, when ignoring the logarithmic correction:

$$s \sim \Lambda \sim \frac{\pi}{\sqrt{w_c - w}}. \tag{5.87}$$

Finally, we find that the critical solutions for $w \nearrow w_c$ take the form:

$$Y_{\mathrm{sc}}(Q) = Y_{\mathrm{pp}}(Q)\exp\left(-\beta\sqrt{x_-}\right) = Y_{\mathrm{pp}}(Q)\exp\left(-\beta\sqrt{m^2+b^2}\,\mathrm{e}^{-\frac{\varphi}{2}}\right), \quad \beta \in \mathbb{R}^+. \tag{5.88}$$

The above limiting procedure leaves a free parameter β because the boost is only restricted by the scaling (5.87). In other words, we find a whole ray of critical solutions $\cong \mathbb{R}^+$. The situation is comparable to the metallic phase, where, when symmetry-transforming the $\mathrm{U}(1)_{\mathrm{i}\sigma_3}$-invariant solution Y_{ac} with $g_s,\ s > 0$, we obtain a ray of solutions ($\cong \mathbb{R}^+$).

The center of the disk is part of the metallic moduli space because the Y_{ac} represents a distinct metallic solution. In contrast, the case $\beta = 0$ in (5.88) yields the pp solution and does not belong to the sc solution space. Correspondingly, it can be identified with $\mathrm{U}(1) \times \mathbb{R}^+ \cong D^2 \setminus \{o\}$, where o denotes the center of the disk D^2.

As a consistency check, we will see in the following section, Section (5.4), that the scaling of the spectral integral 3.73 does not depend on the constant β entering Y_{sc}.

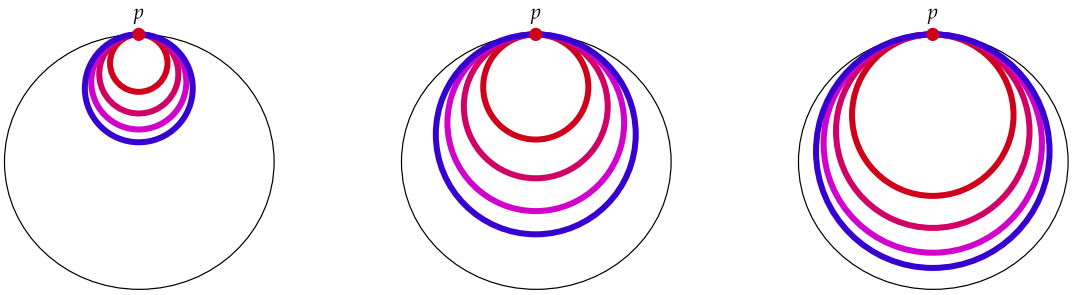

Figure 5.1: Three solutions Y_{sc} for different values of $\beta > 0$, centered at a boundary point p of the Poincaré disk D. The colored curves indicate contour lines of Y_{sc} (red corresponds to large values, blue to small values). In Chapter 6, it will become clear that the solutions Y_{sc} are constant on horocycles centered at the boundary point p.

In the following section, we will find that the solution just constructed indeed corresponds to a singular continuous spectrum.

5.4 Scaling of $K_{n,\varepsilon}$ for Y_{sc}

We now go back to Section 3.4, Eq. (3.73) and use Y_{sc} to calculate the scaling of the correlator $K_{n,\varepsilon}$:

$$K_{n,\varepsilon} = \int \mathrm{d}\mu(Q)\, \mathrm{e}^{-\mathrm{Tr}(\varepsilon\sigma_3)Q}\, Y_{\mathrm{sc}}(Q), \tag{5.89}$$

where Y_{sc} is the critical solution (5.88). Again, we emphasize that in Eq. (5.89) the explicit symmetry-breaking term has been sent to zero: $\widetilde{\varepsilon}, \widetilde{\delta} \to 0$. Hence an extremal Gibbs state, represented by the solution Y_{sc} (5.88), has been selected by the system. Inserting the solution (5.88) into (5.89) we obtain:

$$\lim_{\varepsilon\to 0} K_{n,\varepsilon} = \lim_{\varepsilon\to 0} \int \mathrm{d}\mu(Q)\, \mathrm{e}^{-\varepsilon \mathrm{Tr} Q\sigma_3}\, Y_{\mathrm{pp}}(Q)\, \mathrm{e}^{-\beta\sqrt{\mathrm{Tr}Q(\sigma_3 - \mathrm{i}\sigma_2)}}. \tag{5.90}$$

It remains to calculate the scaling behavior of the integral (5.90):

$$K_{n,\varepsilon} \sim \frac{1}{\pi} \int_{\mathbb{R}} \mathrm{d}\varphi \int_{\mathbb{R}} \mathrm{d}m \int_{\mathbb{R}} \mathrm{d}b\ \mathrm{e}^{-2w_V^2 m^2 - 2\mathrm{i}Em - \varepsilon \mathrm{e}^{\varphi} - \beta\left((m^2+b^2)\mathrm{e}^{-\varphi}\right)^{\frac{1}{2}}}. \tag{5.91}$$

To begin, we note that the ε divergence comes from the large φ region. The scale for m is given by $1/w_V$, so it is small. When also b is small, the rightmost term in (5.91), $(m^2+b^2)\,\mathrm{e}^{-\varphi}$, is independent of φ. The scaling of the integral then merely comes from the factor $\exp(-\varepsilon\,\mathrm{e}^{\varphi})$ and is logarithmic in ε. In hindsight, it will be clear that we can neglect this divergence. For large b it is helpful to transform m, b to polar-type coordinates:

$$m = r\cos(\theta), \quad b = r\sin(\theta), \quad r(.) \in \mathbb{R}^+, \quad \theta(.) \in (0, 2\pi). \tag{5.92}$$

We obtain:

$$K_{n,\varepsilon} \sim \frac{1}{\pi}\int_{\mathbb{R}} \mathrm{d}\varphi\, \mathrm{e}^{-\varepsilon \mathrm{e}^{\varphi}} \int_0^{\infty} r\mathrm{d}r\, \mathrm{e}^{-\beta r \mathrm{e}^{-\frac{\varphi}{2}}} \int_0^{2\pi} \mathrm{d}\theta\ \mathrm{e}^{-2w_V^2 r^2 \cos(\theta)^2 - 2\mathrm{i}Er\cos(\theta)}. \tag{5.93}$$

As r is large, we can calculate the θ integral using the saddle point method. We end up with:

$$K_{n,\varepsilon} \sim \int_{\mathbb{R}} \mathrm{d}\varphi\, \mathrm{e}^{-\varepsilon \mathrm{e}^{\varphi}} \int_0^{\infty} \mathrm{d}r\, \mathrm{e}^{-\beta r \mathrm{e}^{-\frac{\varphi}{2}}} \sim \int_{\mathbb{R}} \mathrm{d}\varphi\, \mathrm{e}^{\frac{\varphi}{2}} \mathrm{e}^{-\varepsilon \mathrm{e}^{\varphi}} \sim \varepsilon^{-\frac{1}{2}}. \tag{5.94}$$

We have learned in an introduction 2.2, Subsection 2.2.6, that the scaling (5.94) is indicative of a singular continuous spectrum. The fractal exponent $\alpha = 1/2$ is universal (independent of β). This was expected because β just represents different elements of the sc moduli space; the solutions Y_{sc} for different $\beta > 0$ all occur at the critical point. With the scaling (5.94) we can now complete the table 4.4.2:

spectrum	diagnostic	moduli space of Y
pp	$K_{n,\varepsilon} \sim \varepsilon^{-1}$	single point
ac	$K_{n,\varepsilon} < \infty$	H^2
sc	$K_{n,\varepsilon} \sim \varepsilon^{-\frac{1}{2}}$	$H^2 \setminus \{o\}$

,

and display a typical solution of all three cases:

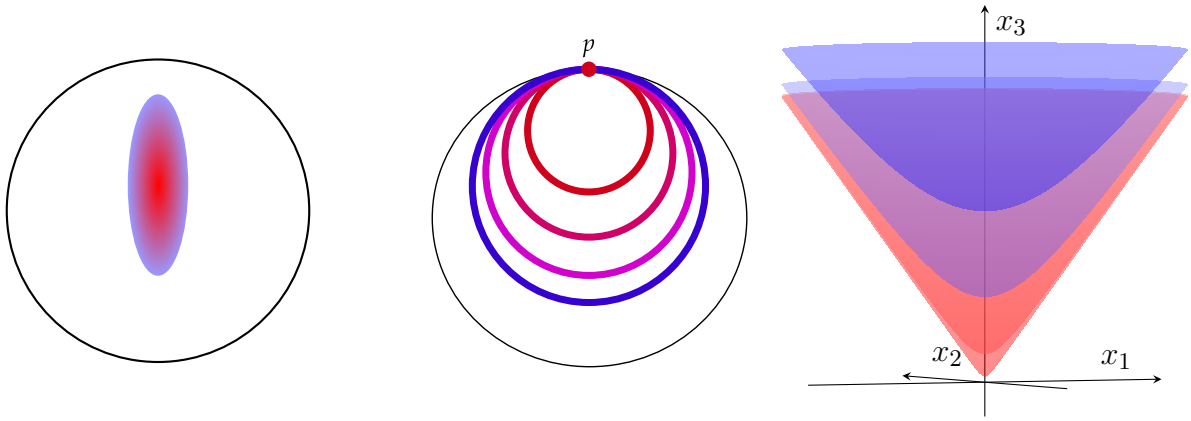

Figure 5.2: Sketch of an ac-, sc-, and pp-type solution: Left(ac): The solution is localized around the center of the Poincaré disk, reflecting symmetry breaking to a compact subgroup. Middle (sc): The solution concentrates along horocycles centered at a boundary point p, indicating partial symmetry breaking to a nilpotent subgroup. Right (pp): The solution is constant on a fixed hyperboloid and decays in the massive direction. The full hyperbolic symmetry is intact.

6 Algebraic characterization

We here delve deeper into the algebraic structure of our symmetry group $G = \mathrm{SU}(1,1)$ (or $\mathrm{SL}(2,\mathbb{R})$). We will introduce different group decompositions:

$$G = KA_+K, \quad G = ANK \quad G = NAK, \tag{6.1}$$

and see how they lead to the different coordinates we have used throughout this work. Of course, similar results also hold in the general case of non-compact semisimple Lie groups, and we will keep the language fairly general.

Next, with these decompositions in hand, we can characterize the different solutions $Y_{\mathrm{ac}}, Y_{\mathrm{sc}}, Y_{\mathrm{pp}}$ on an algebraic level, and we answer the question which subgroup leaves the critical solution Y_{sc} invariant. The symmetry characterization of the two phases and the critical points, and their connection to the spectral types, delivers a rather complete picture of the phase diagram for the Wegner model and, by universality, for Anderson-type transitions in general.

6.1 An algebraic intermezzo

6.1.1 Structure of Lie algebra-Compact, Abelian and nilpotent subalgebras and corresponding subgroups

As we have already used several times in this work, the Lie algebra of $\mathrm{SU}(1,1)$, $\mathrm{su}(1,1)$ is the vector space

$$\mathrm{su}(1,1) = \mathrm{span}_{\mathbb{R}}\{\mathrm{i}\sigma_3, \sigma_1, \sigma_2\}. \tag{6.2}$$

For our purposes, it is convenient to switch to the real Lie algebra

$$\mathfrak{g} \equiv \mathrm{sl}(2,\mathbb{R}) = \mathrm{span}_{\mathbb{R}}\{\mathrm{i}\sigma_2, \sigma_3, \sigma_1\}. \tag{6.3}$$

by using the Lie algebra isomorphism

$$\mathrm{i}\sigma_3 \to \mathrm{i}\sigma_2, \ \sigma_1 \to \sigma_3, \ \sigma_2 \to \sigma_1. \tag{6.4}$$

The corresponding Lie groups, $\mathrm{SU}(1,1)$ and $\mathrm{SL}(2,\mathbb{R})$ are isomorphic as Lie groups. In the following, we will thus write $G = \mathrm{SL}(2,\mathbb{R})$. A Cartan involution on $\mathfrak{g}$ is given by

$$\theta(X) = -X^t, \tag{6.5}$$

where t denotes the transpose of a matrix. θ is a Lie algebra homomorphism:

$$\theta([X,Y]) = [\theta(X),\theta(Y)],\ X,Y \in \mathfrak{g}. \tag{6.6}$$

The eigenspaces of θ with eigenvalue $+1$, $\mathfrak{k}$, and eigenvalue -1, $\mathfrak{p}$, are given by

$$\mathfrak{k} = \mathrm{span}_{\mathbb{R}}\{\mathrm{i}\sigma_2\},\ \mathfrak{p} = \mathrm{span}_{\mathbb{R}}\{\sigma_3,\sigma_1\},\ \mathfrak{g} = \mathfrak{k}\oplus\mathfrak{p}. \tag{6.7}$$

One easily checks that

$$[\mathfrak{k},\mathfrak{k}] \subseteq \mathfrak{k},\ [\mathfrak{p},\mathfrak{p}] \subseteq \mathfrak{k},\ [\mathfrak{k},\mathfrak{p}] \subseteq \mathfrak{p}. \tag{6.8}$$

From the first of the above identities, it follows that $\mathfrak{k}$ is a Lie subalgebra. It is called a (maximal) compact subalgebra. It generates a compact subgroup $K \subset G$. Indeed,

$$K = \exp(\mathbb{R}\,\mathrm{i}\sigma_2) \cong \mathrm{U}(1). \tag{6.9}$$

The second identity in Eq. (6.8) shows that $\mathfrak{p}$ is not a Lie subalgebra. However, we can choose a (maximal) Abelian subspace

$$\mathfrak{a} = \mathrm{span}_{\mathbb{R}}\{\sigma_3\} \tag{6.10}$$

of $\mathfrak{p}$. Obviously, it is a Lie subalgebra of $\mathfrak{g}$. We obtain the corresponding subgroup A which is the subgroup with Lie algebra $\mathfrak{a}$:

$$A = \exp(\mathbb{R}\,\sigma_3). \tag{6.11}$$

Next with the Abelian subspace $\mathfrak{a}$ of $\mathfrak{p}$ we construct the restricted root spaces $\mathfrak{g}_\alpha$, $\alpha \in \mathfrak{a}^*$. They are given by

$$\begin{gathered}\mathfrak{g}_{\alpha=+1} = \mathrm{span}_{\mathbb{R}}\left\{\frac{1}{2}(\sigma_1+\mathrm{i}\sigma_2) = \sigma_+\right\},\ \mathfrak{g}_{\alpha=-1} = \mathrm{span}_{\mathbb{R}}\left\{\frac{1}{2}(\sigma_1-\mathrm{i}\sigma_2) = \sigma_-\right\} \\ \mathfrak{g} = \mathfrak{a}\oplus\mathfrak{g}_{+1}\oplus\mathfrak{g}_{-1}.\end{gathered} \tag{6.12}$$

Indeed,

$$[\sigma_3,\sigma_+] = \sigma_+, \quad [\sigma_3,\sigma_-] = -\sigma_-. \tag{6.13}$$

The corresponding restricted roots are $\alpha = \pm 1$. With the restricted root spaces, we can now construct another subgroup, a nilpotent subgroup N. The corresponding Lie subalgebras $\mathfrak{n}_\pm$ are given by the direct sum of the restricted root spaces over the positive or negative restricted roots. [Positive or negative restricted roots are defined with respect to any lexicographic ordering in $\mathfrak{a}^*$]. In the present case, the direct sums consist of only one summand $\mathfrak{g}_{+1}$ or $\mathfrak{g}_{-1}$:

$$\mathfrak{n}_+ = \mathrm{span}_{\mathbb{R}}\{\sigma_+\}, \quad \mathfrak{n}_- = \mathrm{span}_{\mathbb{R}}\{\sigma_-\}. \tag{6.14}$$

The corresponding nilpotent subgroups are

$$N_+ = \exp(\mathbb{R}\sigma_+), \quad N_- = \exp(\mathbb{R}\sigma_-). \tag{6.15}$$

6.1.2 Decompositions

Cartan decomposition

One can show that the mapping

$$K \times \mathfrak{p} \to G, \quad (k,p) \to k\, \exp(p) \tag{6.16}$$

is a diffeomorphism [52, 51]. Now we can define a maximal Abelian subspace in $\mathfrak{p}$ for every $p \in \mathfrak{p}$,

$$\widetilde{\mathfrak{a}} = \mathrm{span}_{\mathbb{R}}\{p\}. \tag{6.17}$$

Furthermore, given two maximal Abelian subspaces $\mathfrak{a}, \widetilde{\mathfrak{a}}$ one can always find an element $k \in K$ such that $\mathfrak{a}$ is obtained from $\widetilde{\mathfrak{a}}$ via conjugation with k [51]. Now let k_p be such that

$$k_p\, p\, k_p^{-1} \in \mathfrak{a}, \quad p \in \widetilde{\mathfrak{a}}. \tag{6.18}$$

Then,

$$k \exp(p) = k\, k_p^{-1} k_p \exp(\mathrm{p})\, k_p^{-1} k_p = k\, k_p^{-1} \exp(k_p\, p\, k_p^{-1})\, k_p \in KAK. \tag{6.19}$$

However, the corresponding KAK decomposition is not unique. Indeed, we could instead choose

$$k_p \to \hat{k}\, k_p, \quad \hat{k} \in \mathcal{N}_K(\mathfrak{a})/\mathcal{C}_K(\mathfrak{a}), \tag{6.20}$$

where $\mathcal{N}_K(\mathfrak{a})$ is the normalizer of $\mathfrak{a}$ in K and $\mathcal{C}_K(\mathfrak{a})$ is the centralizer of $\mathfrak{a}$ in K, and obtain another element in $\mathfrak{a}$. [The quotient coincides with the Weyl group corresponding to the restricted roots α. In the present case, it is simply $\mathbb{Z}_2$]. To

obtain uniqueness, we have to restrict to a subset of $\mathfrak{a}$, for example

$$\mathfrak{a}_+ = \mathbb{R}^+ \sigma_3 \tag{6.21}$$

(the positive Weyl chamber). As an anticipation, we mention that the geometric meaning of this algebraic fact is that the hyperbolic radius in hyperbolic polar coordinates is restricted to the positive real numbers.

From the above considerations, it follows that we have a diffeomorphism

$$G \cong K \times A_+ \times K, \quad A_+ = \exp(\mathbb{R}^+ \sigma_3). \tag{6.22}$$

Iwasawa decomposition

Another theorem states that the mapping

$$K \times A \times N \to G, \quad (k, a, n) \to k\, a\, n \tag{6.23}$$

or equivalently, by concatenating with the group inversion, the mapping

$$N \times A \times K \to G, \quad (n, a, k) \to n\, a\, k \tag{6.24}$$

are diffeomorphisms [43]. Finally, by noting that A normalizes N we obtain a third diffeomorphism:

$$A \times N \times K \to G, \quad (a, n, k) \to a\, n\, k. \tag{6.25}$$

6.2 Coordinates from the decompositions and symmetry properties of the pp, ac, sc solutions

6.2.1 Coordinates

We recall the expansion of our Q field in the Lie algebra generators:

$$\mathrm{i}Q = x_0\, \mathrm{i}\mathbf{1} + x_3\, \mathrm{i}\sigma_3 + x_1\, \sigma_1 + x_2\, \sigma_2 \to x_0\, \mathrm{i}\mathbf{1} + x_3\, \mathrm{i}\sigma_2 + x_1\, \sigma_3 + x_2\, \sigma_1, \tag{6.26}$$

where on the r.h.s. we have performed the isomorphism $\mathrm{su}(1,1) \to \mathrm{sl}(2,\mathbb{R})$. We can also write $\mathrm{i}Q$ in terms of the conjugate group action acting on the m dependent base point:

$$\mathrm{i}Q = g q_0 g^{-1}, \quad g \in \mathrm{SL}(2,\mathbb{R}). \tag{6.27}$$

Hyperbolic polar coordinates

As in the section on the harmonic analysis, Section 5.1, we parameterize

$$q_0 = m\,\mathrm{i}\mathbf{1} + |m|\,\mathrm{i}\sigma_2 = \begin{pmatrix} im & |m| \\ -|m| & im \end{pmatrix}. \tag{6.28}$$

By exploiting the Cartan decomposition of G, $G = KA_+K$, we parameterize:

$$\begin{aligned} \mathrm{i}Q &= \mathrm{e}^{\frac{\phi}{2}\mathrm{i}\sigma_2}\,\mathrm{e}^{\frac{\theta}{2}\sigma_3}\,q_0\,\mathrm{e}^{-\frac{\theta}{2}\sigma_3}\,\mathrm{e}^{-\frac{\phi}{2}\mathrm{i}\sigma_2} \\ &= \begin{pmatrix} \mathrm{i}m + |m|\sinh(\theta)\sin(\phi) & |m|\cosh(\theta) + |m|\sinh(\theta)\cos(\phi) \\ -|m|\cosh(\theta) + |m|\sinh(\theta)\cos(\phi) & \mathrm{i}m - |m|\sinh(\theta)\sin(\phi) \end{pmatrix}, \end{aligned} \tag{6.29}$$

where $\phi \in (0, 2\pi)$, $\theta \in \mathbb{R}^+$. We thus obtain hyperbolic polar coordinates:

$$x_0 = m, \quad x_3 = |m|\cosh(\theta), \quad x_1 = |m|\sinh(\theta)\sin(\phi), \quad x_2 = |m|\sinh(\theta)\cos(\phi). \tag{6.30}$$

To conclude, hyperbolic coordinates stem from the Cartan decomposition of the symmetry group.

Horospherical coordinates

To describe the symmetry-transformed ac-type solutions ${}^{g_s}Y_{\mathrm{ac}}$ and finally the critical solutions Y_{sc}, we switched from hyperbolic polar coordinates to another coordinate system, so-called horospherical coordinates, Eq. (4.29). These come from the Iwasawa decomposition of the symmetry group. The above parameterization of the base point q_0, Eq. (6.28), comes with the difficulty that for $m = 0$ it collapses to the zero matrix, and thus fails to describe the null-orbit $|x_3 = x_1 + \mathrm{i}x_2|$. We here choose an alternative parameterization

$$q_0 = m\,\mathrm{i}\mathbf{1} + \sigma_+ - m^2\,\sigma_- = \begin{pmatrix} \mathrm{i}m & 1 \\ -m^2 & \mathrm{i}m \end{pmatrix}. \tag{6.31}$$

We now parameterize the conjugate G action via the Iwasawa decomposition $AN\tilde{K}$ (here $\tilde{K}$ is the $m-$dependent stabilizer subgroup of q_0):

$$\mathrm{i}Q = \mathrm{e}^{\frac{\varphi}{2}\sigma_3}\,\mathrm{e}^{-b\sigma_-}\,q_0\,\mathrm{e}^{b\sigma_-}\,\mathrm{e}^{-\frac{\varphi}{2}\sigma_3} = \begin{pmatrix} \mathrm{i}m + b & \mathrm{e}^{\varphi} \\ -(m^2 + b^2)\mathrm{e}^{-\varphi} & \mathrm{i}m - b \end{pmatrix}, \tag{6.32}$$

where $b, \varphi \in \mathbb{R}$. This yields the horospherical coordinate system, Eq. (4.29):

$$x_0 = m, \quad x_1 = b, \quad x_2 = \frac{1}{2}(\mathrm{e}^{\varphi} - (m^2+b^2)\mathrm{e}^{-\varphi}), \quad x_3 = \frac{1}{2}(\mathrm{e}^{\varphi} + (m^2+b^2)\mathrm{e}^{-\varphi}). \tag{6.33}$$

Finally, we comment on the name *horospherical* coordinates. The reason is that the integral curves of the action of the nilpotent subgroups N of G on the symmetric space $H^2 = G/K$ are horocycles, while those of the maximal Abelian subgroup A are radial geodesics.

6.3 Symmetry properties of the three solutions $Y_{\rm ac}, Y_{\rm pp}, Y_{\rm sc}$

We are now finally in a position to characterize the three types of solutions on an algebraic level. As above, we here work with the $\mathrm{SL}_2(\mathbb{R})$ picture.

1. **pp**: We already know that the pp-type solution $Y_{\rm pp}$ is invariant under the full symmetry group G. For fixed parameter values, there is only a single extremal Gibbs state. The corresponding typical field configurations restore the full symmetry.

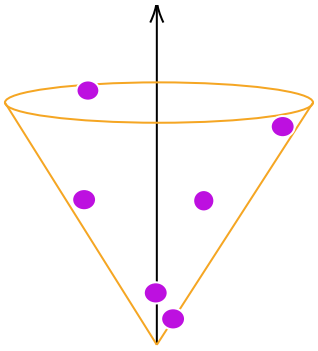

Figure 6.1: Sketch of a typical field configuration in the pp phase: The field fluctuates near the boundary (orange) of the target cone C^3, but explores the whole of the corresponding symmetry group orbits.

2. **ac**: The solution $Y_{\rm ac}$ is a function that only depends on x_0, x_3. It can be written as

$$Y_{\rm ac}(Q) = Y_{\rm ac}(x_0, \mathrm{Tr}(Q\,\mathrm{i}\sigma_2)). \tag{6.34}$$

As such, it is K invariant:

$$Y_{\rm ac}(Q) = Y_{\rm ac}(k\,Q\,k^{-1}), \quad k \in K. \tag{6.35}$$

The transformed ac solutions ${}^{g_s}Y_{\rm ac} = Y_{\rm ac}(g_s^{-1}\,Q\,g_s)$ are invariant under a mod-

ified compact subgroup ${}^{g_s}K = g_s\, K\, g_s^{-1}$, $g_s \in A$:

$$ {}^{g_s}Y_{\rm ac}(Q) = {}^{g_s}Y_{\rm ac}(k_s\, Q\, k_s^{-1}), \quad k_s = g_s k {g_s}^{-1}, \quad k \in K. \tag{6.36} $$

Indeed,

$$ \begin{aligned} &{}^{g_s}Y_{\rm ac}(k_s\, Q\, k_s^{-1}) = Y_{\rm ac}(x_0, \mathrm{Tr}(g_s^{-1}\, g_s\, k\, g_s^{-1}\, Q\, g_s\, k^{-1}\, g_s^{-1}\, g_s\, \mathrm{i}\sigma_2)) \\ &= Y_{\rm ac}(x_0, \mathrm{Tr}(k\, g_s^{-1}\, Q\, g_s\, k^{-1}\, \mathrm{i}\sigma_2)) = Y_{\rm ac}(x_0, \mathrm{Tr}(g_s^{-1}\, Q\, g_s\, \mathrm{i}\sigma_2)) = {}^{g_s}Y_{\rm ac}(Q). \end{aligned} \tag{6.37} $$

3. **sc**: The expression for the sc solution from the end of Section 5.3 reads:

$$ Y_{\rm sc}(Q) = Y_{\rm pp}(Q) \exp\left(-\beta\sqrt{m^2 + b^2}\, \mathrm{e}^{-\frac{\varphi}{2}}\right), \quad \beta \in \mathbb{R}^+. \tag{6.38} $$

Recalling that the hyperbolic coordinates come from the Iwasawa decomposition (6.32) we can write $Y_{\rm sc}$ as

$$ Y_{\rm sc}(Q) = Y_{\rm sc}(x_0, \mathrm{Tr}(-Q\, \frac{\sigma_1 + \mathrm{i}\sigma_2}{2})) = Y_{\rm sc}(x_0, \mathrm{Tr}(Q\, \sigma_+)). \tag{6.39} $$

Eq. (6.39) reveals that the critical solution $Y_{\rm sc}$ is N_+-invariant:

$$ Y_{\rm sc}(Q) = Y_{\rm sc}(n_+\, Q\, n_+^{-1}), \quad n_+ \in N_+ = \exp(\mathbb{R}\, \sigma_+). \tag{6.40} $$

We finally note that in the derivation of $Y_{\rm sc}$ we sent the symmetry group parameter s of the maximal Abelian subgroup $A = \exp(\mathbb{R}\, (\sigma_1 \to \sigma_3))$ to $+\infty$. Of course, this choice is not dictated. We could also send $s \to -\infty$. The solution thus obtained has the form

$$ \widetilde{Y_{\rm sc}}(Q) = {}^{g_s \to -\infty}Y_{\rm ac}(Q) = Y_{\rm pp}(Q) \exp\left(-\beta\, \mathrm{e}^{\frac{\varphi}{2}}\right) = Y_{\rm sc}(x_0, \mathrm{Tr}(Q\, \sigma_-)). \tag{6.41} $$

Now it is invariant under the other nilpotent subgroup in $\mathrm{SL}(2, \mathbb{R})$, $N_- = \exp(\mathbb{R}\, \sigma_-)$, whose Lie algebra is the negative restricted root space $\mathfrak{n}_- = \mathfrak{g}_{-1}$:

$$ \widetilde{Y_{\rm sc}}(Q) = \widetilde{Y_{\rm sc}}(n_-\, Q\, n_-^{-1}), \quad n_- \in N_-. \tag{6.42} $$

In summary, we have obtained two classes of critical solutions, which are both N-invariant (N_+ or N_-). On an algebraic level, they simply differ in the choice of positive or negative restricted root space as the Lie algebra of N.

6.3.1 Moduli spaces of ac and sc solutions for fixed system parameters

We finish by substantiating the claims about the ac and sc moduli space from Section 3.4.5. Recall that in the construction of the symmetry-transformed ac solutions and also the sc solutions, we have fixed the one-parameter subgroup $g_s = \exp((s/2)\,\sigma_1)$, $s \in \mathbb{R}$. In the present chapter we made use of the isomorphism $\mathrm{su}(1,1) \to \mathrm{sl}(2,\mathbb{R})$, that sends σ_1 to $\sigma_3 \in \mathfrak{a}$. After applying the isomorphism, σ_3 is the generator of the maximal Abelian subgroup A. Of course, the above fix of a one-parameter subgroup is not dictated. We could have chosen other one-parameter subgroups, that is, other maximal Abelian subalgebras $\widetilde{\mathfrak{a}} = \mathrm{span}_{\mathbb{R}}\{p\}$, $p \in \mathfrak{p}$. The set of maximal Abelian subalgebras $\widetilde{A}$ thus obtained is homeomorphic to the space of lines in $\mathbb{R}^2 \cong \mathfrak{p}$ passing through the origin. This space is the real projective space $\mathbb{R}P^1$.

1. **ac moduli space**: By fixing another maximal Abelian subalgebra $\widetilde{A}$ we obtain two other rays of symmetry transformed ac solutions $\{{}^{\widetilde{g}_s}Y_{\mathrm{ac}},\, s > 0\}$ and $\{{}^{\widetilde{g}_s}Y_{\mathrm{ac}},\, s < 0\}$ which are both homeomorphic to $\mathbb{R}^+$. Thus for every point in $\mathbb{R}P^1$ we obtain two rays $\cong \mathbb{R}^+$, and the resulting space can be identified with the punctured plane. Together with the $\mathrm{U}(1)_{\mathrm{i}\sigma_2}$-invariant solution Y_{ac}, which is the center of the ac moduli space, the full ac moduli space thus can be identified with

$$\mathbb{R}^2 \cong D^2. \tag{6.43}$$

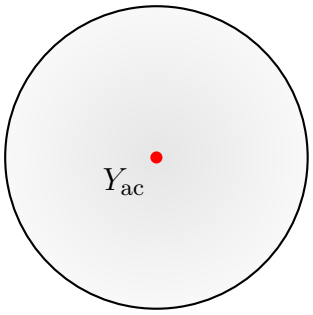

Figure 6.2: Moduli space $H^2 \cong D^2$ of ac type solutions ${}^{g}Y_{\mathrm{ac}}$.

Due to the identification with extremal Gibbs states, an ac-type solution corresponds to a cluster of typical field configurations. Because of the symmetry under compact subgroups, the cluster have compact support. For the center of the disk, the corresponding cluster is a tubular neighborhood of the center half-axis of C^3.

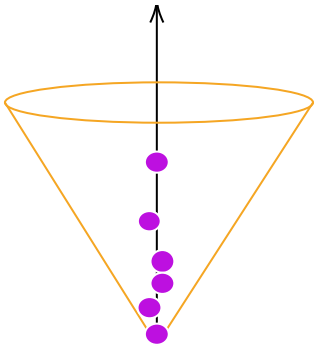

Figure 6.3: Sketch of a typical field configuration in the metallic phase. In this case the field clusters around the center half-axes (black arrow).

2. **sc moduli space**: We have already seen that, according to a specific choice of a maximal Abelian subalgebra, we obtain two nilpotent subalgebras $\widetilde{N}_{\pm}$. Each of them characterizes a class of sc-type solutions because these are invariant under the groups $\widetilde{N}_{\pm}$. In other words, for every element in $\mathbb{R}P^1$ we obtain two classes of sc-type solutions $\{\pm\}$. The set of classes so obtained is a circle:

$$\mathbb{R}P^1 \times \{\pm\} \cong S^1. \tag{6.44}$$

The geometric meaning of this statement is that horocycles can be characterized by their "center", i.e., the boundary point of the Poincaré disk where they are centered at. Furthermore, for a fixed choice of maximal Abelian subgroup $\widetilde{A}$ and a corresponding choice of nilpotent subgroup $\pm$, the class of sc-type solutions still has a free parameter $\beta \in \mathbb{R}^+$ (see Eq. (5.88), Section 5.3, Chapter 5). The entire moduli space of sc-type solutions can thus be identified with

$$S^1 \times \mathbb{R}^+ \cong D^2 \setminus \{o\}, \tag{6.45}$$

where o denotes the center of D^2.

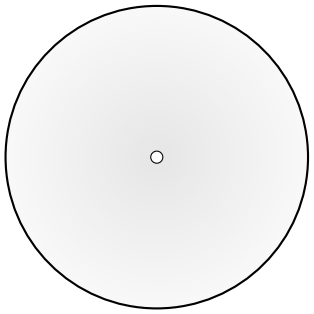

Figure 6.4: Moduli space $D^2 \setminus \{o\}$ of sc-type solutions Y_{sc}.

Again, an sc-type solution corresponds to a critical extremal Gibbs state and a cluster of a typical field configuration. Now the cluster is non-compact and centered around a ray on the boundary cone of C^3 from the tip to infinity.

However, it does not restore the full hyperbolic symmetry. The symmetry-breaking mechanism at criticality is distinct from that in the metallic phase.

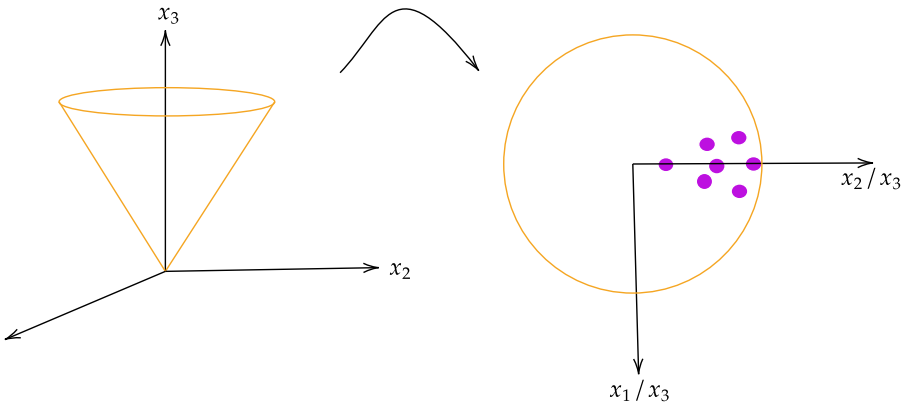

Figure 6.5: Sketch of a typical field configuration at criticality. Now the field clusters around a ray ending at a certain boundary point on the boundary of the Poincaré disk.

Finally, we comment a bit more on the positive constant β entering the sc-type solutions. Geometrically, the magnitude of $\beta > 0$ controls the extent of the support of Y_{sc} around the boundary point it is centered at. It follows that it controls the strength of the typical field fluctuations around this boundary point (the transverse field fluctuations) in the corresponding extremal Gibbs state.

7 Conclusion

In this dissertation, we have extended the analytical approach to Anderson transitions in high dimensions by solving the Wegner 1-orbital model in an approximation exact on the Bethe lattice and likely valid for the calculation of local observables in high dimensions. In low dimensions ($d = 2 + \varepsilon$), the nature of the critical point is well-understood: the one-parameter scaling hypothesis, proposed in [2], can be confirmed by a renormalization group treatment of the nonlinear σ-model. In contrast, in the case of high lattice dimensions, the nature of the critical point is still an ongoing debate. Our work identifies a novel field-theoretical mechanism of spontaneous symmetry breaking, intimately connected to the non-compact nature of the symmetry group:

$$\mathrm{SU}(1,1) \cong \mathrm{SL}(2,\mathbb{R}). \tag{7.1}$$

In a sense, this identification reconciles the insulating phase, the metallic phase, and the critical points by mapping the physics governing these regimes to different spontaneous symmetry breaking scenarios of the same symmetry group. While the full non-compact symmetry remains intact in the insulating phase and breaks down to a compact subgroup K in the metallic phase, it breaks down to a nilpotent subgroup N at criticality:

regime	symmetry
insulating	$\mathrm{SL}(2,\mathbb{R}) = G$
metallic	$\mathrm{U}(1) \cong K \subset G$
critical	$\mathbb{R} \cong N \subset G$

Table 7.1: Symmetry-breaking mechanisms in our field theory

By partially restoring the non-compact symmetry at criticality, this novel symmetry-breaking scenario quite naturally corresponds to a singular continuous spectrum of the Wegner Hamiltonian 3.1.

Due to the connection of the observable

$$K_{n,\varepsilon} = \mathbb{E}(|G_{n,n}(E + \mathrm{i}\varepsilon)|^2) \tag{7.2}$$

to the spectral types, we set up a field theory to express it as the field-theoretical expectation value of a local field operator. One main analytical tool we used in this dissertation is the mapping of a field theory on high-dimensional lattices to a supersymmetric integral equation, the AAT integral equation (3.50). We have argued that the solutions of this integral equation correspond to extremal Gibbs states (restricted to the distinct site n) of the field theory. After further mapping the supersymmetric integral equations to a "bosonic" integral equation (3.90), we then studied the solution spaces of that equation. Importantly, using the tools of harmonic analysis, we obtain a closed formula for the critical manifold in the limit $K \to \infty$

$$K(w_c) = \frac{1}{\sqrt{2}} \frac{w_c}{\ln(w_c)} \exp\left(\frac{E^2}{2w_V^2}\right), \tag{7.3}$$

and study the critical behavior of the metallic solutions ${}^{g}Y_{\mathrm{ac}}$ for $w \nearrow w_c$. By combining this knowledge with the non-compact nature of the symmetry group, we constructed the critical, N-invariant solutions Y_{sc} by performing a coupled limit: $w \nearrow w_c$, and the parameter of a Lorentz transformation $s \to \infty$ such that

$$s \sim \frac{1}{\sqrt{w_c - w}}. \tag{7.4}$$

Finally, by delving deeper into the structure of the symmetry group $SL(2,\mathbb{R})$, we demonstrated that Y_{sc} is indeed N-invariant.

Invoking the principle of universality and recalling that the novel field-theoretical scenario can be described in purely algebraic terms that should not depend on the exact microscopic details of the Wegner Hamiltonian, we expect that this phenomenon occurs for a wider class of Anderson transitions. In addition, any non-compact semisimple Lie group possesses an Iwasawa decomposition $G = KAN$. Therefore, one can in principle expect symmetry-breaking scenarios similar to the one presented here in a wide class of effective field theories with non-compact symmetry orbits.

In summary, we expect that our work may serve as a foundation for the study of other field theories with non-compact symmetry, and that mechanisms similar to the one detected here can be found.

One of the most interesting open problems in the study of Anderson transitions is whether or not the critical point is described by a conformal field theory. In the introduction, it has been portrayed that the no-CFT argument, presented in e.g. [66], relies on the absence of spontaneous symmetry breaking at criticality. Our work sheds new light on this open question by challenging the assumption of an absence of symmetry breaking. An interesting direction for future work is to understand more deeply the consequences of our results for the CFT versus no-CFT

debate.

An additional task for the future is to clarify the connections between the novel field-theoretical mechanism and the recent results from numerical works [35, 36] and from the scaling analysis [89]. The outcome of these works is that two (instead of one!) relevant scales appear at the transition, even though in [89], the one-parameter scaling is recovered for large system sizes.

We hope that the perspective developed in this work contributes to a deeper structural understanding of Anderson transitions in high dimensions and provides a starting point for further analytical investigation of systems with non-compact symmetries.

Bibliography

[1] R. Abou-Chacra, P. W. Anderson, and D. J. Thouless. A self-consistent theory of localization. *J. Phys. C*, 6:1734, 1973. doi:10.1088/0022-3719/6/10/009.

[2] E. Abrahams, P.W. Anderson, D.C. Licciardello, and T.V. Ramakrishnan. Scaling theory of localization – absence of quantum diffusion in 2 dimensions. *Phys. Rev. Lett.*, 42:673, 1979. doi:10.1103/PhysRevLett.42.673.

[3] M. Aizenman and S. Molchanov. Localization at large disorder and at extreme energies: An elementary derivations. *Commun. Math. Phys.*, 157:245, 1993. doi:10.1007/BF02099760.

[4] M. Aizenman, R. Sims, and S. Warzel. Stability of the absolutely continuous spectrum of random Schrödinger operators on tree graphs. *Prob. Theor. Relat. Fields*, 136:363, 2006. doi:10.1007/s00440-005-0486-8.

[5] M. Aizenman and S. Warzel. Resonant delocalization for random Schrödinger operators on tree graphs. *J. Eur. Math. Soc.*, 15:1167, 2013. doi:10.4171/JEMS/389.

[6] M. Aizenman and S. Warzel. *Random operators.* American Mathematical Society, 2015. ISBN: 1470419130.

[7] A. Altland and B. Simons. *Condensed matter field theory.* Cambridge University Press, 2023. ISBN: 978-1-108-49460-1.

[8] B. L. Altshuler, Y. Gefen, A. Kamenev, and L.S. Levitov. Quasiparticle lifetime in a finite system: A non-perturbative approach. *Phys. Rev. Lett.*, 78:2803, 1997. doi:10.1103/PhysRevLett.78.2803.

[9] B. L. Altshuler and V. E. Kravtsov. Random Cantor sets and mini-bands in local spectrum of quantum systems. *Ann. Phys.*, 452:169300, 2023. doi:10.1016/j.aop.2023.169300.

[10] P. W. Anderson. Absence of diffusion in certain random lattices. *Phys. Rev.*, 109:1492, 1958. doi:10.1103/PhysRev.109.1492.

[11] D. Baeriswyl, D. K. Campbell, J. M. P. Carmelo, F. Guinea, and E. Louis. *The Hubbard model*. Springer New York, NY, 1995. ISBN: 978-1-4899-1044-8.

[12] F. Berezin. *Introduction to superanalysis*. Springer, 1987. ISBN: 9027716684.

[13] H. A. Bethe. Statistical theory of superlattices. *Proc. R. Soc. Lond. A*, 150:552, 1935. doi:10.1098/rspa.1935.0122.

[14] G. Biroli, A. K. Hartmann, and M. Tarzia. Critical behavior of the Anderson model on the bethe lattice via a large-deviation approach. *Phys. Rev. B*, 105:094202, 2022. doi:10.1103/PhysRevB.105.094202.

[15] R. Carmona and J. Lacroix. *Spectral theory of random Schrödinger operators*. Birkhäuser, 1990. ISBN: 146128841X.

[16] C. Castellani and L. Peliti. Multifractal wavefunction at the localization threshold. *J. Phys. A: Math. Gen.*, 19:429, 1986. doi:10.1088/0305-4470/19/8/004.

[17] D. Damanik, M. Embree, A. Gorodetski, and S. Tcheremchantsev. The fractal dimension of the spectrum of the Fibonacci Hamiltonian. *Commun. Math. Phys.*, 280:499, 2008. doi:10.1007/s00220-008-0451-3.

[18] R. del Rio, S. Jitomirskaya, N. Makarov, and B. Simon. Singular continuous spectrum is generic. *Bull. Amer. Math. Soc.*, 31:208, 1994. doi:10.1090/S0273-0979-1994-00518-X.

[19] M. Disertori and T. Spencer. Anderson localization for a supersymmetric sigma model. *Commun. Math. Phys.*, 300:659, 2010. doi:10.1007/s00220-010-1124-6.

[20] M. Disertori, T. Spencer, and M. R. Zirnbauer. Quasi-diffusion in a 3d supersymmetric hyperbolic sigma model. *Commun. Math. Phys.*, 300:435, 2010. doi:10.1007/s00220-010-1117-5.

[21] F. J. Dyson, E. H. Lieb, and B. Simon. Phase transitions in quantum spin systems with isotropic and nonisotropic interactions. *J. Stat. Phys.*, 18:335, 1978. doi:10.1007/BF01106729.

[22] K. B. Efetov. Supersymmetry and theory of disordered metals. *Adv. Phys.*, 32:53, 1983. doi:10.1080/00018738300101531.

[23] K. B. Efetov. *Supersymmetry in disorder and chaos*. Cambridge University Press, 1997. ISBN: 0521470978.

[24] K. B. Efetov, A. I. Larkin, and D. E. Khmeniskii. Interaction of diffusion modes in the theory of localization. *Sov. Phys. JETP*, 52:568, 1980.

[25] L. Erdös, A. Knowles, H.T. Yau, and J. Yin. Delocalization and diffusion profile for random band matrices. *Commun. Math. Phys.*, 323:367, 2013. doi:10.1007/s00220-013-1773-3.

[26] F. Evers, A. Mildenberger, and A. D. Mirlin. Multifractality at the Quantum Hall Transition: Beyond the parabolic paradigm. *Phys. Rev. Lett.*, 101:116, 2008. doi:10.1103/PhysRevLett.101.116803.

[27] F. Evers and A. D. Mirlin. Anderson transitions. *Rev. Mod. Phys.*, 80:355, 2008. doi:10.1103/RevModPhys.80.1355.

[28] R. P. Feynman. Space-time approach to non-relativistic quantum mechanics. *Rev. Mod. Phys.*, 20:367, 1948. doi:10.1103/RevModPhys.20.367.

[29] G. B. Folland. *Real analysis: modern techniques and their applications*. Wiley, 1999. ISBN: 0471317160.

[30] R. Froese, D. Hasler, and W. Spitzer. Absolutely continuous spectrum for the Anderson model on a tree: A geometric proof of Klein's theorem. *Commun. Math. Phys.*, 269:239, 2006. doi:10.1007/s00220-006-0120-3.

[31] J. Fröhlich and T. Spencer. Absence of diffusion in the Anderson tight binding model. *Commun. Math. Phys.*, 88:151, 1983. doi:10.1007/BF01209475.

[32] Y. V. Fyodorov and H. J. Sommers. Statistics of resonance poles, phase shifts and time delays in quantum chaotic scattering. *J. Math. Phys.*, 38:1918, 1997. doi:10.1063/1.531919.

[33] A. M. García-García and E. Cuevas. Dimensional dependence of the metal-insulator transition. *Phys. Rev. B*, 75:174, 2007. doi:PhysRevB.75.174203.

[34] I. García-Mata, O. Giraud, B. Georgeot, J. Martin, R. Dubertrand, and G. Lemarié. Scaling theory of the anderson transition in random graphs: Ergodicity and universality. *Phys. Rev. Lett.*, 118:166801, 2017. doi:10.1103/PhysRevLett.118.166801.

[35] I. Garcia-Mata, J. Martin, O. Giraud, B. Georgeot, R. Dibertrand, and G. Lemarié. Two critical localization lengths in the anderson transition on random graphs. *Phys. Rev. Res.*, 2:1, 2020. doi:10.1103/PhysRevResearch.2.012020.

[36] I. Garcia-Mata, J. Martin, O. Giraud, B. Georgeot, R. Dibertrand, and G. Lemarié. Critical properties of the Anderson transition on random graphs: Two-parameter scaling theory, Kosterlitz-Thouless type flow, and many-body localization. *Phys. Rev. B*, 106:214202, 2022. doi:10.1103/PhysRevB.106.214202.

[37] H. O. Georgii. *Gibbs measures and phase transitions*. De Gruyter, 2011. ISBN: 9783110250299.

[38] N. Goldenfeld and R. Haydock. Phase diagram for Anderson disorder: Beyond single-parameter scaling. *Phys. Rev. B*, 73:45, 2006. doi:10.1103/PhysRevB.73.045118.

[39] L. P. Gor'kov, A. I. Larkin, and D. E. Khmel'nitskii. Particle conductivity in a two-dimensional random potential. *JETP Lett.*, 30:248, 1979.

[40] I. A. Gruzberg, A. D. Mirlin, and M. R. Zirnbauer. Classification and symmetry properties of scaling dimensions at Anderson transitions. *Phys. Rev. B*, 87:125, 2013. doi:10.1103/PhysRevB.87.125144.

[41] T. Guhr, A. Müller-Gröling, and H. A. Weidenmüller. Random-matrix theories in quantum physics: common concepts. *Phys. Rep.*, 299:189, 1998. doi:10.1016/S0370-1573(97)00088-4.

[42] P. Heinzner, A. Huckleberry, and M. R. Zirnbauer. Symmetry classes of disordered fermions. *Commun. Math. Phys.*, 257:725, 2005. doi:10.1007/s00220-005-1330-9.

[43] S. Helgason. *Differential geometry, Lie groups, and symmetric spaces*. American Mathematical Society, 1978. ISBN: 0821828487.

[44] S. Helgason. *Groups and geometric analysis*. American Mathematical Society, 1984. ISBN: 0821826735.

[45] R. B. Israel. *Convexity in the theory of lattice gases*. Princeton Series in Physics, 1979. ISBN: 9780691635002.

[46] S. Jitomirskaya and B. Simon. Operators with singular continuous spectrum: Iii. almost periodic Schrödinger operators. *Commun. Math. Phys.*, 165:201, 1994. doi:10.1007/BF02099743.

[47] K. Jüngling and R. Oppermann. Effects of spin interactions in disordered electronic systems: Loop expansions and exact relations among local gauge invariant models. *Z. Phys. B*, 38:93, 1980. doi:10.1007/BF01598749.

[48] F. J. Karcher, I. A. Gruzberg, and A. D. Mirlin. Generalized multifractality at metal-insulator transitions and in metallic phases of two-dimensional disordered systems. *Phys. Rev. B*, 106:104, 2022. doi:10.1103/PhysRevB.106.104202.

[49] A. Klein. Spreading of wave packets in the Anderson model on the Bethe lattice. *Commun. Math. Phys.*, 177:755, 1996. doi:10.1007/BF02099546.

[50] A. Klein. Extended states in the Anderson model on the Bethe lattice. *Adv. Math.*, 133:163, 1998. doi:10.1006/aima.1997.1688.

[51] A. Knapp. *Lie groups beyond an introduction.* Birkhäuser, 1996. ISBN: 0817642595.

[52] A. Knapp. Structure theory of semisimple Lie groups. *Proc. Symp. PureMath.*, 61, 1997.

[53] B. Kramer and A. MacKinnon. Localization: Theory and experiment. *Rep. Prog. Phys.*, 56:1469, 1993. doi:10.1088/0034-4885/56/12/001.

[54] V. E. Kravtsov, B. L. Altshuler, and L. B. Ioffe. Non-ergodic delocalized phase in Anderson model on bethe lattice and regular graph. *Ann. Phys.*, 389:148, 2018. doi:10.1016/j.aop.2017.12.009.

[55] V. E. Kravtsov, I. M. Khaymovich, E. Cuevas, and M. Amini. A random matrix model with localization and ergodic transitions. *New J. Phys.*, 17:122002, 2015. doi:10.1088/1367-2630/17/12/122002.

[56] Y. Last. Quantum dynamics and decompositions of singular continuous spectra. *J. Func. An.*, 142:406, 1996. doi:10.1006/jfan.1996.0155.

[57] P. A. Lee and T. V. Ramakrishnan. Disordered electronic systems. *Rev. Mod. Phys.*, 57:287, 1985. doi:10.1103/RevModPhys.57.287.

[58] G. Lemarié, H. Lignier, D. Delande, P. Szriftgiser, and J. C. Garreau. Critical state of the Anderson transition–between a metal and an insulator. *Phys. Rev. Lett.*, 105:090601, 2010. doi:10.1103/PhysRevLett.105.090601.

[59] J. Lindinger and A. Rodríguez. Multifractal finite-size scaling at the Anderson transition in the unitary symmetry class. *Phys. Rev. B*, 96:134, 2017. doi:10.1103/PhysRevB.96.134202.

[60] A. D. Mirlin and Y. V. Fyodorov. Localization transition in the Anderson model on the Bethe lattice: Spontaneous symmetry breaking and correlation functions. *Nucl. Phys. B*, 366:507, 1991. doi:10.1016/0550-3213(91)90028-V.

[61] A. D. Mirlin and Y. V. Fyodorov. Distribution of local density of states, order parameter function, and critical behavior near the Anderson transition. *Phys. Rev. Lett.*, 72:526, 1994. doi:10.1103/PhysRevLett.72.526.

[62] N. F. Mott. Conduction in glasses containing transition metal ions. *J. Non-Cryst. Solids*, 1:1, 1968. doi:10.1016/0022-3093(68)90002-1.

[63] H. Obuse, A. R. Subramaniam, A. Furusaki, I. A. Gruzberg, and A. W. W. Ludwig. Boundary multifractality at the Integer Quantum Hall Plateau Transition: Implications for the critical theory. *Phys. Rev. Lett.*, 101:116, 2008. doi:10.1103/PhysRevLett.101.116802.

[64] F. W. J. Olver, A. B. Olde Daalhuis, D. W. Lozier, B. I. Schneider, R. F. Boisvert, C. W. Clark, B. R. Miller, B. V. Saunders, H. S. Cohl, and M. A. McClain. Nist digital library of mathematical functions (dlmf), 2026. Release 1.2.6. URL: https://dlmf.nist.gov/.

[65] L. Onsager. Crystal statistics.I. A two-dimensional model with an order-disorder transition. *Phys. Rev.*, 65:117, 1944. doi:10.1103/Phys.Rev.65.117.

[66] J. Padayasi and I. A. Gruzberg. Conformal invariance and multifractality at anderson transitions in arbitrary dimensions. *Phys. Rev. Lett.*, 131:266, 2023. doi:10.1103/PhysRevLett.131.266401.

[67] L. Pastur and A. Figotin. *Spectra of random and almost-periodic operators*. Springer, 1992. ISBN: 9783642743481.

[68] C. Preston. *Random fields*. Springer, 1976. ISBN: 978-3540381938.

[69] A. M. M. Pruisken and L. Schäfer. The Anderson model for electron localization nonlinear σ model, asymptotic gauge invariance. *Nucl. Phys. B*, 200:20, 1982. doi:10.1016/0550-3213(82)90056-6.

[70] M. Puschmann, D. Hernangómez-Pérez, B. Lang, S. Bera, and F. Evers. Quartic multifractality and finite-size corrections at the Spin Quantum Hall transition. *Phys. Rev. B*, 103:235, 2021. doi:10.1103/PhysRevB.103.235167.

[71] M. Reed and B. Simon. *Methods of modern mathematical physics, vol. I.* Elsevier, 1980. ISBN: 0125850506. doi:10.1016/B978-0-12-585001-8.X5001-6.

[72] R. Del Rio, S. Jitomirskaya, Y. Last, and B. Simon. Operators with singular continuous spectrum: Iv. hausdorff dimensions, rank one perturbations, and localization. *J. A. Math.*, 69:153, 1996. doi:10.1007/BF02787106.

[73] R. Del Rio, N. Makarov, and B. Simon. Operators with singular continuous spectrum: Ii. rank one operators. *Commun. Math. Phys.*, 165:59, 1994. doi:10.1007/BF02099737.

[74] A. Rodriguez, L. J. Vasquez, K. Slevin, and R. A. Römer. Multifractal finite-size scaling and universality at the Anderson transition. *Phys. Rev. B*, 84:134, 2011. doi:10.1103/PhysRevB.84.134209.

[75] D. Ruelle. *Statistical mechanics–Rigorous results.* Imperial College Press, 1999. ISBN: 9810238622.

[76] M. Schreiber and I. Gruzberg. Dimensionality dependence of the metal-insulator transition in the Anderson model of localization. *Phys. Rev. Lett.*, 76:1687, 1996. doi:10.1103/PhysRevLett.76.1687.

[77] A. Schwarz and O. Zaboronsky. Supersymmetry and localization. *Commun. Math. Phys.*, 183:463, 1997. doi:10.1007/BF02506415.

[78] L. Schäfer and F. Wegner. Disordered system with n orbitals per site: Lagrange formulation, hyperbolic symmetry, and Goldstone modes. *Z. Phys. B*, 38:113, 1980. doi:10.1007/BF01598751.

[79] P. Sierant, M. Lewenstein, and A. Scardicchio. Universality in Anderson localization on random graphs with varying connectivity. *SciPost Phys.*, 15:45, 2023. doi:10.21468/SciPostPhys.15.2.045.

[80] B. Simon. Operators with singular continuous spectrum: I. general operators. *Ann. Math.*, 141:131, 1995. doi:10.2307/2118629.

[81] P. Stollmann. *Caught by disorder*. Birkhäuser, 2001. ISBN: 9781461266440.

[82] R. S. Strichartz. Fourier asymptotics of fractal measures. *J. Func. An.*, 89:154, 1990. doi:10.1016/0022-1236(90)90009-A.

[83] A. Sütő. Singular continuous spectrum on a cantor set of zero Lebesgue measure for the Fibonacci Hamiltonian. *J. Stat. Phys.*, 56:525, 1989. doi:10.1007/BF01044450.

[84] E. Tarquini, G. Biroli, and M. Tarzia. Critical properties of the anderson localization transition and the high dimensional limit. *Phys. Rev. B*, 95:204, 2017. doi:10.1103/PhysRevB.95.094204.

[85] D. J. Thouless. Electrons in disordered systems and the theory of localization. *Phys. Rep.*, 13:93, 1974. doi:10.1016/0370-1573(74)90029-5.

[86] K. S. Tikhonov, A. D. Mirlin, and M. A. Skvortsov. Anderson localization and ergodicity on random regular graphs. *Phys. Rev. B*, 94:220203, 2017. doi:10.1103/PhysRevB.94.220203.

[87] L. Ujfalusi and I. Varga. Finite-size scaling and multifractality at the Anderson transition for the three Wigner-Dyson symmetry classes in three dimensions. *Phys. Rev. B*, 91:184, 2015. doi:10.1103/PhysRevB.91.184206.

[88] A. C. D. van Enter, R. Fernández, and A. D. Sokal. Regularity properties and pathologies of position-space renormalization-group transformations: Scope and limitations of Gibbsian theory. *J. Stat. Phys.*, 72:879, 1992. doi:10.1007/BF01048183.

[89] C. Vanoni, B. L. Altshuler, V. E. Kratsov, and A. Scardicchio. Renormalization group analysis of the Anderson model on random regular graphs. *PNAS*, 121:e2401955121, 2024. doi:10.1073/pnas.2401955121.

[90] J. J. M. Verbaarschot, H. A. Weidenmüller, and M. R. Zirnbauer. Grassmann integration in stochastic quantum physics: The case of compound-nucleus scattering. *Phys. Rep.*, 129:367, 1985. doi:10.1016/0370-1573(85)90070-5.

[91] D. Vollhardt and P. Wölfle. Diagrammatic, self-consistent treatment of the Anderson localization problem in $d \leq 2$ dimensions. *Phys. Rev. B*, 22:4666, 1980. doi:10.1103/PhysRevB.22.4666.

[92] F. Wegner. Mobility edge problem – continuous symmetry and a conjecture. *Z. Phys. B*, 35:207, 1979. doi:10.1007/BF01319839.

[93] F. Wegner. Inverse participation ratio in $2+\varepsilon$ dimensions. *Z. Phys. B*, 36:209, 1980. doi:10.1007/BF01325284.

[94] F. Wegner. Bounds on the density of states in disordered systems. *Z. Phys. B*, 44:9, 1981. doi:10.1007/BF01292646.

[95] F. J. Wegner. Electrons in disordered systems – scaling near the mobility edge. *Z. Phys. B*, 25:327, 1976. doi:10.1007/BF01315248.

[96] F. J. Wegner. Disordered system with n orbitals per site – $n = \infty$ limit. *Phys. Rev. B*, 19:783, 1979. doi:10.1103/PhysRevB.19.783.

[97] N. Wiener. *The Fourier integral and certain of its applications*. Cambridge University Press, 1933. ISBN: 0521358841.

[98] E. P. Wigner. Characteristic vectors of bordered matrices with infinite dimensions. *Ann. Math.*, 62:548, 1955. doi:10.2307/1970079.

[99] E. P. Wigner. On the distribution of the roots of certain symmetric matrices. *Ann. Math.*, 67:325, 1958. doi:10.2307/1970008.

[100] E. Witten. Topological quantum field theory. *Commun. Math. Phys.*, 117:353, 1988. doi:10.1007/BF01223371.

[101] H. T. Yau and J. Yin. Delocalization of one-dimensional random band matrices. 2025. doi:arXiv:2501.01718v4.

[102] M. R. Zirnbauer. Localization transition on the Bethe lattice. *Phys. Rev. B*, 34:394, 1986. doi:10.1103/PhysRevB.34.6394.

[103] M. R. Zirnbauer. Fourier analysis on a hyperbolic supermanifold with constant curvature. *Commun. Math. Phys.*, 141:503, 1991. doi:10.1007/BF02102812.

[104] M. R. Zirnbauer. The supersymmetry method of random matrix theory. 2004. doi:10.48550/arXiv.math-ph/0404057.

[105] M. R. Zirnbauer. The integer quantum Hall plateau transition is a current algebra after all. *Nucl. Phys. B*, 941:458, 2019. doi:10.1016/j.nuclphysb.2019.02.017.

8 Appendices

8.1 Derivation of field theory on lattices $\mathbb{G}$

The derivation is similar in spirit to the derivation of the AAT integral equation in Section 3.3.3. With the observable

$$K^{\Gamma}_{n,\varepsilon} = \mathbb{E}(G^{\Gamma}_n(E+\mathrm{i}\varepsilon)\, G^{\Gamma}_n(E-\mathrm{i}\varepsilon)), \tag{8.1}$$

the derivation of the field theory is very transparent. We work on a finite sublattice Γ with boundary conditions on the complement Γ^c. We begin by defining field-theoretical states that contain complex retarded $(+)$ variables $u_n, n \in \mathbb{G}$ or complex advanced $(-)$ variables $v_n, n \in \mathbb{G}$:

$$\begin{aligned} \langle \bullet \rangle_{+,\Gamma} &\equiv \mathrm{Det}(\varepsilon - \mathrm{i}(E-h)) \int \prod_{j\in\Gamma} \frac{\mathrm{d}^2 u_j}{\pi} \;\bullet\; \mathrm{e}^{\mathrm{i}\overline{u}\cdot_\Gamma (E+\mathrm{i}\varepsilon-h)u}, \\ \langle \bullet \rangle_{-,\Gamma} &\equiv \mathrm{Det}(\varepsilon + \mathrm{i}(E-h)) \int \prod_{j\in\Gamma} \frac{\mathrm{d}^2 v_j}{\pi} \;\bullet\; \mathrm{e}^{-\mathrm{i}\overline{v}\cdot_\Gamma (E-\mathrm{i}\varepsilon-h)v}, \end{aligned} \tag{8.2}$$

where

$$\overline{u}\cdot_\Gamma (E+\mathrm{i}\varepsilon-h)u \equiv \sum_{j,j'\in\overline{\Gamma}} \overline{u}_j\, (E+\mathrm{i}\varepsilon-h)_{j,j'}\, u_j, \tag{8.3}$$

and equivalently for v. The determinants in the expressions (8.2) ensure the normalization of the states. To perform the expectation value with respect to the disorder $\mathbb{E}$, we rewrite them as Berezin integrals of Gaussian type. We use the identity:

$$\mathrm{Det}(A) = \prod_{j\in\Gamma} \frac{\partial^2}{\partial\zeta_j \partial\overline{\zeta_j}}\, \mathrm{e}^{\overline{\zeta}\cdot_\Gamma A\zeta} \tag{8.4}$$

for suitable matrices A. We then arrive at:

$$\begin{aligned}\langle\bullet\rangle_{+,\Gamma} &\equiv \int \prod_{j\in\Gamma} \frac{\mathrm{d}^2 u_j}{\pi} \otimes \frac{\partial^2}{\partial\zeta_j \partial\overline{\zeta_j}} \bullet\ \mathrm{e}^{\mathrm{i}\overline{u}\cdot_\Gamma (E+\mathrm{i}\varepsilon-h)u - \mathrm{i}\overline{\zeta}\cdot_\Gamma (E+\mathrm{i}\varepsilon-h)\zeta},\\ \langle\bullet\rangle_{-,\Gamma} &\equiv \int \prod_{j\in\Gamma} \frac{\mathrm{d}^2 v_j}{\pi} \otimes \frac{\partial^2}{\partial\omega_j \partial\overline{\omega_j}} \bullet\ \mathrm{e}^{-\mathrm{i}\overline{v}\cdot_\Gamma (E-\mathrm{i}\varepsilon-h)v + \mathrm{i}\overline{\omega}\cdot_\Gamma (E-\mathrm{i}\varepsilon-h)\omega}.\end{aligned} \tag{8.5}$$

We observe that with the states $\langle\bullet\rangle_{\pm,\Gamma}$ one can express retarded and advanced Green's functions as a field-theoretical expectation value of local field operators:

$$\begin{aligned}\mathrm{i}G_n^\Gamma(E+\mathrm{i}\varepsilon) &= \langle\overline{\zeta_n}\zeta_n\rangle_{+,\Gamma}\\ -\mathrm{i}G_n^\Gamma(E-\mathrm{i}\varepsilon) &= \langle\overline{\omega_n}\omega_n\rangle_{-,\Gamma}.\end{aligned} \tag{8.6}$$

Accordingly, we find

$$K_{n,\varepsilon}^\Gamma = \mathbb{E}\left(\langle\overline{\zeta_n}\zeta_n\rangle_{+,\Gamma}\,\langle\overline{\omega_n}\omega_n\rangle_{-,\Gamma}\right). \tag{8.7}$$

We now introduce the supervectors:

$$\Phi_j = \begin{pmatrix} u_j \\ v_j \\ \zeta_j \\ \omega_j \end{pmatrix}, \quad \widetilde{\Phi}_j = \begin{pmatrix} \overline{u_j} & -\overline{v_j} & \overline{\zeta_j} & \overline{\omega_j} \end{pmatrix}. \tag{8.8}$$

By transforming $\zeta \to -\zeta$, $\omega \to -\omega$ (while keeping $\overline{\zeta}, \overline{\omega}$), and abbreviating

$$\int_{\Phi,\widetilde{\Phi}} \equiv \int \prod_{j\in\Gamma} \frac{\mathrm{d}^2 u_j}{\pi}\frac{\mathrm{d}^2 v_j}{\pi} \otimes \frac{\partial^2}{\partial\zeta_j \partial\overline{\zeta_j}}\frac{\partial^2}{\partial\omega_j \partial\overline{\omega_j}}, \tag{8.9}$$

we obtain for the product of the two states:

$$\langle\bullet\rangle_{+,\Gamma}\,\langle\bullet\rangle_{-,\Gamma} = \int_{\Phi,\widetilde{\Phi}} \bullet\ \mathrm{e}^{\mathrm{i}\widetilde{\Phi}\cdot_\Gamma (E+\mathrm{i}\varepsilon\Sigma_3-h)\Phi}, \tag{8.10}$$

where the product $\cdot_\Gamma$ now also contains the vector indices of Φ_j, α, β. Next we perform the disorder average $\mathbb{E}$ (we use Einstein sum convention):

$$\begin{aligned}&\mathbb{E}\left(\mathrm{e}^{-\mathrm{i}\widetilde{\Phi}_{\alpha,j} h_{j,j'} \Phi_{\alpha,j'}}\right) = \mathrm{e}^{-\frac{1}{2}\widetilde{\Phi}_{\alpha,j}\Phi_{\alpha,j'}\widetilde{\Phi}_{\beta,l}\Phi_{\beta,l'}\mathbb{E}(h_{j,j'}h_{l,l'})}\\ &= \mathrm{e}^{-\frac{1}{2}w_V^2 (-1)^{|\alpha|}(\Phi\otimes\widetilde{\Phi})_{\alpha\beta,j}(\Phi\otimes\widetilde{\Phi})_{\beta\alpha,j} - w_T^2 A_{j,j'}(-1)^{|\alpha|}(\Phi\otimes\widetilde{\Phi})_{\alpha\beta,j}(\Phi\otimes\widetilde{\Phi})_{\beta\alpha,j'}}\\ &= \mathrm{e}^{-\frac{1}{2}w_V^2 \sum_{j\in\Gamma}\mathrm{STr}\mathcal{Q}_j^2 - w_T^2 \sum_{jj'\in\overline{\Gamma}} A_{jj'}\mathrm{STr}\mathcal{Q}_j\mathcal{Q}_{j'}}.\end{aligned} \tag{8.11}$$

Combining the above with the deterministic site-diagonal terms, we finally obtain:

$$K^{\Gamma}_{n,\varepsilon} = \langle -\overline{\zeta_n}\zeta_n\overline{\omega_n}\omega_n\rangle_{\Gamma}, \tag{8.12}$$

where the state reads:

$$\langle \bullet_n\rangle_{\Gamma} = \int \prod_{j\in\Gamma} \mathcal{D}\mathcal{Q}_j \ \bullet_n \ \mathrm{e}^{-S_{\Gamma}}, \tag{8.13}$$

and

$$\begin{aligned} &S_{\Gamma} = S_{\mathrm{reg}\Gamma} + S_{V\Gamma} + S_{T\Gamma}, \quad S_{\mathrm{reg}\Gamma} = \sum_{j\in\Gamma} \mathrm{STr}\,(\varepsilon\Sigma_3)\,\mathcal{Q}_j\,, \\ &S_{V\Gamma} = \sum_{j\in\Gamma} \mathrm{STr}\left(-\mathrm{i}E\mathcal{Q}_j + \tfrac{1}{2}w_V^2\mathcal{Q}_j^2\right), \quad S_{T\Gamma} = w_T^2 \sum_{jj'\in\overline{\Gamma}} A_{jj'}\,\mathrm{STr}\,\mathcal{Q}_j\mathcal{Q}_{j'}. \end{aligned} \tag{8.14}$$

8.2 Expressing the Laplacian (3.88) in terms of K_i, D

One proves the identity (3.92) by a straightforward calculation. We start by expressing

$$\Delta^{\flat} = K_3^2 - K_2^2 - K_1^2 + D^2 + D \tag{8.15}$$

in terms of the coordinate vector fields $\frac{\partial}{\partial x_i} \equiv \partial_{x_i}$.

$$\begin{aligned} &K_3^2 = (x_1\,\partial_{x_2} - x_2\,\partial_{x_1})\,(x_1\,\partial_{x_2} - x_2\,\partial_{x_1}) = x_1^2\,\partial_{x_2}^2 + x_2^2\,\partial_{x_1}^2 - x_1\,\partial_{x_1} - x_2\,\partial_{x_2} - 2x_1\,x_2\,\partial_{x_1}\,\partial_{x_2}, \\ &K_2^2 = (x_3\,\partial_{x_1} + x_1\,\partial_{x_3})(x_3\,\partial_{x_1} + x_1\,\partial_{x_3}) = x_3^2\,\partial_{x_1}^2 + x_1^2\,\partial_{x_3}^2 + x_3\,\partial_{x_3} + x_1\,\partial_{x_1} + 2x_1\,x_3\,\partial_{x_1}\,\partial_{x_3}, \\ &K_1^2 = (x_2\,\partial_{x_3} + x_3\,\partial_{x_2})(x_2\,\partial_{x_3} + x_3\,\partial_{x_2}) = x_2^2\,\partial_{x_3}^2 + x_3^2\,\partial_{x_2}^2 + x_2\,\partial_{x_2} + x_3\,\partial_{x_3} + 2x_2\,x_3\,\partial_{x_2}\,\partial_{x_3}, \\ &D^2 + D = \left(\sum_{\mu=0}^{3} x_\mu\,\partial_{x_\mu}\right)^2 + \sum_{\mu=0}^{3} x_\mu\,\partial_{x_\mu} = x_0^2\,\partial_{x_0}^2 + x_1^2\,\partial_{x_1}^2 + x_2^2\,\partial_{x_2}^2 + x_3^2\,\partial_{x_3}^2 + 2x_0\,\partial_{x_0} + ... \\ &... + 2x_1\,\partial_{x_1} + 2x_2\,\partial_{x_2} + 2x_3\,\partial_{x_3} + 2x_0\,x_1\,\partial_{x_0}\,\partial_{x_1} + 2x_0\,x_2\,\partial_{x_0}\,\partial_{x_2} + 2x_0\,x_3\,\partial_{x_0}\,\partial_{x_3} + ... \\ &... + 2x_1\,x_2\,\partial_{x_1}\,\partial_{x_2} + 2x_1\,x_3\,\partial_{x_1}\,\partial_{x_3} + 2x_2\,x_3\,\partial_{x_2}\,\partial_{x_3}, \\ &\Delta^{\flat} = (x_3^2 - x_2^2 - x_1^2)\,(\partial_{x_3}^2 - \partial_{x_2}^2 - \partial_{x_1}^2) + x_0^2\,\partial_{x_0}^2 + 2x_0\,\partial_{x_0} + 2x_0\,x_1\,\partial_{x_0}\,\partial_{x_1} + ... \\ &... + 2x_0\,x_2\,\partial_{x_0}\,\partial_{x_2} + 2x_0\,x_3\,\partial_{x_0}\,\partial_{x_3}. \end{aligned} \tag{8.16}$$

Next we rewrite the middle term of Eq. (3.92):

$$\begin{aligned} &2D\circ x_0\,\partial_{x_0} = 2\left(\sum_{\mu=0}^{3} x_\mu\,\partial_{x_\mu}\right)\circ x_0\,\partial_{x_0} = 2x_0^2\,\partial_{x_0}^2 + 2x_0\,\partial_{x_0} + 2x_0\,x_1\,\partial_{x_0}\,\partial_{x_1} + ... \\ &... + 2x_0\,x_2\,\partial_{x_0}\,\partial_{x_2} + 2x_0\,x_3\,\partial_{x_0}\,\partial_{x_3}. \end{aligned} \tag{8.17}$$

Finally, we obtain:

$$\begin{aligned}
&\frac{1}{4}(x_3^2-x_2^2-x_1^2)^{-1}\left(\Delta^\flat - 2D\circ x_0\,\partial_{x_0}+(x_0^2+x_1^2+x_2^2-x_3^2)\,\partial_{x_0}^2\right)\\
&=\frac{1}{4}(x_3^2-x_2^2-x_1^2)^{-1}\,(x_3^2-x_2^2-x_1^2)\,(\partial_{x_3}^2-\partial_{x_2}^2-\partial_{x_1}^2-\partial_{x_0}^2)\\
&=\frac{1}{4}\left(\partial_{x_3}^2-\partial_{x_0}^2-\partial_{x_1}^2-\partial_{x_2}^2\right)=\Delta.
\end{aligned} \tag{8.18}$$

8.3 Calculation of g integral over H^2

Here we calculate the remaining integral in (5.37) over the hyperboloid H^2:

$$\begin{aligned}
I&=\int_{H^2}\mathrm{d}g'\left(1+w_T^2\frac{\partial}{\partial w_T^2}\right)\mathrm{e}^{-w_T^2\,\mathrm{Tr}\,q_0g'q_0{g'}^{-1}}\varphi_{0,\lambda}(\theta')\\
&=2\int_{\mathbb{R}^+}\sinh(\theta')\,\mathrm{d}\theta'\left(1+w_T^2\frac{\partial}{\partial w_T^2}\right)\mathrm{e}^{-2w_T^2mm'-2w_T^2|mm'|\cosh(\theta')}\varphi_{0,\lambda}(\theta').
\end{aligned} \tag{8.19}$$

An efficient way to calculate the θ' integral in (8.19) is to change coordinates to $t:H^2\to\mathbb{R}$, and $b:H^2\to\mathbb{R}$. These are connected to hyperbolic polar coordinates as follows:

$$\begin{gathered}
\cosh(\theta)+\sinh(\theta)\cos(\phi)=\mathrm{e}^t,\quad \cosh(\theta)=\cosh(t)+\frac{1}{2}\mathrm{e}^t b^2,\\
dg=\frac{1}{\pi}\sinh(\theta)\,\mathrm{d}\theta\,\mathrm{d}\phi=\frac{1}{\pi}\mathrm{e}^t\,\mathrm{d}t\,\mathrm{d}b.
\end{gathered} \tag{8.20}$$

We recall the integral expression for the zonal spherical functions:

$$\varphi_{0,\lambda}(\theta)=\int_0^{2\pi}\frac{\mathrm{d}\phi}{2\pi}\frac{1}{(\cosh(\theta)+\sinh(\theta)\cos(\phi))^{\frac{1}{2}+\mathrm{i}\lambda}}. \tag{8.21}$$

By inserting the integral formula (8.21) into the second row of Eq. (8.19), and using that the integral kernel is independent of ϕ, we can exchange ϕ integration with the multiplication by the integral kernel. It follows that we can express the whole integral in the coordinates (8.20). We arrive at:

$$\begin{aligned}
&I=\frac{1}{\pi}\int_{\mathbb{R}}\int_{\mathbb{R}}\mathrm{e}^{t'}\mathrm{d}t'\mathrm{d}b'\left(1+w_T^2\frac{\partial}{\partial w_T^2}\right)\mathrm{e}^{-2w_T^2mm'-2w_T^2|mm'|\left(\cosh(t')+\frac{1}{2}\mathrm{e}^{t'}{b'}^2\right)}\times\ldots\\
&\ldots\times\mathrm{e}^{-\frac{t'}{2}-\mathrm{i}\lambda t'}.
\end{aligned} \tag{8.22}$$

We now perform the integrals:

$$\begin{aligned} I &= \frac{1}{\sqrt{\pi}}\left(1+w_T^2\frac{\partial}{\partial w_T^2}\right)\int_{\mathbb{R}}\mathrm{d}t'\frac{1}{\sqrt{w_T^2|mm'|}}\mathrm{e}^{-2w_T^2mm'-2w_T^2|mm'|\cosh(t')}\cos(\lambda t') \\ &= \frac{2}{\sqrt{\pi}}\left(1+w_T^2\frac{\partial}{\partial w_T^2}\right)\frac{1}{\sqrt{w_T^2|mm'|}}\mathrm{e}^{-2w_T^2mm'}K_{\mathrm{i}\lambda}(2w_T^2|mm'|), \end{aligned} \tag{8.23}$$

where K denotes the modified Bessel function of the second kind. Finally, performing the parameter derivative yields the desired result (5.38):

$$\begin{aligned} I = \frac{1}{\sqrt{\pi}}\frac{1}{\sqrt{w_T^2|mm'|}}\Big((1-4w_T^2mm')K_{\mathrm{i}\lambda}(2w_T^2|mm'|) - ... \\ ... - 2w_T^2|mm'|(K_{1+\mathrm{i}\lambda}(2w_T^2|mm'|)+K_{1-\mathrm{i}\lambda}(2w_T^2|mm'|))\Big). \end{aligned} \tag{8.24}$$

8.4 Scaling of λ^*

We here argue how λ^* scales with the disorder strength w. For $\lambda\in\mathbb{C}$ the eigenvalues $e_w(\lambda)$ of the linearized operator (5.4) at disorder strength w, as a function of the harmonic parameter λ, has a saddle point at $\lambda=0$. Consequently, we have for small λ:

$$e_w(\lambda) = e_w(0) - |e_w''(0)|\,\lambda^2 + ... \tag{8.25}$$

Here e_w'' denotes the second derivative with respect to λ. Now λ^* fulfills:

$$\lambda^* = \sqrt{\frac{e_w(0)-1}{|e_w''(0)|}}. \tag{8.26}$$

In principle, we could calculate λ^* exactly from the result for the eigenvalues $e_w(\lambda)$ from the harmonic analysis. However, here we are interested only in the scaling, which can be anticipated with a faster argument. For $w\nearrow w_c$, the denominator in Eq. (8.26) stays finite, whereas the enumerator goes to zero. From the harmonic analysis, we know that (up to a logarithmic correction)

$$e_w(0) \sim \frac{K}{w}. \tag{8.27}$$

For $w_c - w \ll 1$ we expand $e_w(0)$ around w_c and obtain:

$$e_w(0) \approx 1 + \frac{w_c - w}{w_c}. \tag{8.28}$$

For λ^*, we find the scaling:

$$\lambda^* \sim \sqrt{w_c - w}, \quad w_c - w \ll 1. \tag{8.29}$$